UNIVERSIDADE FEDERAL DE MINAS GERAIS

Escola de veterinária

Departamento de Clinica e Cirurgia

Programa de Pós-graduação em ciência animal

Thaynara Parente de Carvalho

Pericytes modulate endothelial inflammatory response during bacterial infection

Belo Horizonte (MG)

Escola de Veterinária - ´UFMG

2023

Thaynara Parente de Carvalho

Pericytes modulate endothelial inflammatory response during bacterial infection

Defesa de tese apresentada ao programa de Pós-graduação em Ciência Animal da Universidade Federal de Minas Gerais, como requisito para a obtenção do título de Doutora em Ciência Animal.

Orientador: Prof. Dr. Renato de Lima Santos
Co-orientadoras: Profª. Dra. Tatiane Alves da Paixão e
Profª. Dra. Reneé M. Tsolis
Área de concentração: Patologia Animal

Belo Horizonte (MG)

2023

Carvalho, Thaynara Parente de,1993 -
C331p Pericytes modulate endothelial inflammatory response during bacterial infection/ Thaynara Parente de Carvalho. -2023.
148 f.il

Orientador: Renato de Lima Santos
Coorientadores: Tatiane Alves da Paixão
Reneé M. Tsolis
Tese (Doutorado) apresentado à Escola de Veterinária da Universidade Federal de Minas Gerais para obtenção do título de Doutora em Ciência animal
Área de Concentração: Patologia Animal.
Bibliografias: f. 16 a 17.

1. Doenças - Teses - 2. Medicina veterinária- Teses – 3. Ciência animal - Teses –
I. Santos, Renato de Lima - II. Paixão, Tatiane Alves da – III. Tsolis, Reneé M – IV. Universidade Federal de Minas Gerais, Escola de Veterinária - V. Título.

CDD – 636.089

Bibliotecária responsável Cristiane Patrícia Gomes – CRB2569
Biblioteca da Escola de Veterinária, Universidade Federal de Minas Gerais.

UNIVERSIDADE FEDERAL DE MINAS GERAIS
ESCOLA DE VETERINÁRIA
COLEGIADO DO PROGRAMA DE PÓS-GRADUAÇÃO EM CIÊNCIA ANIMAL

FOLHA DE APROVAÇÃO

THAYNARA PARENTE DE CARVALHO

Tese submetida à banca examinadora designada pelo Colegiado do Programa de Pós-Graduação em CIÊNCIA ANIMAL, como requisito para obtenção do grau de DOUTOR em CIÊNCIA ANIMAL, área de concentração em Patologia Animal.

Aprovado(a) em 28 de abril de 2023, pela banca constituída pelos membros:

Dr.(a). Renato de Lima Santos- Orientador(a)

Dr.(a). Alexander Birbrair

Dr.(a). Roberto Mauricio Carvalho Guedes

Dr.(a). Mariana Xavier Byndloss

Dr.(a). Vladimir Diaz-Ochoa

Documento assinado eletronicamente por **Renato de Lima Santos**, **Professor do Magistério Superior**, em 28/04/2023, às 16:24, conforme horário oficial de Brasília, com fundamento no art. 5º do Decreto nº 10.543, de 13 de novembro de 2020.

Documento assinado eletronicamente por **Alexander Birbrair**, **Professor do Magistério Superior**, em 02/05/2023, às 11:58, conforme horário oficial de Brasília, com fundamento no art. 5º do Decreto nº 10.543, de 13 de novembro de 2020.

Documento assinado eletronicamente por **Roberto Mauricio Carvalho Guedes**, **Professor do Magistério Superior**, em 18/05/2023, às 12:09, conforme horário oficial de Brasília, com fundamento no art. 5º do Decreto nº 10.543, de 13 de novembro de 2020.

Documento assinado eletronicamente por **Mariana Xavier Byndloss**, **Usuária Externa**, em 29/05/2023, às 17:43, conforme horário oficial de Brasília, com fundamento no art. 5º do Decreto nº 10.543, de 13 de novembro de 2020.

Documento assinado eletronicamente por **Vladimir Emiliano Diaz-Ochoa**, **Usuário Externo**, em 23/06/2023, às 12:04, conforme horário oficial de Brasília, com fundamento no art. 5º do Decreto nº 10.543, de 13 de novembro de 2020.

A autenticidade deste documento pode ser conferida no site https://sei.ufmg.br/sei/controlador_externo.php?acao=documento_conferir&id_orgao_acesso_externo=0, informando o código verificador **2240934** e o código CRC **DA26105D**.

UNIVERSIDADE FEDERAL DE MINAS GERAIS
ESCOLA DE VETERINÁRIA
COLEGIADO DO PROGRAMA DE PÓS-GRADUAÇÃO EM CIÊNCIA ANIMAL

FOLHA DE APROVAÇÃO

THAYNARA PARENTE DE CARVALHO

Tese submetida à banca examinadora designada pelo Colegiado do Programa de Pós-Graduação em CIÊNCIA ANIMAL, como requisito para obtenção do grau de DOUTOR em CIÊNCIA ANIMAL, área de concentração em Patologia Animal.

Aprovado(a) em 28 de abril de 2023, pela banca constituída pelos membros:

Dr.(a). Renato de Lima Santos- Orientador(a)

Dr.(a). Alexander Birbrair

Dr.(a). Roberto Mauricio Carvalho Guedes

Dr.(a). Mariana Xavier Byndloss

Dr.(a). Vladimir Diaz-Ochoa

Documento assinado eletronicamente por **Renato de Lima Santos**, **Professor do Magistério Superior**, em 28/04/2023, às 16:24, conforme horário oficial de Brasília, com fundamento no art. 5º do Decreto nº 10.543, de 13 de novembro de 2020.

Documento assinado eletronicamente por **Alexander Birbrair**, **Professor do Magistério Superior**, em 02/05/2023, às 11:58, conforme horário oficial de Brasília, com fundamento no art. 5º do Decreto nº 10.543, de 13 de novembro de 2020.

Documento assinado eletronicamente por **Roberto Mauricio Carvalho Guedes**, **Professor do Magistério Superior**, em 18/05/2023, às 12:09, conforme horário oficial de Brasília, com fundamento no art. 5º do Decreto nº 10.543, de 13 de novembro de 2020.

Documento assinado eletronicamente por **Mariana Xavier Byndloss**, **Usuária Externa**, em 29/05/2023, às 17:43, conforme horário oficial de Brasília, com fundamento no art. 5º do Decreto nº 10.543, de 13 de novembro de 2020.

Documento assinado eletronicamente por **Vladimir Emiliano Diaz-Ochoa**, **Usuário Externo**, em 23/06/2023, às 12:04, conforme horário oficial de Brasília, com fundamento no art. 5º do Decreto nº 10.543, de 13 de novembro de 2020.

A autenticidade deste documento pode ser conferida no site https://sei.ufmg.br/sei/controlador_externo.php?acao=documento_conferir&id_orgao_acesso_externo=0, informando o código verificador **2240934** e o código CRC **DA26105D**.

Agradecimentos/ Acknowledgments

Uma frase que define minha caminhada na pós graduação, vem de uma musica chamada de Psiu da Liniker :“Pra quem não sabia contar gotas, cê aprendeu a nadar”

Meu crescimento com o doutorado foi muito além do cientifico. Realmente, aprendi a contar gotas e a nadar. E eu queria agradecer a todos que me ajudaram, seja os que me jogaram na agua ou por ensinar a dar a braçada. E acima de tudo, aos que me deram as oportunidades, as explicitas e implicitas.

Agradeço aos que me proporcionaram as maiores oportunidades, meus queridos pais de criação. Seu José Ribamar (*in memorian*) e a Maria Elizabeth E o que seria de mim sem os sermões? Como dizia a outra musica “Eu tenho a senha pra correr em todo canto. Humildade e disciplina dos sermão que mãe me deu”.

Agradeço a oportunidade de ter conhecido o meu futuro marido Daniel (agora vai ter que casar). Esse doutorado teria menos graças se não fosse você para fofocar no fim do dia. Obrigada pelo apoio. Te amo. Obrigada também pela segunda familia que você me deu, e que me recebeu tão bem. Obrigada aos meus futuros sogros pelo apoio incondicional e incentive para eu seguir firmes em minhas escolhas, Aparecida e Ronan. E as futuras cunhadas, Priscilla e Sarah, exemplos de sororidade e amor. Co-cunhado Rafael, que tem as um jeito leve de viver. E o pequeno Bebento, só amor.

Agradeço aos meus inumeros irmãos, primos (que estão na mesma categoria de irmãos), tios, tias, e pais biologicos. Em especial gostaria de agradecer a Tauan, Satiro Filho, Ruth, Emely, Benjamim, Sofia, Cecilia, Gui, Elenilson, Estefany, Frank, Tania, Telma, Tárcio e Tamara. Foram meu apoio emocional, e sempre estavam ansiosos para a minha volta a Teresina, nem que fosse para reclamar sobre algo de mim. Aos meus amigos de Teresina, quase irmãos, em especial Marina, Leticia, Thiago, Tatiane Carvalho e a queridissima prof Silvia.

Agradeço imensamente aos meus roomates e amigos Ayisa e Lucas. Obrigada pelo companherismo, por todos os episodios de Ru Paul, por todos os papos não academicos e academicos. Foram essenciais e fizeram o ambiente muito mais agradavel.

Agredeço a todos os amigos companheiros de setor que fiz na UFMG, todos dispostos a ajudar e compartilhar os conhecimentos. Em especial Monique, Menina Laice, Mirtha, Clarissa, Daniel, Noelly, Larissa, Nayara, Jefferson e Pamela. Espero que todos tenham um imenso sucesso, pois todos merecem.

Agradeço a todos os funcionários da UFMG. Em especial ao Luiz, seu João, Leimar, Valéria, dona Beth e Vita. Que além do seus trabalhos, mostraram gentileza, amizade e várias conversas que ajudam a alegrar os dias. Sem vocês a UFMG não funciona.

Agradeço ao professor Alexander Birbrair, por ter me apresentado o modelo de camundongos transgênicos essencial para esse trabalho. Além das diversas sugestões durante todo o doutorado.

Agradeço aos professores do setor de Patologia Veterinária da escola de Veterinária da UFMG, Nátalia, Renato, Roberto, Rógeria, Roselene e Ayisa, por todos os ensinamentos de patologia. Vocês me ensinaram muito mais do que ler lamina, me ensinaram a ser profissionais éticos. Em especial para a professora Ayisa, parabéns! Aos professores que não estão mais no setor mas tive a chance de aprender com eles, Paula e Felipe. Muito orbigada pela preocupação e incentivos.

Agradeço ao meu orientador Renato que me deu chance desde do mestrado, e agora no doutorado. E ainda acreditou que eu poderia muito mais, mesmo que eu mesma não tivesse tanta certeza. Além de me ajudar ativamente, principalmente na fase final do doutorado. Agradeço imensamente a minha co-orientadora Tatiane, que mulher! Eu admiro e me inspiro em mulheres forte, e a senhora é uma delas. Ambos são exemplos de competência professional, e sou grata por tudo.

Furthermore, I would like to thank Renée, my other co-PI, who welcomed me with open arms in her lab almost for one year. I am so grateful to have had you as a mentor and I am so

grateful that I was able to learn so much from you. Also, I would like to thank her for the new opportunities.

I thank for all Tsolis' and Baulmer's Lab team. Special Jee-Yon (and Eugene, of course), Sophie, Aurore, Brianna, Vlad, Scott, Amber (that always has a cat picture for showed for me), and Leticia. For make my time in Davis so pleasant.

I also thanks for the people that help me to make Davis home, Sylvia, Ana, Alix and Denise. You are friends, and bring all the latino-america kidness for this distant lands.

Agradeço a todos os orgão de fomento CAPES e CNPq por financiar meu doutorado e meu projeto. Sem o apoio destes orgão nada disso seria possivel.

“Not in knowledge is happiness, but in the acquisition of knowledge”

Edgar Allan Poe

Resumo

Os pericitos são células pluripotentes mesenquimais, localizadas ao redor dos vasos sanguíneos. Há evidências que o pericito tem papel importante no desenvolvimento de doenças metabólicas e infecciosas, como nos casos de infecções por citomegalovírus e *Bartonella henselae*. Apesar da importância reconhecida destas células e ainda não há estudos que tenham investigado a interação e papel do pericito frente a infecções com bactérias intracelulares, como *Brucella ovis* e *Listeria Monocytogenes*, e o papel direto da interação do pericito com as células endoteliais. O objetivo deste trabalho foi investigar o papel do pericito frente a infecção bacteriana *in vitro* e *in vivo.* Pericitos foram infectados com *B. ovis* e *L. monocytogenes* e observou-se que estas céluulas são pouco permissivas à infecção por ambas as bactérias. Foi realizada co-cultura de células endoteliais e pericitos (2:1, respectivamente) ou células endoteliais isoladas em cultivo, que foram estimuladas com *B. ovis, L. monocytogenes,* ou LPS de *Escherichia coli* em baixa doses. Após estimulo foi demonstrado que a presença do pericito diminui a transcrição e expressão de moléculas de adesão (PECAM-1 e ICAM-1) e moléculas pro-inflamatórias (CCL-2 e IL-6). Em modelo murino com depleção de pericitos infectados com *B. ovis* e *L. monocytogenes* por via intraperitoneal foi observada intensa reação inflamatória com peritonite fibrinosa, lesão ausente nos animais não-depletados. Também foi observado aumento de CCL-2 no soro dos animais depletados Em seguida, foi investigagdo o mecanismo pelo qual estas células se comunicam. Foi mensurado a produção de conexinas (conexina 43, 30.2, 37 e 40), na co-cultura sendo que a conexina 43 foi a mais abundante, A conexina 43 foi bloqueada, usando-se um inibidor químico (GAP19) ou por meio de mRNA de interferência (siRNA). Quando há bloqueio da conexina-43 há um aumento de molécula de adesão e pro-inflamatórias, demonstrando a função das conexina-43 para essa co-cultura. *In vivo,* camundongos tratados com GAP19 e infectados com *B. ovis* há aumento de carga bacteriana no fígado e baço, com significativo aumento da concentração de CCL-2 no soro. Todos os resultados demonstram que pericito modula resposta inflamatória das células endoteliais frente a estímulos bacterianos usados neste trabalho (*B. ovis* e *L. monocytogenes*).

Palavras-chave: Junções Gap, quimiocinas, diapedeses, peritonite.

Abstract

Pericytes are pluripotent mesenchymal cells located around blood vessels. There is evidence that the pericyte plays a significant role in the development of metabolic and infectious diseases, including cytomegalovirus and *Bartonella henselae* infections. Taking into account the importance of these cells and a lack of previous studies on the role of pericytes during bacterial infections, the goal of this study was to investigate the interaction and function of the pericytes in infections caused by intracellular bacteria, including *Brucella ovis* and *Listeria monocytogenes*, and the direct effect of the pericyte on endothelial cells. This study described the role of the pericyte during bacterial infection *in vitro* and *in vivo*. Inoculation of cultured pericytes with *B. ovis* and *L. monocytogenes* demonstrated that pericytes are not permissive to intracellular bacterial infections. Co-cultured endothelial cells and pericytes (2:1 respectively) or endothelium alone were inoculated with *B. ovis* or *L. monocytogenes*, or stimulated with LPS at a low concentration. Under those conditions the presence of pericytes decreased and expression of adhesion molecules (PECAM-1 and ICAM-1) and pro-inflammatory molecules (CCL-2 and IL-6). The presence of fibrinous peritonitis was observed in a murine model with depletion of pericytes infected with *L. monocytogenes* and *B. ovis* via the intraperitoneal route, whereas none of non-depleted control mice developed peritonitis under the same experimental conditions. Depleted mice had increased levels of CCL-2 in the serum. In addition, we measure the levels of connexins expressed in our co-culture, and the one with more expression between the endothelial cells and pericytes was connexin-43. To investigate how endothelial cells and pericytes communicate, we blocked connexin 43 using a chemical inhibitor (GAP19) or silence Connexin-43 expression using siRNA. Innibition of connexin-43 function led to an increase in expression of adhesion and pro-inflammatory molecules, demonstrating the function of connexin-43. Mice treated with GAP19 *in vivo* and infected with *B. ovis* had increased bacterial loads in the liver and spleen, and elevated CCL-2 levels in their sera. All results demonstrate that pericytes modulate the inflammatory response of endothelial cells to bacterial stimuli.

Keywords: Gap junctions, chemokines, diapedesis, peritonitis.

Figure List

Chapter I

Chapter II

Table List

Abbreviations list

BBB	Blood brain barrier
BRB	Blood retina barrier
CAMs	Cell adhesion molecules
CD105	Cluster differentiation 105
CD13	Cluster differentiation 13
CD146	Adhesion molecules
CFU	Colony formation unit
Cx-43	Connexin 43
DAMPs	Damage-associated molecular patterns
DT	Diphtheria toxin
ECs	Endothelial cells
hMSC	Human mesenchymal stem cells
ICAM-1	Intercellular adhesion molecule-1
Ip	Intraperitoneal
Iv	Intravenous
LPS	Liposaccharides
MOI	Multiplicity of infection
LDH	Lactate dehydrogenase
NG-2	Glial nerve antigen-2
NOD-NLRs	Nucleotide-binding oligomerizantion domin-like
PAMPs	Pathogen-associated molecular patterns
PDGF	Platelet derived growth factor
PDGFR-β	Platelet derived growth factor receptor beta
PECAM-1	Vascular adhesion molecule-1
PMN	Polymorphonuclear
PRR	Pattern-recognition receptor
RGS-5	G signal regulatory protein-5
TEER	Transendothelial electrical resistance

TLR	Toll-like receptors
TIR	Toll/Interleukin-1 receptor
α-SMA	Smooth muscle α-actin

SUMMARY

INTRODUCTION

Pericytes are a heterogeneous cell population found around endothelial cells on blood vessels. They possess a great capacity of differentiation. It has been demonstrated that pericytes express various human mesenchymal stem cells (hMSC) markers. Neuron-glial antigen 2 proteoglycan (NG2) and platelet-derived growth factor receptor beta (PDGFRβ) seem the most reliable markers to identify arterial and capillary pericytes, especially when combined (Navarro et al., 2016; Yamazaki and Mukouyama, 2018). The NG2 glycoprotein, also known as chondroitin sulfate proteoglycan-4 (CSPG-4), is a cell surface component that plays an essential role in pericyte maturation, turning them into proliferative, motile cells that participate in the process of remodeling and neovascularization (Ozerdem et al, 2001; Ozerdem et al, 2002; Ozerdem et al, 2003; Couchman, 2003; Gibby et al, 2012).

The role of pericytes in angiogenesis and control of blood flow is well known (Hall et al., 2014; Ferland-McCollough et al., 2018; Nikolakopoulou et al., 2019). Additionally, during inflammation, postcapillary pericytes express the CXCL1 chemokine that allows neutrophil transmigration to the damaged or inflamed tissues [38] (Girbl et al., 2018). Activated precapillary and capillary pericytes, in turn, express ICAM-1, MIF, CCL2, and CXCL8 to attract and activate transmigrated neutrophils and macrophages, which can migrate faster and directional interstitial than non-activated leukocytes (Stark et al., 2013). Interaction between pericytes and T lymphocytes leads to differentiation of T regulatory lymphocytes, primarily immune suppressive. These studies highlight the pivotal role of pericytes in activating and regulating both arms of the immune response.

In addition to their physiological functions, pericytes have been implicated in disease development and recrudescence, such as neurological disorders, cancer and diabetic-related conditions and others (Hall et al., 2014; Ferland-McCollough et al., 2018; Nikolakopoulou et al., 2019). There is also evidence that pericytes may be implicated in diseases caused by viral and bacterial pathogens, such as human cytomegalovirus and *Bartonella henselae* (Varanat et al., 2013; Wilkerson et al., 2015; Aronoff et al., 2017), though the role of such cell types in bacterial infections remains unclear. Since pericytes have high plasticity and are players in disease development, this study aimed at investigating the role of pericytes in bacterial infections based

on the role of pericytes in inducing or suppressing inflammation in the context of different pathologic conditions. So, we aimed to test the hypothesis that pericytes modulate inflammation during bacterial infections.

CHAPTER I

Literature review

1.0 Pericytes

Pericytes are mesenchymal cells localized around blood vessels. They have a long cytoplasm with numerous projections that interacts with endothelial cells. Their nuclei are oval and prominent. Pericytes are present in all vascular tissues of mammals. The major function of these cells is angiogenesis and control of vascular stability (Armulik et al., 2011). These cells are attached to the basement membrane that surrounds and support the blood vessels. Pericytes can directly interact with endothelial cells and other cell types such as neurons and astrocytes, by direct physical contact and through autocrine and paracrine regulations (Balabanov et al., 1998; Dore-Duffy et al., 2005).

It is important to note that pericytes possess a complex phenotype and a heterogeneous distribution. Many markers have been used to identify these cells, including PDGF- platelet derived growth factor subunit β receptor (PDGFR- β), glial nerve antigen-2 (NG-2), G signal regulatory protein-5 (RGS-5), smooth muscle α-actin (α-SMA), desmedin, aminopeptidase N (CD13), endoglin (CD105), adhesion molecules (CD146), among others (Diaz-Flores, et al., 2009). However, the pericyte population is diverse, and not all pericytes express all markers, making homogeneous characterization of these cells not achievable (Armulik et al., 2011). Identification of pericytes in routine histologic sections is challenging and imprecise, but these cells may be identified by ultrastructural analysis, and/or markers such as NG-2 and PDGFR- β proteins associated with the perivascular localization of the cells (Armulik et al., 2005).

Many researchers divide pericytes into three subclasses based on their phenotypes: 1) pericytes located in the arteriole-capillaries, with most part of the cytoplasm in contact with endothelial cells and with contractile characteristics; 2) pericytes located in venules and post capillaries that have a shorter cytoplasm when compared to the others; 3) pericytes located capillary (Attwell et al., 2016; Berthiaume et al., 2018). However, despite the differences between

these three subclasses, a recent study by Vanlandewijck et al (2018) showed that there is no difference in the mRNA profile between these subclasses of pericytes.

Pericytes interacted primarily with endothelial cells through peg-and-socket junctions as well as through the juxtracrine and paracrine mediators. The main paracrine mediators know are TGF-β, angiopoietin 1/ 2, VEGF, and PDGF-β (Sweeney et al., 2016). The direct cross talking between endothelial cells and Pericytes is essential for the development, maturation and formation of blood vessels (Armulik et al., 2011). Pericytes also interacted with tissues cells, one example is the interaction with astrocytes and neurons. Astrocytes secrete prostaglandin E2 that binds to its receptor in pericytes (Mishra et al., 2016). Neurons interacted with pericytes through neurotransmitters. The effects depend of the neurotransmitter that can induce relaxation (Glutamate) or contraction (noradrenaline) of pericytes (Peppiatt et al., 2006; Hall et al., 2014). Approximately 25% of all pericyte research investigates the function of these cells in the brain (Brown et al., 2019).

Pericytes help maintain vascular homeostasis and angiogenesis (Armulik et al., 2011; Sweeney et al., 2016). Many other functions of these cells have been studied from different biological aspects in recent years. Such the influence in the chemotaxis process, blood coagulation, role in the immune function by regulating lymphocytes activation (Birbrar et al., 2019). Pericytes are involved in the development of some local and systemic disorders and diseases, such as neurological diseases, cancer and diabetes (Hall et al., 2014; Nikolakopoulou et al., 2019). Since pericytes are complex cells with high plasticity and involve in several pathologies, it is essential the acquisition of knowledge about pericyte cells in the diseases, immune response and interaction with other cells, likely endothelial cells.

1.2 Pericyte and endothelial cell junctions

Pericyte embrace the abluminal endothelial surface of almost all arterioles, venules and capillaries. Ultrastructural analyses demonstrated interdigitating contacts between pericytes and endothelial cells (Shepro and Morel, 1993). The junctions between pericytes and endothelial cells are of the peg-and-socket type (Armulik et al., 2011). Pegs appear to be the result of fusion of

either pericyte or endothelial cells, resulting in indentations within the opposing cell type. There is strong evidence from the anchoring of two cell types to each other as well as the observations of enriched expression of signaling proteins and the presence of specialized vesicular structures at dorms and sockets for cellular cross-signalization (Figure 1). Maturation and stability of blood vessels invoke the formation dynamics of endothelial-pericyte junctions, apical-basal polarity and control of the cytoskeleton to modulate cell shape (Wakui et al., 2006).

Peg-and socket contacts are formed by N-cadherin-dependent adherent junctions and channels of connexin (mostly cx-43) gap junctions (Winkler et al., 2011). The other significant type of contact is focal adhesion plaques, in which the extracellular matrix connects pericyte with endothelial cells indirectly via integrin dependent cell adhesions of both cell types (Winkler et al., 2011). The expression of functional N-cadherin is required for the normal attachment and spreading of pericyte to endothelial cells monolayer. Pericyte induces increased expression of N-cadherin in endothelial cells *in vitro* (McGuire et al., 2011). N-cadherin allows transmission of signals between two cells, which interacts with and activates Trio, a dual Rac1/RhoA guanine nucleotide exchange factor that induces the recruitment of VE-cadherin to endothelial-endothelial junctions thereby physically stabilizing the endothelial barrier (Kruse et al, 2019). As a result, Pericyte improved the blood barrier properties of the monolayer of endothelial cells (McGuire et al. 2011).

Connexin-based gap junctions clear the way for intercellular communication between numerous cell types. These junctions formed channels to pass small molecules (<1.2 kDa) like ions, second messengers and small metabolites between cells (Mathias et al., 2010). Gap junctions are formed for connexons. And connexons are formed for six molecules connexins and allow the transfer of ions, second messengers such as cAMP, and other small molecules between pericyte and endothelial cells (Armulik et al., 2005; Winkler et al., 2011; Kruse et al., 2019). Gap junctions are the only junctional structures conserved in all multicellular organisms, from mesoza to mammals (Phelan, 2005). A connexin is a protein with four transmembrane domains, two extracellular loop domains, an intracellular loop domain, and N- and C-terminal domains. In humans, there are 21 recognized connexins, whereas there are 20 known connexins in the mouse (Jiang, 2006). Each type of connexin can form a gap junction channel just by themselves (homotypic) or with other connexins. Connexins are named based on protein predicted molecular

weight (such as Connexin 43 MW ~43 kD). With some nomenclature differences, homologous connexins have different names in different species, likely Connexin 30.2 in mice (compatiable with connexin 30 in human) (Nielsen et al., 2012). Gap junctions of endothelial cells and pericytes are rich in connexin-43 (Cx-43) (Gerhardt and Betsholtz, 2003; Armulik et al., 2005; Maeda and Tsukihara, 2011; Winkler et al., 2011; Kruse et al., 2019). In co-culture between pericytes and endothelial cells, CX-43 was significantly expressed, suggesting that gap junctions play an important role in cell-to-cell communication (Brandt et al., 2019).

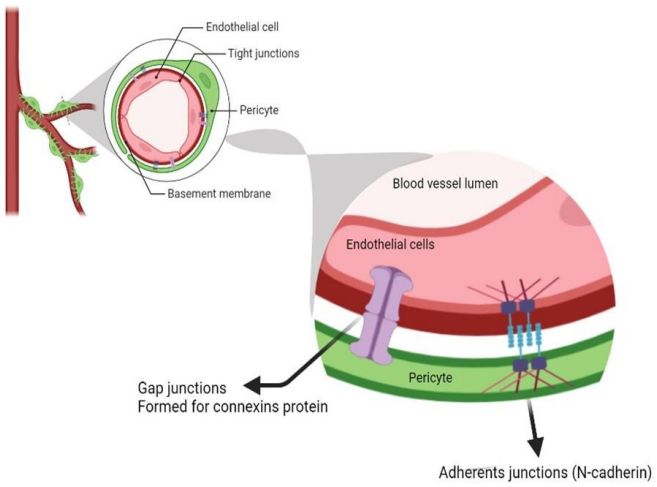

Figure 1.1 Localization of pericytes around endothelial cells with the peg-and-socket junctions. Pericyte and endothelial cells interaction and interconnections. These two cells are physical attachment and showed junctions of Peg-and-socket type. These junctions are rich in Gap junctions (connexons) and adherents' junctions (N-cadherin). Created with Biorender.com.

It is known that gap junctions are essential for the endothelial differentiation of mural cells precursors during vessel assembly. Besides, the loss of Cx-43 may be linked to the functional decline of pericyte functions such as homeostatic and supporting vascular stability (von Tell et al., 2006). In retinal tissue, the increase in glucose in the blood stream (similar to diabetes) reduced Cx-43 expression *in vitro* and compromised connectivity and stability of endothelial cells (Okamoto et al., 2019). Furthermore, when Cx-43 expression is downregulated

promotes vascular cell loss and increased permeability (Tien et al., 2014). Therefor, Cx-43 is essential for blood barrier maintenance (Okamoto et al., 2019).

1.3 Pericytes are an important component of blood tissues barrier

Because of their ability to form a barrier to protect tissues and organs from pathogens, blood vessels play an essential role in homeostasis of mammals. One of the best characterized blood barriers is in the brain, known as the blood brain barrier (BBB). BBB is a physical and functional barrier with the function of preventing several molecules, substances, and microorganisms from entering the central nervous system. The central nervous system is a complex and organized tissue, whose function depends on the direct of biochemical equilibrium. The BBB maintains the balance that allows the nervous system to function properly. BBB is composed by cerebral capillaries, whose endothelial cells are arranged juxtaposed with high transendothelial electrical resistance and low vascular permeability (Stanimirovic and Fredman, 2012).

For endogenous and therapeutic molecules to enter the brain parenchyma, they must cross the BBB, which is composed of a complex cellular architecture with endothelial cells delimitating blood vessels, pericytes and basement membranes around the endothelial cells, and astrocytes extending their end-feet to the abluminal side of vessels (Figure 1.2) (Abbott et al., 2010). This organization results in the formation of tight junctions between endothelial cells and others that limit paracellular transport and transcytosis (Hajal et al., 2021). This uniquely restrictive interface between blood and parenchyma protects the brain against toxins and pathogens (Hajal et al., 2018). In general, BBB function is essential and complex, which consists of making sure that there is an adequate concentration of ions in the nervous system. This is to preventing exotoxins, endotoxins and some infectious agents from reaching there. Further, in case of failure, BBB is supposed to regulate immune response, preventing tissue damage (Stanimirovic and Fredman, 2012). A healthy and functional BBB implies that the components of the cells are working properly (Dong, 2018). An intact BBB has low paracellular permeability

and high transendothelial electrical resistance (TEER) (Ayloo and Gu, 2019). Endothelial cells, astrocytes and pericytes secrete extracellular matrix components that control local permeability (Zhang et al., 2020).

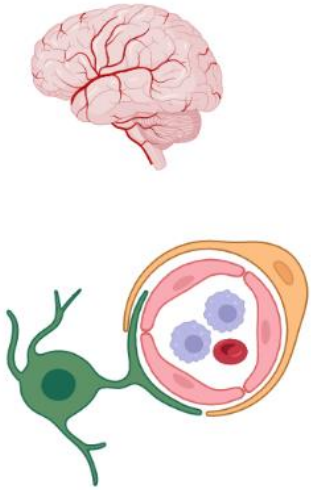

Figure 1.2 Cells component of blood brain barrier. BBB are formed for different types of cells, such as endothelial cells (pink), perycites (yellow) and astrocytes (green). Together these cells control the permeability of nervous system and wich substance can goes in or out. Created with BioRender

The pericytes are essential to the maintenance of BBB integrity, angiogenesis regulation and cerebral blood flow control (Li et al., 2017). In the nervous system, permeability is controlled by complexes of endothelial junctions (Armulik et al., 2005). Pericytes control and regulate several junctions (V-cadherin, CX-43, ZO-1, and claudin 5) between endothelial cells and astrocytes, thereby affecting permeability. Depletion of pericytes increased blood vessel permeability (Armulik et al., 2010; Sengillo et al., 2013; Perrot et al., 2020). *In vivo,* pericyte deficiency was not associated with changes in endothelial monolayer polarization or with signs of fenestration of blood vessels (Armulik et al., 2010). The breakdown of the blood-brain barrier due to pericyte loss is thought to accelerate neurodegeneration diseases such as Alzheimer's. These events probably happen due to the accumulation of toxins in the central nervous system (Sagare et al., 2013; Sengillo et al., 2013; Kisler et al., 2017). Furthermore, pericytes showed to be crucial

to post-ischemic phase recovery, they migrate to injury sites and contribute to BBB and tissues repair (Geranmayeh et al., 2019).

Another important blood barrier is the blood-retina barrier (BRB), which keeps the retina in a state of homeostasis by restricting the entry of substances and maintaining strict ionic and metabolic gradients. Any disruption in BRB could cause macular edema, which is associated with ischemic retinopathies, including diabetic retinopathy and other degenerative diseases (Vinores, 2010). The BRB is divided into internal and external parts. In the inner part of BRB, there are tightly connected capillary endothelial cells covered with pericyte and Muller glial cells. These cells nourish the inner two thirds of the retina. In the outer part of BRB there are tightly connected pigment epithelial cells responsible for maintaining the retinal integrity (Cunha et al., 2011; Campochiaro 2015). Pericytes, likely in BBB, perform several functions, including angiogenesis, vascular remodeling, regression and stabilization, and generation and maintenance of the blood barrier (Hamilton et al, 2010; Armulik et al, 2011; Korn and Augustin, 2015).

Pericyte also contributes to the blood barrier of the placenta (Demir, 1989; Ohlsson et al., 1999). There is, however, no clear understanding of the specific role of these cells in the placenta, and the effects of pericyte absence or presence on toxic effects maternal and fetal health. Studies in humanized mice with pericyte reduction showed an increase in maternal blood pressure and reduction of fetal weight (Takimoto et al., 1996). Depletion of pericyte platelet derived growth factor receptor beta (PDGFR-β) deficiencies showed system microvascular dysfunction, including the placenta (Levéen et al., 1994; Soriano et al., 1994; Ohlsson et al., 1999). However, the relationship between pericyte depletion, placental abnormalities and fetal microvasculature disorders is still not well understood. Other critical cells that limited this study is that PDGFR-β deficient mice also had a decrease in trophoblast number because of expression of PDGFR-β (Goustin et al., 1985; Ohlsson et al., 1999).

1.4 How is endothelial cells behavior in depletion of pericytes?

Throughout vertebrates, pericytes and endothelial cells have a physical attachment and are continually interconnected to maintain microvascular homeostasis. A disturbance in this interaction is associated with the onset and progression of a variety of pathologic processes (Carmeliet, 2003). A molecule secreted by each cell was capable of directly affecting the metabolism of the other cell. For example, for the blood vessels to properly exercise the physiologic functions, they must be mature (stable endothelial cells and covered by mural cells). To stabilize endothelial cells channels, angiogenic endothelial cells release PDGF-β to chemoattract platelet derived growth factor receptor beta (PDGFR-β) positive pericytes (Hellberger et al., 2010; Gaelgen et al., 2009). The absence of pericytes results in loss of vascular integrity and stability. The depletion of pericyte resulted vessel leakage of toxic substances (such as glutamate in cerebrospinal fluid), vasogenic edema, and microaneurysms (Quaegebeur et al., 2010; Ogura et al., 2017; Nikolakopoulou et al., 2019).

The loss of pericytes in the central nervous system is associated with chronic and acute disorders (Hall et al., 2014). The pericytes are sensitive to changes in tissues, such as hypoxia, and they die easily after strokes (Kisler et al., 2017) or brain trauma (Zehebdner et al., 2018). Besides, massive pericyte absences were reported in Alzheimer's disease (Sweeney et al., 2016). However, the cause of pericytes loos is still unknown, but there are some causes, consequences, and effects of these losses in the nervous system. Also, it is unclear if these cells can be changed to replace them with new ones. Many models for investigating what happens in the nervous system have been developed over the past few years. One model used for specific depletion of pericyte cells is transgenic mice Cre line models for PDGFR-β or NG2 or both (Cuttler et al., 2011; Nikolakopoulou et al., 2019). This model is usually associated with other transgenic mice iDTR mice that selectively express diphtheria toxin receptor (DTR) (Buch et al., 2005) in pericytes. A second important animal model for decreased pericytes in tissue is the application of antibodies against PDGFRβ (anti-PDGFRβ mAb) (Ogura et al., 2017).

The retina is another tissue with lesions due to pericyte loss. According to Tu et al., 2011, retinal vessels, pericyte was essential for homeostasis. Pericyte loss in the retina is associated with diabetic retinopathy, due to resulting in microaneurysms, proliferation of new blood vessels, and hyperpermeability (Cogan et al., 1961). New blood vessels proliferated without being properly oriented to sprout. These are associated with downstream of VEGF signal

(Adamis et al., 2008). In general, all consequences of pericyte loss in retina caused a hypoperfusion and hypoxia, leading to aberrant formation of non-functional blood vessels that directly cause blindness from vitreous hemorrhage and retinal detachment (Antonetti et al., 2012). Diabetic retinopathy is a multifactorial disease mostly caused by blood glucose levels, and high blood pressure (Cogan et al., 1961; Liew et al., 2009; Cheung et al., 2010). Hyperglycemia leads microangiopathy, including microaneurysms, hemorrhages, basement membrane thickening and pericyte loss (Cheung et al., 2010).

Also in retinal tissue, inflammation increase is reported in diabetes (Adamis et al., 2008). Currently, it is unknown what factors induced this leukocyte infiltration and how the absence of pericyte influenced diapedesis. However, endothelial cells without pericyte showed an upregulation in inflammatory and adhesion molecules, such as *Ccl2, Vcam1, Tnfα,* and *Il6* (Ogura et al, 2017).

In tumor progression, angiogenesis is essential to maintain the tumor microenvironment. Defective/absence of pericyte-endothelial cells interaction is one of the major causes of dysfunctional tumor vasculature and hypoxia. This combination of facts favors cancer growth and metastasis (Song et al., 2005). Pericytes play a crucial role in the angiogenesis in the tumor microenviroment, the depletion of pericyte (Ng2+) in cancer model decreased the size of tumor (Birbrair et al., 2014; Picolo et al., 2021) Nevertheless, pericyte abundance and deficiency occur in different types of tumors during vascularization (Wong et al., 2020). Pericytes and endothelial cells can form a “shield” to protect tumor cells from cancer therapy and immune surveillance (Meng et al., 2015). It is difficult to determine the exact function of pericytes in the tumor's environment. However, could be critical cells in tumor progression modulation.

1.5 **Diapedesis**

Leukocyte migration, vascular permeability, and soluble factors are all involved in the inflammation response. Mammals have leukocytes from the bloodstream as a defense mechanism. Nevertheless, this process requires a finely orchestrated cascade of events that

involves a number of molecules from different cells, including leukocytes and endothelial cells. Diapedesis is the term for this coordinated process. It is understood that there are at least three steps in diapedesis, namely rolling, adhesion and transmigration and each step is specifically regulated (Springer, 1994).

The initial step of the inflammation response is a reorganization of endothelial cells' surface to capture floating circulating neutrophils (Lefort and Ley, 2012). An increase in adhesive molecules on endothelial luminal surface was stimulated by tissue inflammatory molecules. Leukocytes bind to selectin (low affinity) molecules on endothelial cells. The first step, "rolling," is characterized by weak and transient adhesive interactions between neutrophils and endothelial surfaces using these molecules (Lefort and Ley, 2012).

Interstitial leukocyte migration occurs due to chemokine gradient. The action of chemokines on the endothelial luminal surface triggers the activation of leukocytes integrins that facilitate adhesion and arrest via interactions with diverse ligand expression endothelial surface. Neutrophils are the earliest lines of defense against invading microorganisms and play a central role in innate immunity and the inflammatory process (Phillipson and Kubes, 2011). Major molecules in the initiation of cell-cell contact between leukocytes and endothelial cells are the Ig-like cell adhesion molecules (CAMs), such as intercellular adhesion molecule-1 (ICAM-1/CD54), ICAM-2/CD102, vascular cell adhesion molecule-1 (VCAM-1/CD106) and platelet endothelial cell adhesion molecule-1 (PECAM-1/CD31) (Timmerman et al., 1988; Schnoor et al., 2015). Firm adhesion is followed by a transmigration process. Furthermore, neutrophils respond to chemokines and undergo a drastic cell rearrange from round to flat and polarized. In blood vessels, neutrophil polarization is essential for them to migrate or crawl along the endothelial lumen surface to reach nearby sites. Once neutrophils pass through the endothelial barrier, the cell must cross the pericyte layer within the venular basal membrane before reaching the inflamed interstitial tissues (Ley et al., 2007; Muller, 2011).

Pericytes are essential components of the wall of microvascular vessels. Directly wrapped around endothelial cells, they are in a strategic position at the interface between circulating blood cells and the interstitial space (Armulik et al., 2005). The role of pericytes in

diapedesis is still unclear. What is known is that pericytes interact directly with neutrophils (Girbl et al., 2018).

Besides, leukocyte diapedesis is commonly observed along specific paths, which is, several leukocytes are leaving through the same area. These specific regions have lower levels of extracellular matrix proteins in the venular basement membrane, such as laminin 8, laminin 10, collagen IV, and nidogen (Wang et al., 2006; Voisin et al., 2010). These specific areas correspond to the gap between the cells (Wang et al., 2006). A total of four neutrophils were observed to have migrated between two pericyte cells and not in the middle of the pericyte body (Voisin et al., 2010). This suggests that pericyte presence and position influences leukocyte diapedesis route. In the sepsis process induced by LPS treatment, pericytes in the microvascular network was found to be essential to prevent vascular leakage and excessive leukocyte recruitment in sepsis (Zheng et al., 2016). In addition, without pericytes, autoimmune neuroinflammation had an increased number of neutrophils infiltration. Pericyte depletion *in vivo* showed an upregulation of ICAM-1 and VCAM-1 in the central nervous system. (Torok et al., 2021).

1.6 **Endothelial cells in the innate immune cells?**

Endothelial cells (ECs) compose blood vessels, such as a single layer of cells called the endothelium. The endothelium exhibits selective permeability. The endothelial cells have many functions, which can be categorized into three main categories: Trophic, tonic, and trafficking. In physiologic conditions, ECs are directly involved in metabolic homeostasis (trophic function), vascular stabilization (tonic functions and vascular permeability), coagulation and cell extravasation (trafficking) (Wilson and Ye, 2014). As part of its role in controlling and regulating coagulation activity (anticoagulation and pro-coagulation mechanisms), ECs express inhibitors and procoagulants, such as factor X and thrombomodulin (Moncada and Vane, 1981). The endothelium layer permeability could happen via two pathways: paracellular and transcellular.

Several classes of receptors can help recognize microorganisms and endogenous molecules released during cell injury, including pattern-recognition receptor (PRR). PRR efficiently recognizes pathogen-associated molecular patterns (PAMPs) and danger-associated molecular patterns (DAMPs). In mammals, there are five families of PRR, including toll-like

receptors (TLRs) and NOD-like receptors (NLRs) are the most characterized (Said-Sadier and Ojcius, 2012). ECs are constantly exposed to circulating factors and pathogenic stimuli, such as Pathogen-associated molecular pattern (PAMPs) and Damage-associated molecular pattern (DAMPs,) which predispose them to damage, and disrupt blood flow and selective barrier function (Campasi and Fagagna, 2007). Inflammation can cause different reactions in the endothelium response. ECs become activated, display increased leakiness, enhanced leukocyte adhesiveness, and pro-coagulant activity, and form new vessels. ECs can express various TLRs (Heidemann et al., 2006), including TLR1, TLR2 (Edfeldt et al., 2002), TLR3 (Tissari et al., 2005), TLR4 (Spitzer et al., 2002), TLR5 (Maser et al., 2005), TLR7, TLR8 (Tissari et al., 2005), and TLR9 (Kebir et al., 2015). Other immune receptors expressed in ECs are NODs (1 and 2). Human endothelial cells infected with *Listeria monocytogenes* can increased production of NOD receptors naturally (Opitz et al., 2009). In addition to their innate immune roles, ECs also participate in the adaptive host immune response. ECs are capable of expressing both MHC I and MHC II class molecules, serving as antigen-presenting cells (APC) (Marelli-berg and Jarmin, 2004).

There was a connection between the anti-inflammatory response of endothelial cells and the anticoagulant state. This happens because both pathways share molecular components. One example is the anticoagulant protein C pathway, composed of thrombomodulin and endothelial protein C receptor (EC membrane surface expression). Protein C is produced in large quantities in the liver. Protein C is anti-coagulation and anti-inflammatory molecule (Dahlback and Villoutreix, 2005). Thrombomodulin directly inhibits leukocyte adhesion to activated endothelium and prevents more ECs activation (Abeyama et al., 2005). Another connection between coagulation and the inflammatory response are protease-activated receptors (PARs). Coagulation leads to the activation of a plethora of proteases, including Xa, VIIa, and IIa (thrombin). The PARs play a role in innate immunity, and regulate vascular tone and permeability, EC proliferation and angiogenesis (Cirino et al., 2003).

1.7 **Pericytes and immunity**

Pericytes can directly respond to inflammatory stimuli, likely LPS, TNF-α, IL-1β, and INF-γ, producing CCL-2, CCL-3, CCL4, CXCL1, CXCL10, CXCL11, IL-6, IL-13, and TNF-α

(Navarro et al., 2016). Other roles in inflammation in response to these strong stimuli include increased vascular permeability due to induction of nitric oxide synthase (iNOS). The generation of nitic oxide acts as a relaxing factor which is responsible for vasodilation. Pericytes stimulated with TNF-α, IL-1β, and IFN-γ promotes upregulation of cyclooxygenase-2 (COX-2) responsible for the production of pro-inflammatory prostaglandins (Navarro et al., 2016).

As a result of stimulation with LPS, pericytes can express and upregulate TLR4 in the lungs (Edelman et al., 2006). That suggests that pericytes can recognize Gram-negative bacteria LPS. However, it still not known how these cells response after the recognition of a pro-inflammatory stimulus that is different of the classical LPS. NOD1 and NOD2 mediate the cytoplasmic recognition of peptidoglycan fragments (Nishio et al., 2011). Pericytes in cell culture can express NOD1 and is functional. However, NOD2 was barely detected (Navarro et al., 2016). A pericyte that expresses PRR in culture suggests that these cells could serve as immune sentinels. However, it is still unknown how these cells modulate immunity in mammals.

Most of the studies describe the pericyte act as a barrier of blood vessels. And the function of these cells in the inflammatory response has been underestimated. Pericytes act as sensors and regulators of inflammatory processes in leukocyte migration (Stark et al., 2013). The recent researchers suggested that pericytes are responsible for inflammation in diseases for chronic inflammation. One example is in mice with peritoneal dialysis, that had a catheter implant showed pericytes with a significantly contributed to peritoneal membrane alterations, fibrosis and new vessel formation. Besides, pericytes directly control neutrophil influx in acute inflammation (Zheng et al., 2016).

1. **Brucellosis**

The number of new cases of brucellosis in humans per year is estimated at 500,000, which is a worldwide spread zoonotic disease. However, this number could be underestimated (Laine et al., 2022). It is causedby Gram-negative, facultative intracellular coccobacilli (Corbel, 2006), which belongs to the α-2 subclass of Proteobacteria (Moreno et al., 2006). In general, α-2 Proteobateria are abundant in diverse environments, terrestrial and marine (Moñoz-Gomes et al.,

2019). Like some other Proteobacteria, *Brucella* spp. have adopted intracellular life styles, making this group of pathogens significant to humans and animals (Moreno et al., 2006).

Brucella spp. can infect various host species (Corbel, 2006). Despite members of the *Brucella* genus having a close genetic relationship (~97% of similarity) (Tsolis, 2002; Suárez-Esquivel et al., 2020), the genus includes six "classical" species, which were named according to their preferred host: *B. abortus* (cattle), *B. melitenis* (goats and sheep), *B. ovis* (sheep), *B. suis* (pigs), *B. canis* (dogs), and *B. neotomae* (desert rats) (Veger et al., 1987; Moreno et al., 2002). Besides the "classical" *Brucella* species, the genus has expanded over the last years with the recognition of novel species (Occhialini et al., 2022), including *B. ceti* (cetaceans) and *B. pinnipedialis* (pinnipeds) (Foster et al., 2007), *B. microti* (common vole), *B. papionis* (baboon) (Whatmore et al., 2014; Whatmore et al., 2015) and *B. vulpis* (red fox) (Scholz et al., 2016). More recently described were *Brucella*-like organisms isolated from amphibians, which have a functional flagellum (Soler-Lloréns et al., 2016; Eisenberg et al., 2017). However, some of the preferred hosts are still unknown, such as *B. inopinata* isolated from one human breast implant (Scholz et al., 2010). One novel species has been characterized in bats in Brazil with *Brucella* sp DNA amplification for bats tissues, and histologic lesions in epipidymis associated immunomarker for *Brucella* sp, associated with lesions. However, we need more studies to determine whether the species is a new species or just another host for an existing species. New *Brucella* species were described in various hosts and niches, illustrating an ongoing expansion.

Brucella spp. utilize a large set of virulence factors to circumvent host defenses. During acute infection, the low immunogenicity of *Brucella*' LPS favors a silent infection. *Brucella* spp. are much less endotoxic than Enterobacteriaceae and protects bacteria against antibacterial peptides, complement-mediated killing, and phagocytosis by macrophages (Allen et al., 1998; Barquero-Calvo et al., 2007). Effector proteins secreted through the *virB* operon-encoded type IV secretion system (T4SS) enable *Brucella* to control vesicle trafficking into the host cell so a replicative niche is established promoting bacterial survival intracellularly (Celli et al., 2003). Furthermore, *Brucella* uses its virulence factors to inhibit cell death to chronically persist within macrophages, apparently alternatively activated (Fernandez-Prada et al., 2003; Xavier et al., 2013; Kerrines et al., 2018).

A variety of cell types can interact with and be invaded by *Brucella* spp. (de Figueiredo et al., 2015) leading to distinct brucellosis manifestations. Brucellosis is primarily related to damage to the reproductive tract in animals, though bacterial tropism in several tissues can trigger different clinical manifestations in humans, such as arthritis and meningitis (Mantur et al., 2007; Olsen and Palmer, 2014). After ingestion, the bacterium crosses the intestinal barrier through invasion of M-cells (Paixão et al., 2009) and spreads throughout the system within macrophages (de Figueiredo et al., 2015). *Brucella* spp. can interact with placental trophoblasts resulting in a big inflammatory reaction. Since a strong inflammatory response is triggered in the placenta (Liu et al., 2019; Byndloss et al., 2019). *In vitro*, *Brucella* invaded and survived within endothelial cells (Ferrero et al., 2011). A recent study suggests that *Brucella* could interact with human brain microvascular endothelial cells, but could not traverse to the central nervous system, unless it was internalized by transmigrating monocytes (Miraglia et al., 2018). These studies highlight that our understanding of the host-pathogen interaction of *Brucella* spp. may largely benefit from studying new cell types and their roles in brucellosis.

2.2 **Brucellosis in human and their natural preferential hosts**

Brucellosis is a contagious infectious zoonosis with worldwide distribution. Pappas et al. (2006) emphasize the importance of meeting the needs of a neglected and reemerging zoonosis. Bovine brucellosis results in significant economic loss (Mcdermottt et al., 2013; Santos et al., 2013), mostly due to abortion, sub-fertility or infertility in herds, and reduction of milk production (Xavier et al., 2009; Carvalho Neta et al., 2010; Poester et al., 2013). The most pathogenic strain of is *B. melitensis*. It estimated that 1 to 10 bacteria can provoke the infection, while *B. abortus* and *B. suis* show intermediary zoonotic potential, and *B. canis* has a lower zoonotic potential. *B. ovis* is not considered pathogenic for humans (Young, 1995; Godfroid, 2005; Xavier et al., 2009 and 2010). *B. neotomae* was also considered apathogenic for humans, however there was evidence of a human infection with *B. neotomae*, which was found in the cerebrospinal fluid of two patients with neurobrucellosis (Suáres-Esquivel et al., 2017). However,

the number of newly reported human cases remains unclear and underestimated (Laine et al,. 2022). In addition, it remains unclear the zoonotic rule of “non-classical” *Brucella* in humans.

Transmission occurs through mucosa contact with contaminated animal secretions, by ingestion or aerosol. The most significant means of transmission for many *Brucella* species in animals is sexual transmission. In *B. ovis,* females can have a significant role in male infection (Brown et al., 1973; Xavier et al., 2010). In cows, sexual role is determinant for spread the bacteria, the infection can occur even through infected semen in use for artificial insemination (Rankin, 1965). For humans, transmission also could be for ingestion or aerosol. The source of infection could be contaminated secretions from the placenta, female ou male genital organs and mammary gland. Ingestion of no pasteurized milk or laboratory or vaccine accidents with live strains may infect humans as well (Young, 1983; Corbel, 1993; Corbel, 2006; Xavier et al., 2009; Carvalho Neta et al., 2010). There is the possibility of venereal transmission in humans (Xavier et al., 2010), although it is considered to be an uncommon mode of transmission.

The clinical manifestation of brucellosis depends on species of host and *Brucella* (Xavier et al., 2009 and 2010), but in general, results in highly relevant economic losses for the animal industry due abortions, sub-fertility or infertility, and reduction of milk production (Mcdermott et al., 2013; Santos et al., 2013). The infection by *B. ovis* causes chronic epididymitis in sheep with decreased fertility (Carvalho Junior et al., 2012) and rarely leads to abortions or neonatal mortalities (Ficapal et al., 1998). Conversely, *B. abortus* and *B. melittensis* cause abortions in cows and rams during the last trimester of pregnancy, weak litter, placenta retention, and necrotizing placentitis (Xavier et al., 2009; Carvalho Neta et al., 2010; Poester et al., 2013). In males, *B. abortus* causes orquitis and epididymitis (Corbel et al., 2006). In dogs, *B. canis* causes high neonatal mortality (Souza et al., 2018). *B. suis* results in a systemic infection in swine, which can also result in a decrease in reproductive index (Poester et al., 2013). In human patients, brucellosis is associated with a chronic and debilitating disease, although the mortality rate is low. Common clinical symptoms in acute phase are intermittent or undulating fever and fatigue. In chronic phase of infection is common to see osteomyelitis, arthritis, spondylitis, endocarditis and neurobrucellosis (Lubani et al., 1986; Corbel, 2006; Franc et al., 2018; Cross et al., 2019).

In humans with nervous system involvement, neurobrucellosis occurs in 5-10% of cases. However, it has been estimated up to 30% depending on the cohort studied. There is a rare but important manifestation of this illness (Gul et al., 2008; Yetkin et al., 2006; Guven et al., 2013). The species of *Brucella* that most commonly causes neurobrucellosis is *B. melitensis*, but cases have also been associated with *B. suis, B. abortus, B. neotomae, B. pinnepidialis* and *B. ceti* infections (Wallach et al., 2002; Sohn et al., 2003; Villalobos-Vindas et al., 2017). There has been no report of neurobrucellosis in natural hosts such as cattle, goats, sheep, pigs or dogs. It is important to note, however, that neurobrucellosis in cetaceans is an important and common manifestation associated with *B. ceti* infection (Guzman-Verri et al., 2012). Non-human primates may develop neurobrucellosis after exposure to *Brucella* (Grilló et al., 2012, Lee et al., 2013), but mice do not develop neurobrucellosis (Grilló et al., 2012).

Neurobrucellosis in human manifests with symptoms that are due to inflammatory changes, and it is the most severe clinical manifestation of brucellosis. When the nervous system is damaged, multiple symptoms may appear. The cerebrospinal fluid exhibited high protein contents, low glucose levels, and leukocytosis, primarily lymphocytes (Pappas et al., 2005). It is also a significant disease that might have been the cause of chronic and severe headaches, fever, photophobia and vomiting (Bouza et al., 1987; Young, 1995). Less frequent symptoms are nuchal rigidity, focal motor, sensitive and sensory syndromes, mainly with visual impairment and psychiatric manifestations such as depression, amnesia, and psychosis (Bouza et al., 1987; Young, 1989). Encephalitis and myelitis are both due to the direct presence of the bacterium in the cerebral tissue and the spinal cord (Mclean et al., 1992).

Affected cetaceans develop opisthotonos, tremors, seizures, disorientation, and a general inability to buoyancy. Pathological gross findings are not specific and consist of hiperemic meninges and brains, as well as an increase in cerebrospinal fluid volume and cellularity. Generally, cetaceans presente nonsuppurative meningoencephalitis, characterized by infiltration of lymphocytes, plasma cells, and macrophages (Gonzalez et al., 2002). It is possible to find bacteria into the neuvous tissue lesion and the cerebrospinal fluid (Foster et al., 2002; González et al., 2002; Munoz et al., 2006; Jauniaux et al., 2010).

2.3 Mouse model tissue tropism

Preferential host experimental infection of small ruminants and cows can be used to understand brucellosis. However, studies on preferential hosts can be challenging and is not economically viable, as well as ethically problematic. To test vaccines against brucellosis, mice models were introduced in 1911. After a few decades, mice were used for diagnostic purposes to identify *Brucella* pathogenic strains (Grilló et al., 2012). Mice infection depends on *Brucella* species, dose and mode of infection, and on the mouse strain (Enright et al., 1990; Baldwin and Parent, 2002; Ko and Splinter, 2003; Silva et al., 2010; Grilló et al., 2012; Carvalho et al., 2016). In the last decade, the mouse model has been extensively used as a model, providing a significant contribution to several aspects of brucellosis including immunology, host-pathogen interactions, pathogenesis and vaccinology (Silva et al., 2011; Grilló, 2012; Carvalho et al., 2016).

Aside from infections in natural hosts and experimental infections of small ruminants (Anderson et al., 1986; Meador and Deyoe, 1986), there is information available about *Brucella* spp. emerged from experimental models such as the mouse (Young et al., 1979; Bosseray, 1980; Tobias et al 1993) and guinea pigs (Braude, 1951; Hensel et al., 2022). Particularly the mouse has been extensively used as an animal model for *Brucella* spp. contributing significantly to several aspects of brucellosis, including immunology, host-pathogen interactions, pathogenesis, and vaccination (Silva et al., 2011; Grilló et al., 2012; Carvalho et al., 2016). The mouse model became even more relevant due to technical difficulties such as biocontainment needs, for experimental infections in natural hosts. There are a variety of routes by which mice may be challenged, including oral, intragastric, intraperitoneal, intravenous, or intratracheal. Bacteria may be recovered from the spleen and liver after a period of one to seven days (Paixão et al., 2009; Grilló et al., 2012; Silva et al., 2011; Silva et al., 2015; Carvalho et al., 2016). Interestingly, *B. melitensis* can cause systemic infection in mice after intragastric inoculation without causing any intestinal lesion or inflammation in the intestinal mucosa. There is evidence that M-cells are specifically targeted by *B. melitensis* to cross the intestinal epithelial layer (Paixão et al., 2009). The findings of the mouse model are similar to those described in cattle that have been infected with *B. abortus* (Ackermann et al., 1998).

Brucella-infected mice exhibit areas with inflammatory infiltrates composed of neutrophils during the early stages of infection (first 3 to 4 days after infection). In the chronic stages of infection, macrophages and epithelioid macrophages form microgranulomas, forming an inflammatory infiltrate primarily containing macrophages. *Brucella* can be detected in phagocytic cells, especially macrophages (Silva et al., 2011; Grilló et al., 2012; Carvalho et al., 2016). In the spleen of *Brucella*-infected mice, there is an increase in organ size and weight associated with inflammation reaction (splenitis). At approximately 7-10 days post infection, the number of intracellular *Brucella* spp. in macrophages reaches its peak (Silva et al., 2011; Grilló et al., 2012). Another tissue investigated and considered critical for *Brucella* persistence is the bone marrow. Persistence of *B. abortus* or *B. canis* has been demonstrated in mice bone marrow, coinciding with the chronicity of the disease in this animal model (Chacón-Diaz et al., 2015; Gutiérrez-Jiménez et al., 2018). In mice infected with *B. abortus*, histopathological changes in the bone marrow include granulomas and an increase in multipotent progenitor and active hematopoietic stem cells, neutrophils, and CD4+ T lymphocytes. The three types of cells infected in bone marrow with *B. abortus* 2308 expressing red fluorescent protein were monocytes, neutrophils, and granulocyte-macrophage progenitors (GMP). At 8 days post infection, the proportion of neutrophils containing bacteria was greater than other cells, but significantly decreased after 30 days. Interestingly, *B. abortus* resists killing by neutrophils, induces premature death of these cells and *B. abortus*-infected neutrophils display phosphatidylserine on their cell membrane, which favors phagocytosis of infected neutrophils by macrophages. Therefore, apparently *B. abortus* adopts a "Trojan horse'' strategy by using infected neutrophils as vehicles for the dispersion throughout the host mononuclear phagocytic system (Gutiérrez-Jiménez et al., 2018; Gutiérrez-Jiménez et al., 2019).

In chronic brucellosis in cattle and camels in showed hygromas are often caused by *Brucella* (Omer et al., 2010). Furthermore, humans suffering from brucellosis frequently display symptoms of osteoarticular complications in chronic phases (Corbel, 2006). Bioluminescent *B. melitensis* was used in mouse models to identify bacteria dissemination to osteoarticular tissues. In mice, the skeletal complications also occurs during the chronic phase of infection. In 26 weeks after infection, the bacteria provoked massive infiltration of inflammatory cells in synovial joints of hind paws, with pannus and bone lesions (Magnani et al., 2013). Mice models of arthritis, and

probably in natural hosts, demonstrate that CXCR2 is involved in arthritis. *Knockout* mice for CXCR2 showed a marked reduction in bacteria levels in joints. Perhaps one complementary treatment for human osteoarthritis provoked by *Brucella* is blocking CXCR2 (Lacey et al., 2016).

Brucella has a preference for the reproductive tract of domestic animals. Considering that male genital tract is also affected in brucellosis, Izadjoo et al. (Izadjoo et al., 2008) developed a male mouse model to study *Brucella*'s genitourinary pathogenesis. Testis, epididymis, or both were infected in 13 of 57 animals (22.8%) inoculated with *B. melitensis* strain 16M, with histiocytic inflammation in the testicular peri-arterial tissue and the superficial lymph nodes. *B. ovis*, which causes lesions primarily in the male genital system of sheep (Carvalho Júnior et al., 2012), is capable of infecting mice in which it induces systemic lesions that are similar to those induced by other *Brucella* species in the mouse, but it does not consistently result in lesions in the genital system (Silva et al., 2011), indicating that in this particular case the mouse is a suitable model for infection, but not necessarily a model for the disease or tissue tropism.

The placenta is a complex and transient structure in mammalians' pregnant uteri. It might be morphologically classified into various categories. The mouse placenta is hemochorial and discoid. This is quite distinct from the placenta of domestic ruminants, which are highly susceptible to *Brucella*-induced abortion and have synepitheliochorial and cotyledonary placentas (Poester et al., 2013; Roberts et al., 2016). Despite these morphologic differences, pregnant mice have been employed as a model for *Brucella*-induced placentitis and fetal loss (Tobias et al., 1993; Kim et al., 2005; Byndloss et al., 2019; Tsai et al., 2022; Braz et al., 2022; Poveda- Urkixo et al., 2022). *B. abortus* colonizes and persists in pregnant mice's placenta and uterus. In the mouse placenta, *B. abortus* infects trophoblastic giant cells localized mostly in the periphery of the placenta. However, it may also be found extracellularly, particularly in association with necrosis. Histologically, infected placentas develop marked necrosis and mild neutrophil infiltration in spongiotrophoblastic zone extending into the decidua basalis (Tobias et al., 1993). At the junctional zone of the infected placenta, trophoblastic giant cells may have dark blue and granular cytoplasm. This is because of intracellular bacteria. *Brucella* may also exist in the spongiotrophoblast, endodermal cells of the visceral yolk sac adjacent to Reichert's membrane remnants. Considering the importance of placentitis and abortion in natural hosts (Moreno et al., 2006; Poester et al., 2013) and the lack of mechanistic studies in these species, the mouse model

significantly contributed to the identification of pathogen and host mechanisms involved in *B. abortus*-induced placentitis. Indeed, in the mouse, the effector *Brucella* protein VceC triggers the endoplasmic reticulum (ER) stress response (Byndloss et al., 2019), which is linked to inflammation in *B. abortus*-infected placenta (Keestra-Gounder et al., 2016). This results in trophoblast cell death, inflammation, and fetal loss (Byndloss et al., 2019). VceC-triggered ER stress response is also associated with the induction of tumor necrosis factor alpha (TNF-α), which is associated with placentitis and fetal loss (Tsai et al., 2022). Interestingly, smooth *Brucella* species may have variable pathogenic potential for causing placentitis in pregnant mice, with *B. melitensis* displaying a more intense placental tropism when compared to *B. suis* biovar 2 (Poveda-Urkixo et al., 2022). However, *B. ovis* that is primarily associated with epididymitis in rams (Carvalho junior et al., 2012) is also capable of inducing placentitis and fetal loss in pregnant mice (Braz et al., 2022). Interestingly, non-pregnant uteruses from experimentally infected mice yields markedly lower numbers of *B. abortus* per gram of tissue (Rossetti et al., 2012) than placentas (Salcedo et al., 2013), demonstrating the tropism for the placenta in the pregnant uterus in this model (Tobias et al., 1993). Based on the original studies on "classical" *Brucella* species, a dogma has been established regarding *Brucella* tissue and cell tropisms. The fact that *Brucella* spp. are associated with so many different host species (i.e. brucellosis is not one disease), solid knowledge in this field indicates that *Brucella* spp. stealthily shelters in phagocytic cells in organs of the reticuloendothelial system or monocyte phagocyte system, particularly spleen, liver, bone marrow, and lymph nodes, with a particular tropism for genital organs, specially the placenta in females or epididymis and sexual glands in males (Figure 1.3). However, studies have shown that *Brucella* is capable of infecting and multiplying in a wide variety of cell types cultured during the growth period (Supplementary Table 1).

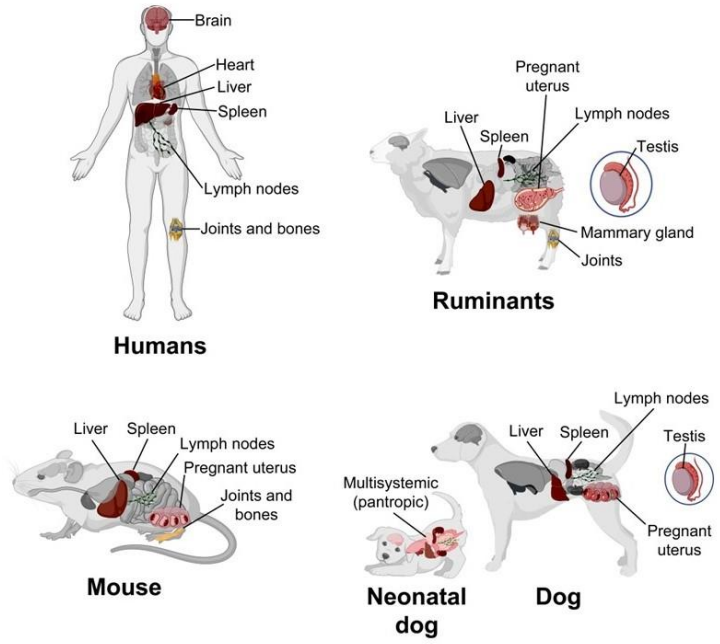

Figure 1.3 Most important target organs in various host species for *Brucella* spp. Target organs and tissues for *Brucella* spp. in natural host (ruminants and dogs), human (as a zoonotic target) and the most used laboratory model (mouse). The organs the are identified and paint showed the distribuction of the pathogen in the host. Created with BioRender.com.

Early studies also evaluated *B. abortus* ability to infect various cultured host cell types (Richardson, 1959). Cell lines were then used as models, not just for evaluating tropism, but to investigate *Brucella* spp. intracellular traffic (Detilleux et al., 1990). *In vitro* studies have verified a large spectrum of susceptible cells to *Brucella* spp. Infection and survival, enhancing knowledge about intracellular pathways, pathogenesis and bringing new insights to control strategies.

It is well known that *Brucella* spp. are rather driven to infect professional phagocytes, including macrophages (Celli, 2006), dendritic cells (Salcedo et al., 2008), monocytes and neutrophils (Barquero-Calvo et al., 2015; Demars et al., 2019). However, *Brucella* survival in different cells has been demonstrated since decade. The importance of these other cells in the maintenance and pathogenesis of bacteria is still unclear. It has been established that *Brucella* can

survive and multiply in placental trophoblasts (Meador et al., 1989). Also, *in vivo* evidence of survival is in erythrocytes, epithelial cells (Souza et al., 2018), fibroblasts, myeloid cells (Demar et al., 2019) and lymphocytes (Goenka et al., 2012).

It is well known that monocytes/macrophages are the main target of *Brucella* infection (Celli, 2006; González-Espinoza et al., 2021), but what else would direct *Brucella* into these cells? In a study with *B. abortus,* it showed that bacteria can directly bind, invade and modulate functional responses in human platelets culture. Additionally, the same study using human monocyte cell line (THP-1) and purified human monocytes from peripheral blood infected showed that platelets increased the number of infected monocytes. Surprisingly, the plates were responsible for the delivery of *Brucella* to monocytes (Trotta et al., 2018). In fact, *B. abortus* establishes platelets-leucocytes complexes mainly with monocytes and PMNs (Trotta et al., 2020) enhancing infection effectiveness and interacting in their functions. It is possible, for example, that infected monocytes have passed through human brain microvascular endothelial cells (HBMEC) culture as a "Trojan horse" (Miraglia et al., 2018).

Bacterial interactions with the intracellular environment have been investigated by *in vitro* infection of macrophages. The multiplicity of infections of macrophages with *Brucella* spp. ranges from 1:1 to 1:1000, including experiments with immortalized cell lines or primary macrophages (Celli et al., 2003; Barqueiro-Calvo et al., 2007; Billard et al, 2007; Delpino et al., 2009; Silva et al., 2011; Gorvel et al., 2014; Ferreiro et al., 2014; Chacon-Diaz et al, 2015; Fernandez et al., 2017, Park et al. 2021). Those types of infections demonstrated that *Brucella* spp. have a preferred intracellular niche and allowed the identification of many *Brucella* virulence factors (Celli et al., 2003; Barqueiro-Calvo et al., 2007; Billard et al., 2007; Delpino et al., 2009; Silva et al., 2011; Gorvel et al., 2014; Ferreiro et al., 2014; Chacon-Diaz et a.l, 2015; Fernandez et al., 2017, Park et al. 2021). Also, this model is useful for assessing bacterial ability to invade, survive, and multiply.

Polymorphonuclear (PMN) neutrophils are also susceptible to *in vivo* or *in vitro* *Brucella* infections. In the intracellular environment of PMN, the bacteria can invade and survive. Usually, when PMN recognize PAMPs of Gram-negative bacteria, they become intensely activated (Colotta et al., 1992). However, *Brucella* resists the hostile intracellular environment of

PMNs, and induces cell death without bacterial replication (Braude et al.,1951b; Ackermann et al., 2005). Why *Brucella* induces a different reaction in PMNs remains unclear. Apoptotic PMNs showed signs to be removed by phagocytic cells, such as macrophages (Laskay et al., 2003). Using this mechanism, the bacterium can spread to other organs while avoiding the innate immune system (Barquero-Calvo et al., 2007; Barquero-Calvo et al., 2015). More studies about the PMNs answer to *Brucella* are essential to understand what happens in the early stages of infections. In addition, they help understand how the bacterium and PMNs interaction helps spread *Brucella* to different host tissues.

Other important culture assay was infection of human trophoblast. Different species of *Brucella* can invade, survivel and multiply in these cells. Infections of these cells did not disturb the production of human chorionic gonadotrophins. In this model, *Brucella* avoid the lysosomal vacuole fusion likely in other cells infections (Salcedo et al., 2013; Garcia-Mendez et al., 2019). This showed a promising too for future investigations of interaction of these cells and bacteria in a controlled environment. However, the studies of *in vitro* infection are limited in human cells line, that exposed a need to investigate what happen in trophoblast from other other hosts.

There have been many different *in vitro* studies that did not constrain professional phagocytic cells. In non-Phagocytic cells infected with *Brucella*, the bacterium can invade, survive and multiply. However, it is not possible to truly understand the true contribution of some cells in the microenvironment of infection *in vivo*. One of the non-phagocytic cells most commonly used to study the *Brucella* intracellular cycle are HeLa cells (Hallimg et al., 1991; Pizarro-Cerda et al., 1998; Guzman-Verri et al., 2001; Rosseti et al., 2012) and endothelial cells (Ferrero et al., 2011; Miraglia et al., 2018). Thus, *B. abortus* seems to skillfully modulate endothelial cells (HMBEC) to allow infection in brain systems, leading to neurobrucellosis. This modulation was enhanced when platelets infected with *B. abortus* activated endothelial cells. This way, endothelial cells increased the transmigration of monocytes and neutrophils (Trotta et al., 2020).

Viglietti et al. (2018) have demonstrated that *B. abortus* active autophagosome-lysosome fusion in infected osteoblast cell line (MC3T3-E1), allows their replication within these vacuoles and also *Brucella* has shown inhibition of deposition of bone matrix by osteoblasts at

the same time that induct matrix metalloproteases-2 secretion which can explain, for instance, the bone loss in human brucellosis with arthritis or discospondylitis. In another study using adipocytes differentiated from fibroblast cell line (3T3-L1), *B. abortus* has showed capacity to replicate in adipocytes and driving proinflammatory cytokines, mainly TNF-α and *Brucella* lipoproteins modulating adipogenesis, opening new questions about the role of adipose tissue in chronic infection (Viglietti et la., 2020).

2.5 Mechanisms of *Brucella* spp. envasion of innate immune response

Brucella spp. avoid or interfere with host innate response, which allows bacterial survival and colonization of various tissues of the host. In comparison to some Gram-negative microbes, such as *Escherichia coli* and *Salmonella enterica*, LPS of *Brucella* spp, which is mostly lipid A, induce low and delayed the inflammatory response in infected hosts (Lapaque et al., 2002). TLR4 is activated by *Brucella* LPS at high concentrations. The *Brucella* LPS portion O chain forms complexes with MHC class II and interferes with the binding in the cells and bacteria in *Brucella*-infected leukocytes (Barquero-Calvo et al., 2007). In addiction LPS of rough *Brucella* spp., also confers elevated resistance to cationic bactericidal peptides of the host complement system (Moren et al., 1981; Freer et al., 1996; Moren et al., 1981).

In the intracellular environment, *Brucella* uses a type IV secretion system (T4SS) to modulate intracellular trafficking through the secretion of effector proteins across host cell membranes into the cytosol (Paschos et al., 2011; Smith et al., 2012). *Brucella* spp. also produce periplasmic cyclic β-1,2-glucan that inhibits phagosome fusion with lysosomes in host cells (Arellano-Reynoso et al., 2005). However, the remaining 10% of bacteria evade host killing mechanisms (Boschiroli et al., 2002). BtpA and BtpB are proteins, that share homology with the eukaryotic Toll/Interleukin-1 receptor (TIR), secreted in the host cytosol, that down-modulate innate immune signaling (Salcedo et al., 2008). TIR domain interaction play a crucial role in activating conserved cellular signal transduction pathways in response to pathogens signals.

These way bacterial TIR proteins interfere with host TLR defense signalling by molecular mimicry (Rana et al., 2013).

The T4SS is a virulence factor present in *Brucella* spp., encoded by the *virB* operon. T4SS plays significant roles in mediating intracellular survival and manipulating the host immune response to infection through the excretion of effector proteins (Celli et al., 2003; Lacerda et al., 2013; Ke et al., 2015). The deletions of various genes within the *virB* operon, or transposons in different *virB* genes, changed *Brucella* spp. that it is unable to convert eBCVs into rBCVs and replicate intracellularly (Comerci et al., 2001; Celli et al., 2003; Celli et al., 2005). Also, an attenuated profile in the murine models of infection, with decreased of *Brucella* systemic colonization (Grillo et al., 2012). T4SS is a system that delivers effector proteins across biological membranes, and it is essential for bacterial intracellular cycle (Juhas et al., 2008; Green and Mescas, 2016).

3.0 Listeriosis

Listeria genus contains a total of 21 species, but few species can cause diseases. *L. monocytogenes* is known as a pathogenic species. *L. monocytogenes* is a Gram-positive intracellular foodborne bacterial pathogen. *L. monocytogenes* may cause gastroenteritis or several manifestations including central nervous system disorders, miscarriage and even death in human patients (Lamond and Freita, 2018; Schlech, 2019; Quereda et al., 2020). CDC estimates that *L. monocytogenes* causes about 1600 illnesses and 260 deaths in the US every year (CDC, 2023).

Listeriosis outbreaks have been linked to unpasteurized milk, milk products, meat, sea products or ready-to-eat food. In ultraprocessed food *L. monocytogenes* is associated to contamination of the equipment, and even forming biofimls (CDC, 2023). As a result of the presence and/or persistence of *L. monocytogenes* pathogens on farms, products containing *L. monocytogenes* may be contaminated before or during processing (Hellstrom et al., 2008; Oevermann et al., 2010; Queiroz et al., 2018). Listeriosis occurs sporadically in cattle, sheep, and

goats, and can also occur in pigs, dogs, cats and some wild animals (Ramaswany et al., 2007; Voetsch et al., 2007). As a result of the isolation of water, soil, and feed from the farm environment and surrounding environment, a variety of contamination sources for the animals were identified (Mohamed et al., 2009; Castro et al., 2018). *L. monocytogenes* infects ruminants and may lead to significant economic losses. The typical manifestations of listeriosis in cattle and small ruminants are gastroenteritis, neurological disease, septicemia and abortions/natimortality. In these animals, infection is also through food, such as silage consumption, as well as through the placenta or contaminated milk (Hellstrom et al., 2008; Oevermann et al., 2010; Queiroz et al., 2018; Whitman et al., 2020). *L. monocytogenes* multiplies abundantly in poorly acidified silage, which is the most common source of infection for ruminants. It was found that ruminants fed high amounts of contaminated silage excreted more bacteria in their feces, and they were more likely to develop clinical diseases (Felon et al., 1986; Felon et al., 1996).

Neurolisteriosis is associated with meningitis, meningoencephalitis and rhombencephalitis (Disson et al., 2012). In human, the more frequent manifestation is menigoencephalitis, while ruminants show only rhombencephalitis. In materno-fetal *L. monocytogenes* manifestations include amniotic inflammation (amnionitis), preterm labor, stillbirths, and spontaneous abortions. A newborn may exhibit microabcesses, granulomatosis, and necrosis, especially in the liver and spleen (Bagatella et al., 2021). *L. monocytogenes* infections most commonly cause septicemia in humans, as well as ruminants, which may develop fever, diarrhea, and multi-organ failure. Although clinically evident, septicemia is uncommon in adult ruminants (Charlie et al., 2017; Bagatella et al., 2021). Abortions in ruminants typically occur during the last trimester of pregnancy, either sporadically or in outbreaks (Bagatella et al., 2021). Importantly, *L. monocytogenes* may also be excreted by healthy ruminants (Nightingale et al., 2004; Ho et al., 2007; Esteban et al., 2009) so farm animals play an important role in the disease cycle.

In ruminants, *L. monocytogenes* enteric colonization is associated with prolonged fecal shedding in asymptomatic animals. However, listeriosis is associated with acute enteritis in sheep and cattle of various ages. The symptoms of the disease in animals are lethargy, anorexia, hyperthermia, and diarrhea. Occasionally, *L. monocytogenes* can cause abomasitis, characterized by multifocal neutrophil infiltrations. The mesenteric lymph nodes can be colonized by *L.*

monocytogenes resulting in a fibrinosuppurative lymphadenitis. Mastitis is a specific clinical manifestation of ruminants, ranging from subclinical chronic interstitial inflammation to severe suppurative inflammation (Bagatella et al., 2021). The route of infection for the mammary tissues may be direct or indirect, in the direct route *L. monocytogenes* invades through the teat canal, whereas the indirect route is through the blood stream (Gitter et al., 1980; Wesley et al., 1989).

L. monocytogenes has a complex life cycle that allows bacteria to spread systemically and evade humoral immunity. *L. monocytogenes* expresses PrfA (positive regulatory factor A), which initiates the transcriptional switch from saprophytic (extra-host environment, such as food and environment) to intra-host adapted. PrfA is thermo-regulated and becomes more efficient at human and other mammalian body temperatures (37°C) (Vazquez-Boland et al., 2001). Bacteria are internalized into cells and are initially located within vacuoles (phagosomes). PrfA induces transcription of other virulence factors essential to the intracellular cycle, mostly present on *Listeria* pathogenicity island (LIPI-1), such as *hly* (LLO), *actA, plcA, plcB,* and *mlp,* essential for the intracellular infection cycle (Kreft et al., 2001; de las Heras et al., 2011; Vasanthakrishnan et al., 2015). *L. monocytogenes* can invade both phagocytes and non-phagocytic cells. The process by which invaders enter phagocytic cells is known as phagocytosis. Conversely, *L. monocytogenes* is internalized into non-phagocytic cells through a process called receptor-mediated endocytosis mediated by two *L. monocytogenes* virulence factors: internalin A and B (InIA and InIB). InIA and InIB bind to membrane receptors of the host cells. InIA binds to E-cadherin and InIB to Met,gC1QR and proteoglycans (Bierne and Cossart, 2007). After 30 minutes of internalization, the *L. monocytogenes*-containing phagossomes start pore-forming due to the action of another bacterial protein named listeriolisin O (LLO) and the phospholipases PlcA and PlcB (Radoshevich and Cossart, 2018). After phagossome lysis, bacteria are transported into the cytosol, where *L. monocytogenes* replicate exponentially. Cytosolic *L. monocytogenes* use a bacterial surface protein (Act A) to stimulate the polymerization of host actin monomers into filaments (Radoshevich and Cossart, 2018; Dowd et al, 2020). The actin of host cells propels *L. monocytogenes* through the cytoplasm to the cell periphery. As a result of these modifications, bacteria are more likely to be engulfed by neighboring cells (Dow et al., 2020). This engulfment process results in the bacteria in double-membranous vacuoles, from which they escape due to the action of LLO and phospholipases (Radoshevich and Cossart, 2018).

Intragastric infection with *L. monocytogenes* (infectious dose of 10^9-10^{11} CFU) mimics an oral infection in mice, which is relatively inefficient, with low system colonization. Intravenous or intraperitoneal inoculations result in a fast systemic spread and colonization so it may result in mortality (Ghanem et al., 2014). However, the IP and IV completely bypass the initial gut phase of infection (Disson et al., 2009). InlA is incompatible with mice E-cadherin (Lecuit et al., 1999). For trying to adapt the murine model infected with oral transmission, two different humanized mouse lines were created. One of these mice is a transgenic mouse that expresses human E-cadherin selectively in enterocytes of the small intestine (Disson et al., 2008) and the other mouse has the E16P mutation that allows for InlA-mediated uptake in all E-cadherin-expressing cells (Jones et al., 2015).

The spleen and liver are colonized by *L. monocytogenes* in a mouse model of oral or IV infection. After a period of time during which exponential replication occurs systemically. The gall bladder functions as a reservoir tissue for extracellular replication (Hardy et al., 2018). At 24 hours after IV infection *L. monocytogenes* reaches the bone marrow (Hardy et al., 2009), but not when infection occurs through the oral route (Hardy et al., 2009; Jones et al., 2017). In the mouse model the nervous system tissues in susceptible BALB/c mice after five days post infection with contaminated food (Bou et al., 2012). In CD1 mice infected multiple times, there was 7-10 days of brain colonization per *L. monocytogenes* after infection (Altira et al., 1999). Contrary to this, IV infection generally does not result in brain dissemination, with the exception of high doses of infection (Berche, 1995).

References

ABBOTT, N. J.; PATABENDIGE, A. A. K.; DOLMAN, D. E. M.; et al. Structure and function of the blood–brain barrier. **Neurobiol. Dis.,** v.37, p.13–25, 2010.

ABEYAMA, K.; STERN, D. M.; ITO, Y.; et al. The N-terminal domain of thrombomodulin sequesters high-mobility group-B1 protein, a novel antiinflammatory mechanism. **J. Clin. Invest.,** v.115, n.5, p.1267–1274, 2005.

ACKERMANN, M.R.; CHEVILLE, N.F.; DEYEOE, B.L. Bovine ileal dome lymphoepithelial cell: endocytosis and transport of *Brucella abortus* strain 19. **Vet. Pathol.**, v.25, p. 28–35, 1988.

ADAMIS, A. P.; BERMAN, A. J. Immunological mechanisms in the pathogenesis of diabetic retinopathy. **Semin Immunophatol.**, v.30, n.2, p. 65–84, 2008.

ALEXANDER, B.; SCHNURRENBERGER, P.R.; BROWN, R.R. Numbers of *Brucella abortus* in the placenta, umbilicus and fetal fluid of two naturally infected cows. **Vet. Rec.**, v.108, p.500, 1981.

ALLEN, C.A.; ADAMS, L.G.; FICHT, T.A. Transposon-derived *Brucella abortus* rough mutants are attenuated and exhibit reduced intracellular survival. **Infect. Immun.**, v.66, p.1008–1016, 1998.

ANDERSON, J.D.; SMITH, H. The metabolism of erythritol by *Brucella abortus*. **J. Gen. Microbiol.**, v.38, p.109–124, 1965.

ANDERSON, T.D.; CHEVILLE, N.F.; MEADOR ,V.P. Pathogenesis of placentitis in the goat inoculated with *Brucella abortus*. II. Ultrastructural studies. **Vet. Pathol.**, v.23, p. 227–239, 1986.

ANTONETTI, D. A.; KLEIN, R.; GARDNER, T. W. Diabetic retinopathy. **N. Engl. J. Med.,** v. 366, n.13, p. 1227-1239, 2012.

ARMULIK, A.; ABRAMSSON, A.; BETSHOLTZ, C. Endothelial/pericyte interactions. **Circ. Res.**, v.97, n.6, p.512–523, 2005.

ARMULIK, A.; GENOVE, G.; BETSHOLTZ, C. Pericytes: developmental, physiological, and pathological perspectives, problems, and promises. **Dev. Cell.**, v.21, p.193–215, 2011.

ARRIOLA BENITEZ, P. C.; PESCE VIGLIETTI, A. I.; ELIZALDE, M. M.; et al. Hepatic stellate cells and hepatocytes as liver antigen-presenting cells during *B. abortus* infection. **Pathogens**, v.9, n.7, p.527, 2020.

ARRIOLA BENITEZ, P. C.; PESCE VIGLIETTI, A. I.; HERRMANN, C. K.; et al. *Brucella abortus* promotes a fibrotic phenotype in hepatic stellate cells, with concomitant activation of the autophagy pathway. **Infect. Immun.**, v.86, n.1, p.e00522-17, 2017.

ARRIOLA BENITEZ, P. C.; SCIAN, R.; COMERCI, D. J.; et al. *Brucella abortus* induces collagen deposition and MMP-9 down-modulation in hepatic stellate cells via TGF-β1 production. **Am. J. Pathol.,** v.183, n.6, p.1918–1927, 2013.

ARRIOLA BENITEZ, P.C.; PESCE VIGLIETTI, A.I.; ELIZALDE, M.M.; et al. Hepatic Stellate Cells and Hepatocytes as Liver Antigen-Presenting Cells during *B. abortus* Infection. **Pathogens**, v.9, n.7,p.527, 2020.

ATTWELL, D.; MISHRA, A.; HALL, C. N.; et al. What is a pericyte? **J. Cereb. Blood. Flow. Metab.**, v.36, n. 2, 2016.

AYLOO, S.; GU, C. Transcytosis at the blood–brain barrier. **Curr. Opin. Neurobiol.**, v. 57, p. 32-38, 2019.

BALABANOV, R.; DORE-DUFFY, P. Role of the CNS microvascular pericyte in the blood-brain barrier. **J. Neurosci. Res.**, v.53, n.6, p. 637-644, 1998.

BARBIER, T.; MACHELART, A.; ZÚÑIGA-RIPA, A.; et al. Erythritol Availability in bovine, murine and human models highlights a potential role for the host aldose reductase during *Brucella* infection. **Front. Microbiol.**, 8, 1088, 2017.

BARQUEIRO-CALVO, E.; CHAVES-OLARTE, E.; WEISS, D. S.; et al. *Brucella abortus* used a stealthy strategy to avoid activation of the innate immune system during the onset of infection. **PloS One,** v. 2, n.7, pe631, 2007.

Barquero-Calvo, E., Mora-Cartín, R., Arce-Gorvel, V., et al. *Brucella abortus* induces the premature death of human neutrophils through the action of its lipopolysaccharide**. PLoS Pathog,** v.11, p.e1004853, 2015.

BARQUERO-CALVO, E.; CHAVES-OLARTE, E.; WEISS, D. S.; et al. *Brucella abortus* uses a stealthy strategy to avoid activation of the innate immune system during the onset of infection. **PloS one**, v.2, n.7, p.e631, 2007.

BERTHIAUME, A. A.; GRANT, R. I.,; MCDOWELL, K. P.; et al. Dynamic Remodeling of Pericytes *In Vivo* Maintains Capillary Coverage in the Adult Mouse Brain. **Cell Rep.**, v.22, n.1, p. 8-16, 2018.

BIALER, M. G.; FERRERO, M. C.; DELPINO, M. V.; et al. Adhesive Functions or Pseudogenization of Type Va Autotransporters in *Brucella* Species. **Front. Cell. Infec. Microbiol.**, v.11, p.607610, 2021.

BIRBRAIR, A. Stem cells heterogeneity-Novel concepts. **Springer,** v.13, p.1-3, 2019.

BIRBRAIR, A.; ZHANG, T.; ZHONG-MIN, W.; et al. Type-2 pericytes participate in the normal and tumoral angiogenesis. **Stem Cells Physiology Pathophysiology,** v.4, p.30-35, 2014.

BILLARD, E.; DORNAND, J.; GROSS, A. Interaction of *Brucella suis* and *Brucella abortus* rough strains with human dendritic cells. **Infect. Immun.**, v.75, n.12, p. 5916–5923, 2007.

BLASCO, J.M.; MOLINA-FLORES, B. Control and eradication of *Brucella melitensis* infection in sheep and goats. **Vet. Clin. North Am. Food Anim**., v.27, p.95–104, 2011.

BOSSERAY, N., 1980. Colonization of mouse placentas by *Brucella abortus* inoculated during pregnancy. **Br. J. Exp. Pathol**., v.61, p.361–368, 1980.

BRANDT, M. M.; VAN DIJK, C. G. M.; MARINGANTI, R.; et al. Transcriptome analysis reveals microvascular endothelial cell-dependent pericyte differentiation.**Sci. Rep.**, v.9, p. 15586, 2019.

BRAUDE, A.I. Studies in the pathology and pathogenesis of experimental brucellosis. I. A comparison of the pathogenicity of *Brucella abortus*, *Brucella melitensis*, and *Brucella suis* for guinea pigs. **J. Infect. Dis**. v.89, p. 76–86, 1951.

BRAZ, H.; SILVA, M.F.; CARVALHO, T.P.; et al. Pathogenesis of *Brucella ovis* in pregnant mice and protection induced by the candidate vaccine strain *B. ovis* Δ*abcBA*. **Vaccine**, v.40, p.4617–4624, 2022.

BROWN, L.S.; FOSTER, C. G.; COURTNEY, J. M.; et al. Pericytes and Neurovascular Function in the Healthy and Diseased Brain. **Front. Cell Neurosci.**, v.13, p282, 2019.

BRUCE, D. Note on the discovery of a microorganism in Malta Fever. **The Practitioner**, v.39, p.161-170; 1887.

BUCH, T.; HEPPNER, F. L.; TERTILT, C.; et al. A Cre-inducible diphtheria toxin receptor mediates cell lineage ablation after toxin administration. **Nat. Methods**, v.2, n.6,p. 419-426, 2005.

BYNDLOSS, M.X.; TSAI, A.Y.; WALKER, G.T.; et al. *Brucella abortus* infection of placental trophoblasts triggers endoplasmic reticulum stress-mediated cell death and fetal loss via type IV secretion system-dependent activation of CHOP. **MBio,** v.10, p. e01538-19, 2019.

CAMPISI, J.; D'ADDA DI FAGAGNA, F. Cellular senescence: when bad things happen to good cells. **Nat. Rev. Mol. Cell .Biol.**, v.8, n.9, p. 729-740, 2007.

CAMPOCHIARO, P.A. Molecular pathogenesis of retinal and choroidal vascular diseases. **Prog. Retin. Eye Res.,** v. 49, p. 67-81, 2015.

CARMELIET, P. Angiogenesis in health and disease. **Nat. Med.**, v.9, p.653-660, 2003.

CARVALHO NETA, A. V.; STYNEN, A. P.; PAIXÃO, T. A.; et al. Modulation of the bovine trophoblastic innate immune response by *Brucella abortus*. **Infect. Immun**, v.76, n.5, p.1897–1907, 2008.

CELLI, J. Surviving inside a macrophage: The many ways of *Brucella*. **Res. Microbiol**, v.157, p.93–98, 2006.

CELLI, J.; DE CHASTELLIER, C.; FRANCHINI, D.M.; et al. *Brucella* evades macrophage killing via *VirB*-dependent sustained interactions with the endoplasmic reticulum. **J. Exp. Med**., v.198, p.545-556, 2003.

CHACÓN-DÍAZ, C.; ALTAMIRANO-SILVA, P.; GONZÁLEZ-ESPINOZA, G.; et al. *Brucella canis* is an intracellular pathogen that induces a lower proinflammatory response than smooth zoonotic counterparts. **Infect. Immun**, v.83, n. 12, p. 4861–4870, 2015.

CHEUNG, N.; MITCHELL, P.; WONG, T. Y. Diabetic retinopathy. **Lancet**, v.376, n.9735, p. 124-136, 2010.

CIRINO, G.; FIORUCCI, S.; SESSA, W. C. Endothelial nitric oxide synthase: the Cinderella of inflammation?. **Trends Pharmacol. Sci.**, v.24, n.2, p. 91-95, 2003.

COGAN, D.G.; TOUSSAINT, D.; KUWABARA, T. Retinal vascular patterns. IV. Diabetic retinopathy**. Arch. Ophthalmol.**, v. 66, p. 366-378, 1961.

CORBEL, M.J. Brucellosis in Humans and Animals. WHO Press, World Health Organization, Switzerland, 2006.

CUNHA-VAZ J.; BERNARDES, R.; LOBO, C. Blood-retinal barrier. **Eur. J. Ophthalmol.,** v.21, p.3-9, 2011.

CUTTLER, A. S.; LECLAIR, R. J.; STOHN, J. P.; et al. Characterization of *Pdgfrb*-Cre transgenic mice reveals reduction of ROSA26 reporter activity in remodeling arteries. **Genesis**, v.49, n.8, p. 673-680, 2011.

DAGGETT, J.; ROGERS, A.; HARMS, J.; et al. Hepatic and splenic immune response during acute vs. chronic *Brucella melitensis* infection using in situ microscopy. **Comp. Immunol. Microbiol. Infect. Dis.**, v.73, p. 101490, 2020.

DAHLBÄCK, B.; VILLOUTREIX, B. O. The anticoagulant protein C pathway. **FEBS Lett**, v.579, n.15, 3310-3316, 2005.

DAVISON, N.J.; CRANWELL, M.P.; PERRETT, L.L.; et al. Meningoencephalitis associated with *Brucella* species in a live-stranded striped dolphin (*Stenella coeruleoalba*) in south-west England. **Vet. Rec**., v. 165, p.86–89, 2009.

DAWSON, C.E.; PERRETT, L.L.; YOUNG, E.J.; et al. Isolation of *Brucella* species from a bottlenosed dolphin (*Tursiops truncatus*). **Vet. Rec**., v.158, p. 831–832, 2002.

DELPINO, M. V.; FOSSATI, C. A.; BALDI, P. C. Proinflammatory response of human osteoblastic cell lines and osteoblast-monocyte interaction upon infection with *Brucella* spp. **Infect. Immun**, v.77, n.3, p.984–995, 2009.

DELPINO, M.V., BARRIONUEVO, P., SCIAN, R. et al. *Brucella*-infected hepatocytes mediate potentially tissue-damaging immune responses**. J. Hepatol.**, v.53, v.1, p. 145-154, 2010.

DEMARS, A.; LISON, A.; MACHELART, A.; et al. Route of infection strongly impacts the host-pathogen relationship. **Front. Immunol**., v.10, p.1589, 2019.

DEMIR, R.; KAUFMANN, P.; CASTELLUCCI, M.; et al. Fetal vasculogenesis and angiogenesis in human placental villi. **Acta. Anat.,** v.136; p. 190-203, 1939.

DETILLEUX, P.G.; DEYOE, B.L.; CHEVILLE, N.F. Entry and intracellular localization of *Brucella* spp. in Vero cells: fluorescence and electron microscopy. **Vet. Pathol**., v.27, p.317–328, 1990.

DÍAZ-FLORES, L.; GUTIÉRREZ, R.; MADRID, J. F.; et al. Pericytes. Morpho function, interactions and pathology in a quiescent and activated mesenchymal cell niche. **Histol. Histopathol.**, V. 24, N. 7, P. 909-969, 2009.

DONG, X. Current strategies for brain drug delivery. **Theranostics**, v. 8, p. 1481-93, 2018.

DORE-DUFFY, P.; BALABANOV, R.; BEAUMONT, T.; KATAR, M. The CNS pericyte response to low oxygen: early synthesis of cyclopentenone prostaglandins of the J-series. **Microvasc. Res**, v. 69, n.1, p. 79-88, 2005.

ECKSTEIN, C.; MOL, J. P. S.; COSTA, F. B.; et al. *Brucella ovis* mutant in ABC transporter protects against *Brucella canis* infection in mice and it is safe for dogs. **PloS one**, v.15, n.4, p.e0231893, 2020.

EDFELDT, K.; SWEDENBORG, J.; HANSSON, G. K.; YAN, Z. Q. Expression of toll-like receptors in human atherosclerotic lesions: a possible pathway for plaque activation**. Circulation**, v.105, n. 10, p.11-58-1161, 2002.

EISENBERG, T.; RIßE, K.; SCHAUERTE, N.; et al. Isolation of a novel 'atypical' *Brucella* strain from a bluespotted ribbontail ray (*Taeniura lymma*). **Antonie Van Leeuwenhoek**. V.110, n.2, p. 221-234, 2017.

ERDOGAN, S.; DUZGUNER, V.; KUCUKGUL, A.; ASLANTAS, O. Silencing of PrP C (prion protein) expression does not affect *Brucella melitensis* infection in human derived microglia cells. **Res. Vet. Sci.**, v.95, n.2, p.368–373, 2013.

FERNÁNDEZ, A. G.; HIELPOS, M. S.; FERRERO, M. C.; et al. Proinflammatory response of canine trophoblasts to *Brucella canis* infection. **PloS one**, v.12, n.10, p.e0186561, 2017.

FERNANDEZ-PRADA, C.M.; ZELAZOWSKA, E.B.; NIKOLICH, M.; et al. Interactions between *Brucella melitensis* and human phagocytes: bacterial surface O polysaccharide inhibits phagocytosis, bacterial killing, and subsequent host cell apoptosis. **Infect. Immun**., v.71, p.2110-2119, 2003.

FERRERO, M. C.; FOSSATI, C. A.; BALDI, P. C. Direct and monocyte-induced innate immune response of human lung epithelial cells to *Brucella abortus* infection. Microbes and infection, v.12, n.10, p.736–747, 2010.

FERRERO, M. C.; FOSSATI, C. A.; BALDI, P. C. Smooth *Brucella* strains invade and replicate in human lung epithelial cells without inducing cell death. **Microb. Infect.**, v.11, n. 4, p.476–483, 2009.

FERRERO, M. C.; FOSSATI, C. A.; RUMBO, M.; BALDI, P. C. *Brucella* invasion of human intestinal epithelial cells elicits a weak proinflammatory response but a significant CCL20 secretion. **FEMS immunology and medical microbiology**, v. 66, n.1, p.45–57, 2012.

Ferrero, M. C.; Hielpos, M. S.; Carvalho, N. B.; et al. Key role of Toll-like receptor 2 in the inflammatory response and major histocompatibility complex class ii downregulation in *Brucella abortus*-infected alveolar macrophages**. Infect. Immun**, v.82, n.2, p. 626–639, 2014.

FERRERO, M.C.; BREGANTE, J.; DELPINO, M.V.; et al. Proinflammatory response of human endothelial cells to *Brucella* infection. **Microbes Infect.**, v. 13, p. 852–861, 2011;

FICHT, T. *Brucella* taxonomy and evolution. **Future Microbiol**., v.5, p.859–866, 2010.

FOSTER, G.; MACMILLAN, A.P.; GODFROID, J.; et al. A review of *Brucella* sp. infection of sea mammals with particular emphasis on isolates from Scotland. **Vet. Microbiol**. v.10, p.563–580, 2002.

FOSTER, G.; OSTERMAN, B.S.; GODFROID, J.; et al. *Brucella ceti* sp. nov. and *Brucella pinnipedialis* sp. nov. for *Brucella* strains with cetaceans and seals as their preferred hosts. **Int. J. Syst. Evol. Microbiol.**, v.57, n. 11, p.2688-2693, 2007.

FOSTER, G.; OSTERMAN, B.S.; GODFROID, J.; et al. *Brucella ceti* sp. nov and *Brucella pinnipedialis* sp. nov. for *Brucella* strains with cetaceans and seals as their preferred hosts. **Int. J. Syst. Evol. Microbiol**., v.57, p.2688–2693, 2007.

FRANC, K.A.; KRECEK, B.C.; HASLER, B.N.; ARENAS-GAMBOA, A.M. Brucellosis remais a neglected disease in the developing world: a call for interdisciplinary action. **BMC Public Health**, v.18, p.125, 2018.

GAENGEL, K.; GENOVÉ, G.; ARMULIK, A.; BETSHOLTZ, C. Endothelial-mural cell signaling in vascular development and angiogenesis. **Arterioscler Thromb Vasc Biol.**, v.29, n.5, p. 630-638, 2009.

GARCÍA SAMARTINO, C.; DELPINO, M. V.; POTT GODOY, C.; et al. *Brucella abortus* induces the secretion of proinflammatory mediators from glial cells leading to astrocyte apoptosis. **The American journal of pathology**, v.176, n.3, p.1323–1338, 2010.

GARCÍA-MÉNDEZ, K. B.; HIELPOS, S. M.; SOLER-LLORENS, P. F.; et al. Infection by *Brucella melitensis* or *Brucella papionis* modifies essential physiological functions of human trophoblasts. **Cellular microbiology**, v.21, n.7, p.e13019, 2019.

GARCÍA-MÉNDEZ, K.B.; HIELPOS, S.M.; SOLER-LLORENS, P.F.; et al. Infection by *Brucella melitensis* or *Brucella papionis* modifies essential physiological functions of human trophoblasts. **Cell. Microbiol**. v.21, p. e13019, 2019.

GENTILINI, M. V.; GIAMBARTOLOMEI, G. H.; DELPINO, M. V. Adrenal Steroids Modulate Fibroblast-Like Synoviocytes Response During *B. abortus* Infection. **Frontiers in endocrinology**, v.10, p.722, 2019

GENTILINI, M. V.; PESCE VIGLIETTI, A. I.; ARRIOLA BENITEZ, P. C.; et al. Inhibition of Osteoblast Function by *Brucella abortus* is Reversed by Dehydroepiandrosterone and Involves ERK1/2 and Estrogen Receptor. **Frontiers in immunology**, v.9, p. 88., 2018.

GERANMAYEH, M. H.; RAHBARGHAZI, R.; FARHOUDI, M. Targeting pericytes for neurovascular regeneration. **Cell Commun. Signal**, v.17, p. 1-13, 2019.

GIAMBARTOLOMEI, G.H.; DELPINO, M.V. Immunopathogenesis of hepatic brucellosis. **Front. Cell. Infect. Microbiol**., v.9, p.423, 2019.

GIRBL, T.; LENN, T.; PEREZ, L.; et al. Distinct Compartmentalization of the Chemokines CXCL1 and CXCL2 and the Atypical Receptor ACKR1 Determine Discrete Stages of Neutrophil Diapedesis. **Immunity,** v.49, n.6, p. 1062-1076, 2018.

GODFROID, J.; CLOECKAERT, A.; LIAUTARD, J.P.; et al. From the discovery of the Malta fever's agent to the discovery of a marine reservoir, brucellosis has continuous been a re-emerging zoonosis. **Vet. Res**., v.36, p.313–326, 2005.

GOENKA, R.; GUIRNALDA, P.D.; BLACK, S.J.; BALDWIN, C.L. B Lymphocytes Provide an Infection Niche for Intracellular Bacterium *Brucella abortus*. **J. Infect. Dis.,** v. 206, p. 91–98, 2012.

GONZÁLEZ, L.; PATTERSON, I.A.; REID, R.J.; et al. Chronic meningoencephalitis associated with *Brucella* sp. infection in live-stranded striped dolphins (*Stenella coeruleoalba*). **J. Comp. Pathol**., v.126, p.147–152, 2002.

GONZÁLEZ-ESPINOZA, G.; ARCE-GORVEL, V.; MÉMET, S.; Gorvel, J-P. *Brucella*: reservoirs and niches in animals and humans. **Pathogens**, v.10, p. 186, 2021

GORVEL, J.P.; MORENO, E.. *Brucella* intracellular life: From invasion to intracellular replication. **Vet. Microbiol.,** v.90, p. 281–297, 2002.

GORVEL, L.; TEXTORIS, J.; BANCHEREAU,; M et al. Intracellular bacteria interfere with dendritic cell functions: role of the type I interferon pathway. **PloS on**e, v.9, n.6, p.e99420, 2014.

GOUSTIN, A. S.; BETSHOLTZ, C.; PFEIFER-OHLSSON, S.; et al. Coexpression of the sis and myc proto-oncogenes in developing human placenta suggests autocrine control of trophoblast growth. **Cell**., v.41, n.1; p.301–312, 1985.

GRILLÓ, M.J.; BLASCO, J.M.; GORVEL, J.P. What have we learned from brucellosis in the mouse model? **Vet. Res.** v. 43, p.1–35, 2012.

Gutiérrez-Jiménez, C.; Hysenaj, L.; Alfaro-Alarcón, A.; et al. Persistence of *Brucella abortus* in the bone marrow of infected mice. **J. Immunol. Res**., v.2018, p.1-8, 2018.

GUTIÉRREZ-JIMÉNEZ, C.; MORA-CARTÍN, R.; ALTAMIRANO-SILVA, P.; et al. Neutrophils as trojan horse vehicles for *Brucella abortus* macrophage infection. Front. Immunol., .v10, p.1012, 2019.

GUZMÁN-VERRI, C.; CHAVES-OLARTE, E.; VON EICHEL-STREIBER, C.; et al. GTPases of the Rho subfamily are required for *Brucella abortus* internalization in nonprofessional phagocytes: direct activation of Cdc42. **J. Biol. Chem**., v.276, p.44435–44443, 2001.

HAJAL, C.; CAMPISI, M.; MATTU, C.; et al. *In vitro* model of molecular and nano-particle transport across the blood-brain barrier. **Biomicrofluidics**, v. 12, p. 42213, 2018.

HAJAL, C.; LEROI, B.; KAMM, R. D.; MAOZ, B. M. Biology and models of the blood–brain barrier. **Annu. Rev. Biomed. Eng.**, v. 23, p. 359-384, 2021.

HALL, C. N.; REYNELL, C.; GESSLEIN, B.; et al. Capillary pericytes regulate cerebral blood flow in health and disease. **Nature**, v.508, n.7494, p. 55-60, 2014.

HALLING, S.M.; DETILLEUX, P.G.; TATUM, F.M.; et al. Deletion of the BCSP31 gene of *Brucella abortus* by replacement**. Infect. Immun**., v.59, p.3863–3868, 1991.

HAMILTON, N. B; ATTWELL, D.; HALL, C. N. Perycite-mediated regulation of capillary diameter: a component of neurovascular coupling in heathl and disease. **Front Neuroenergetics**, v.2, p. 1-4, 2010.

HEID, H.W.; KEENAN, T.W. Intracellular origin and secretion of milk fat globules. **Eur. J. Cell Biol**. 84, 245–258, 2005.

HEIDEMANN, J.; DOMSCHKE, W.; KUCHARZIK, T.; MAASER, C. Intestinal microvascular endothelium and innate immunity in inflammatory bowel disease: a second line of defense? **Infect Immun**, v.74, n.10, p. 5425-5432, 2006.

HELLBERG, C.; OSTMAN, A.; HELDIN, C. H. PDGFand vessel maturation. **Recent Results Cancer Res.,** v. 180, p. 103-114, 2010.

HELLER, M. C.; WATSON, J. L.; BLANCHARD, M. T.; et al. Characterization of *Brucella abortus* infection of bovine monocyte-derived dendritic cells. **Veterinary immunology and immunopathology**, v.149, n.3-4, p.255–261, 2012.

HERNÁND;Z-MORA, G., PALACIOS-ALFARO, J.D.; GONZÁLEZ-BARRIENTOS, R. Wildlife reservoirs of brucellosis: *Brucella* in aquatic environments. **Rev. Sci. Tech**. v.32, p.89–103, 2013.

Hernández-Mora, G.; González-Barrientos, R.; Morales, J.A.; et al. Neurobrucellosis in stranded dolphins, Costa Rica. **Emerg. Infect. Dis**., v.14, p.1430–1433, 2008.

IZADJOO, M.J.; MENSE, M.G.; Bhattacharjee, A.K.; et al. A study on the use of male animal models for developing a live vaccine for brucellosis. **Transbound. Emerg. Dis**., v.55, p. 145–151, 2008.

JANSEN, W.; DEMARS, A.; NICAISE, C.; et al. Shedding of *Brucella melitensis* happens through milk macrophages in the murine model of infection. **Sci. Rep**. v.10, p.9421, 2020.

JIANG, J. X.; GU, S. Gap-junction-and hemichannel-independent actions of connexins. **BBA,** V.1711, N.2, P. 208-214, 2005.

KANG, Y. S., KIRBY, J. E. Promotion and Rescue of Intracellular *Brucella neotomae* Replication during Coinfection with Legionella pneumophila. **Infect. Immun**, v.85, n.5, p.e00991-16, 2017.

KEBIR, D.E.; DAMLAJ, A.; MAKHEZER, N.; FILIP, J. Toll-like receptor 9 signaling regulates tissue factor and tissue factor pathway inhibitor expression in human endothelial cells and coagulation in mice. **Crit. Care Med.**, v.43, n.6, p.e179-189, 2015.

KELEHER, L. L.; SKYBERG, J. A. Activation of bovine neutrophils by *Brucella* spp. **Vet. iImmunol. Immunopathol.**, v.177,p. 1–6, 2016.

KHALAF, O. H.; CHAKI, S. P.; GARCIA-GONZALEZ, D. G.; et al. Interaction of *Brucella abortus* with Osteoclasts: a Step toward Understanding Osteoarticular Brucellosis and Vaccine Safety. Infection and immunity, v.88, n.4, p.e00822-19, 2020.

KISLER, K.; NELSON, A. R.; REGE, S. V.; et al. Pericyte degeneration leads to neurovascular uncoupling and limits oxygen supply to brain. **Nat. Neurosci.**, v. 20, n. 3, p. 406-416, 2017.

KORN, C.; AUGUSTIN, H. G. Mechanisms of vessels pruning and regression. **Dev. Cell.,** v. 34, p. 5-17, 2015.

KRUSE, K.; LEE, Q. S.; SUN, Y.; et al. N-cadherin signaling via Trio assembles adherens junctions to restrict endothelial permeability. **J. Cell Biol.,** v.218, n.1, p. 299-316, 2019.

LACEY, C. A.; PONZILACQUA-SILVA, B.; CHAMBERS, C. A.; et al. MyD88-Dependent Glucose Restriction and Itaconate Production Control *Brucella* Infection. **Infect. Immun**, v.89, n.10, p.e0015621, 2021.

LACEY, C.A.; KELEHER, L.L.; MITCHELL, W.J.; et al. CXCR2 mediates *Brucella*-induced arthritis in interferon γ-deficient mice. **J. Infect. Dis**., v.214, p.151–160, 2016.

LAINE, C. G.; SCOTT, H. M.; ARENAS-GAMBOA, A. M. Human brucellosis: Widespread information deficiency hinders an understanding of global disease frequency. **PLoS Negl. Trop. Dis.**, v.16, n.5, p.e0010404, 2022.

LAINE, C.G.; SCOTT H.M.; ARENAS-GAMBOA, A. Human brucellosis: Widespread information deficiency hinders an understanding of global disease frequency. **Plos Negl. Trop. Dis.** v.16, p.e0010404, 2022.

LARSEN, A. K.; GODFROID, J.; NYMO, I. H. *Brucella pinnipedialis* in hooded seal (*Cystophora cristata*) primary epithelial cells. **Acta Vet.**, v.58, p.9, 2016.

LARSEN, A. K.; NYMO, I. H.; BRIQUEMONT, B.; et al. Entrance and survival of *Brucella pinnipedialis* hooded seal strain in human macrophages and epithelial cells. **PloS one,** v.8, n.12, p. e84861, 2013

LASKAY, T.; VAN ZANDBERGEN, G.; SOLBACH, W. Neutrophil granulocytes—Trojan horses for *Leishmania major* and other intracellular microbes? **Trends Microbiol**. v.11, p.210–214, 2003.

LEFORT, C. T.; LEY, K. Neutrophil arrest by LFA-1 activation. **Front. Immunol.**, v.3, p. 157, 2012.

LETESSON, J. J.; BARBIER, T.; ZÚÑIGA-RIPA, A.; et al. *Brucella* genital tropism: What's on the menu. **Front. Microbiol**., v.8, p.506, 2017.

LEVÉEN, P.; PEKNY, M.; GEBRE-MEDHIN, S.; et al. Mice deficient for PDGF B show renal, cardiovascular, and hematological abnormalities. **Genes. Dev**., v.8; p.1875-1887, 1994.

LI, Y.; LUCAS-OSMA, A.M.; BLACK, S.; et al. Pericytes impair capillary blood flow and motor function after chronic spinal cord injury**. Nat. Med**., v.23, n.6, p.733–741, 2017.

LIEW, G.; KLEIN, R.; WONG, T. Y. The role of genetics in susceptibility to diabetic retinopathy. **Int Ophthalmol Clin**, v.49, n.2, p. 35-52, 2009.

LIU, X.; ZHOU, M.; WU, J.; et al. HMGB1 release from trophoblasts contributes to inflammation during *Brucella melitensis* infection. **Cellular microbiology**, v.21, n.10, p.e13080, 2019.

LUBANI, M.; SHARDA, D.; HELIN, I. Cardiac manifestations in brucellosis. **Arch. Dis. Childh**. , v.61, p.569–572, 1986.

MACEDO, A.A.; GALVÃO, N.R.; SÁ, J.C.; et al. *Brucella*-associated cervical bursitis in cattle. **Trop. Anim. Health. Prod.**, v.51, p.697–702, 2019.

MAEDA, S.; TSUKIHARA, T. Structure of the gap junction channel and its implications for its biological functions. **Cell Mol Life Sci,** v. 68, n.7, p. 1115-1129, 2011.

MAGNANI, D.M.; LYONS, E.T.; FORDE, T.S.; et al. Osteoarticular tissue infection and development of skeletal pathology in murine brucellosis. **Dis Model Mech.**, v.6, p.811–818, 2013.

MARELLI-BERG, F. M.; JARMIN, S. J. Antigen presentation by the endothelium: a green light for antigen-specific T cell trafficking?. **Immunol Lett**, v.93, n.2-3, p. 109-113, 2004.

MATHIAS, R. T.; WHITE, T. W.; GONG, X. Lens gap junctions in growth, differentiation, and homeostasis. **Physiol Rev,** v.90, n. 1, p.179-206, 2010.

MCDERMOTT, J.J.; GRACE, D.; ZINSSTAG, J. Economics of brucellosis impact and control in low-income countries. **Rev. Sci. Tech. De L'oie**,, v.32, p.249–261, 2013.

MCGUIRE, P. G.;RANGASAMY, S.; MAESTAS, J.; DAS A. Pericyte-derived sphingosine 1-phosphate induces the expression of adhesion proteins and modulates the retinal endothelial cell barrier**. Arterioscler Thromb Vasc Biol**, v.31, n.12, p. e107-115, 2011.

MEADOR, V.P.; DEYOE, B.L. Experimentally induced *Brucella abortus* infection in pregnant goats. **Am. J. Vet. Res**., v.47, p.2337–2342, 1986.

MENA-BUENO, S.; POVEDA-URKIXO, I.; IRAZOKI, O.; et al. *Brucella melitensis* Wzm/Wzt System: Changes in the Bacterial Envelope Lead to Improved Rev1Δ*wzm* Vaccine Properties. **Frontiers in microbiology**, v.13, p. 908495, 2022.

MENG, M. B.; ZAORSKY, N. G.; DENG, L.; et al. Pericytes: a double-edged sword in cancer therapy. **Future Oncol**, v.11, n.1, p. 168-179, 2015.

MILILLO, M. A.; TROTTA, A.; SERAFINO, A.; et al. Bacterial RNA Contributes to the Down-Modulation of MHC-II Expression on Monocytes/Macrophages Diminishing $CD4^+$ T Cell Responses. **Frontiers in immunology**, v.10, p. 2181, 2019.

MIRAGLIA, M. C.; RODRIGUEZ, A. M.; BARRIONUEVO, P.; et al. *Brucella abortus* Traverses Brain Microvascular Endothelial Cells Using Infected Monocytes as a Trojan Horse **Frontiers in immunology**, v.8, p.200, 2018.

MIRAGLIA, M. C.; SCIAN, R.; SAMARTINO, C. G.; et al. *Brucella abortus* induces TNF-α-dependent astroglial MMP-9 secretion through mitogen-activated protein kinases. **Journal of neuroinflammation**, v.10, p.47, 2013.

MISHRA, A.; REYNOLDS, J.; CHEN, Y. et al. Astrocytes mediate neurovascular signaling to capillary pericytes but not to arterioles. **Nat Neurosci,** v.19, p. 1619-27, 2016.

MOL, J. P.; COSTA, E. A.; CARVALHO, A. F.; et al. Early transcriptional responses of bovine chorioallantoic membrane explants to wild type, ΔvirB2 or ΔbtpB *Brucella abortus* infection. **PloS one**, v.9, n.9, p.e108606, 2014.

MONCADA, S.; VANE, J.R. Prostacyclin and blood coagulation. **Drugs**, v.21, n.6, p.430-437, 1981.

MORENO E.; CLOECKAERT, A.; MORIYON, I. *Brucella* evolution and taxonomy. **Vet Microbiol**., v.90, p.209–227, 2002

MORENO E.; MORIYÓN I. The genus *Brucella*. In: Dworkin M., Falkow S., Rosenberg E., Schleifer K.H., Stackebrandt E., editors. The prokaryotes. Springer; New York, NY, USA: 2006. pp. 315–456, 2006.

MORENO, E.; MORIYÓN, I. The Genus Brucella. In The Prokaryotes; Dworkin, M., Falkow, S., Rosenberg, E., Schleifer, K.-H., Stackebrandt, E., Eds.; Springer: New York, NY, USA, p. 315–456. 28, 2006.

MORENO, E.; STACKEBRANDT, E.; DORSCH, M.; et al. *Brucella abortus* 16S rRNA and lipid A reveal a phylogenetic relationship with members of the alpha-2 subdivision of the class Proteobacteria. **J. Bacteriol.,** v.172, p. 3569–3576, 1990.

MULLER WA. Mechanisms of leukocyte transendothelial migration. **Annu Rev Pathol,** v.6, p.323-344, 2011.

MUÑOZ-GÓMEZ, S. A.; HESS, S.; BURGER, G; et al. An update phylogeny of the *Alphaproteobacteria* reveals that the parasitic *Rickettsiales* and *Holosporales* have independent origins. **eLife**, v.8, p e423535, 2019.

NAVARRO, R.; COMPTE, M.; ÁLVAREZ-VALLINA, L.; SANZ, L. Immune Regulation by Pericytes: Modulating Innate and Adaptive Immunity. **Front Immunol**, v.7, p. 480, 2016.

NIELSEN, M. S.; ALXESEN, L. N.; SORGEN, P. L.; et al. GAP junctions. **Wiley online Library.,** v.2, n.3, p. 110051, 2012.

NIKOLAKOPOULOU AM, MONTAGNE A, KISLER K, et al. Pericyte loss leads to circulatory failure and pleiotrophin depletion causing neuron loss**. Nat Neurosci**, v. 22, n. 7, p. 1089-1098, 2019.

NIKOLAKOPOULOU, A.M.; MONTAGNE, A.; KISLER, K.; et al. Pericyte loss leads to circulatory failure and pleiotrophin depletion causing neuron loss. **Nat Neurosci,** v.22, p. 1089–1098, 2019.

OGURA S, KURATA K, HATTORI Y, et al. Sustained inflammation after pericyte depletion induces irreversible blood-retina barrier breakdown**. JCI Insight**., v.2, n.3, p. e90905, 2017.

OHLSSON, R.; FALCK, P.; HELLSTRÖM, M.; et al. PDGFB regulates the development of the labyrinthine layer of the mouse fetal placenta. **Developmental biology**, v. 212, n.1; p.124–136, 1999.

OKAMOTO, T.; USUDA, H.; TANAKA, T.; et al. The functional implications of endothelial gap junctions and cellular mechanics in vascular angiogenis. **Cancers**, v.11, n.2, p. 237, 2019.

OPITZ, B.; EITEL, J.; MEIXENBERGER, K.; SUTTORP, N. Role of Toll-like receptors, NOD-like receptors and RIG-I-like receptors in endothelial cells and systemic infections. **Thromb Haemost**, v.102, n.6, p.1103-1109, 2009.

PAIXÃO, T. A.; ROUX, C.M.; DEN HARTIGH, A.B; et al. Establishment of systemic *Brucella melitensis* infection through the digestive tract requires urease, the type IV secretion system, and lipopolysaccharide O antigen. **Infect. Immun.**, v.77, p.4197-4208, 2009.

PAIXÃO, T.A.; ROUX, C.M.; DEN HARTIGH, A.B.; et al.. Establishment of systemic *Brucella melitensis* infection through the digestive tract requires urease, the type IV secretion system, and lipopolysaccharide O antigen. **Infect. Immun**., v.77, p.4197–4208, 2009.

PARK, W. B.; KIM, S.; SHIM, S.; YOO, H. S. Identification of Dendritic Cell Maturation, TLR, and TREM1 Signaling Pathways in the *Brucella canis* Infected Canine Macrophage Cells, DH82, Through Transcriptomic Analysis. **Frontiers in veterinary science**, v.8, p.619759, 2021.

PEPPIATT, C. M.; HOWARTH, C.; MOBBS, P.; ATTWELL, D. Bidirectional control of CNS capillary diameter by pericytes**. Nature**, v.443, n.7112, p. 700-704, 2006.

PESCE VIGLIETTI, A. I.; ARRIOLA BENITEZ, P. C.; GENTILINI, M. V.; et al. *Brucella abortus* Invasion of Osteocytes Modulates Connexin 43 and Integrin Expression and Induces Osteoclastogenesis via Receptor Activator of NF-κB Ligand and Tumor Necrosis Factor Alpha Secretion. **Infect. Immun**, v.84, n.1, p.11–20, 2015.

PESCE VIGLIETTI, A. I.; ARRIOLA BENITEZ, P. C.; GIAMBARTOLOMEI, G. H.; DELPINO, M. V. *Brucella abortus*-infected B cells induce osteoclastogenesis. **Microbes and infection**, v.8, n.9, p.529–535, 2016.

PESCE VIGLIETTI, A. I.; GIAMBARTOLOMEI, G. H.; DELPINO, M. V. Endocrine modulation of *Brucella abortus*-infected osteocytes function and osteoclastogenesis via modulation of RANKL/OPG. **Microbes and infection**, v.21, n. 7, p. 287–295, 2019.

PESCE VIGLIETTI, A. I.; GIAMBARTOLOMEI, G. H.; QUARLERI DELPINO, M. V. *Brucella abortus* Infection Modulates 3T3-L1 Adipocyte Inflammatory Response and Inhibits Adipogenesis. **Frontiers in endocrinology**, v.11, p.585923, 2020.

PHELAN, P. Innexins: members of a evolutionarily conserved family of gap-junction proteins. **BBA,** v.1711, n.2, p.225-245, 2005.

PHILIPSION, M.; KUBES, P. The neutrophil in vascular inflammation. **Nature medicine,** v. 17, n.11, p. 1381-1390, 2011.

PICOLI, C.C.; BRYAN, O.P.G.; SANTOS, G.S.P.; et al. Pericytes cross-talks within the tumor microenvironment. **BBA,** v. 1876, n.2, p.102-104, 2021.

PIZARRO-CERDÁ, J.; MÉRESSE, S.; PARTON, R.G.; et al. *Brucella abortus* transits through the autophagic pathway and replicates in the endoplasmic reticulum of nonprofessional phagocytes. **Infect. Immun.** v.66, p. 5711–5724, 1998.

POESTER, F.P., SAMARTINO, L.E., SANTOS, R.L. Pathogenesis and pathobiology of brucellosis in livestock. **Rev. Sci. Tech**., v.32, p.105–115, 2013.

POVEDA-URKIXO, I., RAMÍREZ, G.A., GRILLÓ, M.J. Kinetics of placental infection by different smooth *Brucella* strains in mice. **Pathogens**, v.11, p.279, 2022.

PUJOL, M.; BORIE, C.; MONTOYA, M.; et al. *Brucella canis* induces canine $CD4^+$ T cells multi-cytokine Th1/Th17 production via dendritic cell activation. **Comparative immunology, microbiology and infectious diseases**, v.62, p. 68–75, 2019.

PUJOL, M.; CASTILLO, F.; ALVAREZ, C.; et al. Variability in the response of canine and human dendritic cells stimulated with *Brucella canis*. **Veterinary research**, v.48, n.1, p.72, 2017.

QUAEGEBEUR, A.; SEGURA, I.; CARMELIET, P. Pericytes: blood-brain barrier safeguards against neurodegeneration? **Neuron.**, v.68, n. 3, p. 321-323, 2010.

RANA, R.R.; ZHANG, M.; SPEAR, A.M.; et al. Bacterial TIR-containing proteins and host innate immune system evasion. **Med. Microbiol. Immunol.,** v.202, p. 1-10, 2013.

RICHARDSON, M. Parasitization in vitro of bovine cells by *Brucella abortus*. **J. Bacteriol.**, v.78, p. 769–777, 1959.

RODRÍGUEZ, A. M.; TROTTA, A.; MELNYCZAJKO, A. P.; et al. *Brucella abortus*-Stimulated Platelets Activate Brain Microvascular Endothelial Cells Increasing Cell Transmigration through the Erk1/2 Pathway. **Pathogens**, v.9, n.9, 708, 2020.

ROSSETTI, C.A.; DRAKE, K.L.; ADAMS, L.G. Transcriptome analysis of HeLa cells response to *Brucella melitensis* infection: a molecular approach to understand the role of the mucosal epithelium in the onset of the *Brucella* pathogenesis. **Microbes Infect**., v.14, p.756–767, 2012.

SABROE, I.; DOWER, S.K.; WHYTE, M.K.D. The role of Toll-like receptors in the regulation of neutrophil migration, activation and apoptosis. **Clin. Infect. Dis**., v.41, p.s421–s426, 2005.

SAGARE, A. P.; BELL, R. D.; ZHAO, Z.; et al. Pericyte loss influences Alzheimer-like neurodegeneration in mice**. Nat Commun**, v.4, p. 2932, 2013.

SAID-SADIER, N.; OJCIUS, D.M. Alarmins, inflammasomes and immunity. **Biomed J**, v. 35, n.6, p. 437-449, 2012.

SALCEDO, S. P.; CHEVRIER, N.; LACERDA, T. L.; et al. Pathogenic brucellae replicate in human trophoblasts. **The Journal of infectious diseases**, v.207(7), 1075–1083.

SALCEDO, S.P.; MARCHESINI, M.I.; LELOUARD, H.; et al. *Brucella* Control of Dendritic Cell Maturation is Dependent on the TIR-Containing Protein Btp1. **Plos Pathog.**, v.4, p.e21, 2008.

SAMARTINO, L.E., ENRIGHT, F.M. *Brucella abortus* differs in the multiplication within bovine chorioallantoic membrane explants from early and late gestation. **Comp Immunol Microbiol Infect Dis**., v.19, n.1, p.55-63, 1996.

SAMARTINO, L.E.; ENRIGHT, F.M. pathogenesis of abortion of bovine brucellosis. **Comp. Immun. MicrobioL infect. Dis**., v.16, p.95–101, 1993.

SANTOS, R.L.; MARTINS, T.M.; BORGES, A.M., PAIXÃO, T.A. Economic losses due to bovine brucellosis in Brazil. **Pesq. Vet. Bras**., v.33, p.759–764, 2013.

SCHNOOR M, ALCAIDE P, VOISIN MB, VAN BUUL JD. Crossing the Vascular Wall: Common and Unique Mechanisms Exploited by Different Leukocyte Subsets during Extravasation. **Mediators Inflamm**, v.2015, p.946509, 2015.

SCHOLZ, H.C.; NÖCKLER, K.; LLNER, C.G.; et al. *Brucella inopinata* sp. nov., isolated from a breast implant infection. **Int. J. Syst. Evol. Microbiol**., v.60, p.801-808, 2010.

SCHOLZ, H.C.; REVILLA-FERNÁNDEZ, S.; AL DAHOUK, S.; et al. *Brucella vulpis* sp. nov., isolated from mandibular lymph nodes of red foxes (*Vulpes vulpes*). **Int. J. Syst. Evol. Microbiol**., v.66, p.2090-2098, 2016.

SCHOLZ, H.C.; REVILLA-FERNÁNDEZ, S.; DAHOUK, S.A.; et al. *Brucella vulpis* sp. nov., isolated from mandibular lymph nodes of red foxes (*Vulpes vulpes*). **Int J Syst Evol Microbiol.**, v.66, p.2090–2098, 2016.

SCIAN, R.; BARRIONUEVO, P.; GIAMBARTOLOMEI, G. H.; et al. Potential role of fibroblast-like synoviocytes in joint damage induced by *Brucella abortus* infection through production and induction of matrix metalloproteinases. **Infection and immunity**, v. 79, n.9, p.3619–3632, 2011

SCIAN, R.; BARRIONUEVO, P.; RODRIGUEZ, A. M.; et al. *Brucella abortus* invasion of synoviocytes inhibits apoptosis and induces bone resorption through RANKL expression. **Infection and immunity**, v.81, n.6, p.1940–1951, 2013.

SENGILLO, J. D.; WINKLER, E. A.; WALKER, C. T.; et al. Deficiency in mural vascular cells coincides with blood-brain barrier disruption in Alzheimer's disease. **Brain Pathol**, v.23, n.3, p. 303-310, 2013.

SHEPRO, D.; MOREL, N. M. Pericyte physiology. **FASEB J,** v.7, n.3, p. 1031-1034, 1993.

SHOLZ, H.C., NÖCKLER, K., GÖLLNER, C., BAHN, P.; et al. *Brucella inopinata* sp. nov., isolated from a breast implant infection**. Int. J. Syst. Evol. Microbiol**. v.60, p.801–808, 2010.

SIDHU-MUÑOZ, R. S.; SANCHO, P.; VIZCAÍNO, N. Evaluation of human trophoblasts and ovine testis cell lines for the study of the intracellular pathogen *Brucella ovis*. **FEMS microbiology letters,** v.36*5*, n.24, p.10.1093, 2018

SIDOR, I.F.; DUNN, J.L.; TSONGALIS, G.J.; et al. A multiplex real-time polymerase chain reaction assay with two internal controls for the detection of *Brucella* species in tissues, blood, and feces from marine mammals. **J. Vet. Diagn. Invest**., v..25, p.72–81, 2011.

SILVA, A.P.C.; MACÊDO, A.A.; SILVA, T.M.; XIMENES, L.C.; et al. Protection provided by an encapsulated live attenuated Δ*abcBA* strain of *Brucella ovis* against experimental challenge in a murine model. Clin. **Vaccine Immunol**., v.22, p.789–797, 2015

SILVA, T. M.; PAIXÃO, T. A.; COSTA, E. A.; et al. Putative ATP-binding cassette transporter is essential for *Brucella ovis* pathogenesis in mice. **Infection and immunity**, v.79, n.4, p.1706–1717, 2011.

SILVA, T.; COSTA, E.A.; PAIXÃO, T.A.; et al. Laboratory animal models for brucellosis research. J. Biomed. **Biotechnol.**, v.2011, p.1-9, 2011

SMITH, H.; WILLIAMS, A.E.; PEARCE, J.H.; et al. Foetal erythritol: a cause of the localization of *Brucella abortus* in bovine contagious abortion. **Nature,** v.193, p. 47–49, 1962.

SOLER-LLORÉNS, P. F.; QUANCE, C. R.; LAWHON, S. D.; et al. A *Brucella* spp. Isolate from a Pac-Man Frog (*Ceratophrys ornata*) Reveals Characteristics Departing from Classical Brucellae. **Front. Immunol**, v.6, p.116, 2016.

SOLER-LLORÉNS, P.F.; QUANCE, C.R.; LAWHON, S.D.; et al. A *Brucella* spp. isolate from a Pac-man frog (*Ceratophrys ornata*) reveals characteristics departing from classical brucellae. **Front. Cell. Infect. Microbiol**., v,6, p.116, 2016.

SONG, S.; EWALD, A. J.; STALLCUP, W; et al. PDGFRbeta+ perivascular progenitor cells in tumours regulate pericyte differentiation and vascular survival. **Nat. Cell Biol**., v. 7, n. 9, p. 870-879, 2005.

SOUZA, T.D.; CARVALHO, T.F.; MOL, J.P.D.S.; et al. Tissue distribution and cell tropism of *Brucella canis* in naturally infected canine foetuses and neonates. **Sci. Rep**. v.8, p.7203, 2018.

SPRINGER TA. Traffic signals for lymphocyte recirculation and leukocyte emigration: the multistep paradigm. **Cell,** v. 76, n.2, p.301-314, 1994.

STANIMIROVIC, D. B.; FRIEDMAN, A. Pathophysiology of the neurovascular unit: disease cause or consequence? **J .Cereb. Blood Flow Metab.**, v. 32, n. 7, p. 1207-1221, 2012.

STARK, K.; ECKART, A.; HAIDARI, S. et al. Capillary and arteriolar pericytes attract innate leukocytes exiting through venules and 'instruct' them with pattern-recognition and motility programs. **Nat. Immunol.**, v. 14, n.1, p. 41-51, 2013.

SUÁREZ-ESQUEVEL, M.; CHAVES-OLARTE, E.; MORENO, E.; GUZMÁN-VERRI, C. *Brucella* genomics: macro and micro evolution. **Int. J. Mol. Sci.**, v.21, n.20, p. 7749, 2020.

SURENDRAN, N.; HILTBOLD, E. M.; HEID, B.; et al. Live *Brucella abortus* rough vaccine strain RB51 stimulates enhanced innate immune response *in vitro* compared to rough vaccine strain RB51SOD and virulent smooth strain 2308 in murine bone marrow-derived dendritic cells. **Vet. microbiol.**, v.147, n.1-2, p.75–82, 2011.

SWEENEY, M. D.; AYYADURAI, S.; ZLOKOVIC, B. V. Pericytes of the neurovascular unit: key functions and signaling pathways. **Nat. Neurosci.**, v. 19, n.6, p. 771-783, 2016.

TAKIMOTO, E.; ISHIDA, J.; SUGIYAMA, F.; et al. Hypertension induced in pregnant mice by placental renin and maternal angiotensinogen. **Science.,** v.274; p. 995-998, 1996.

TIMMERMAN I, DANIEL AE, KROON J, VAN BUUL JD. Leukocytes Crossing the Endothelium: A Matter of Communication**. Int. Rev. Cell**, v.322, p.281-329, 2016.

TISSARI, J.; SIRÉN, J.; MERI, S.; et al. IFN-alpha enhances TLR3-mediated antiviral cytokine expression in human endothelial and epithelial cells by up-regulating TLR3 expression. **J. Immunol.**, v. 174, n.7, p.4289-4294, 2005.

TOBIAS, L.; CORDES, D.O.; SCHURIG, G.G. Placental pathology of the pregnant mouse inoculated with *Brucella abortus* strain 2308. **Vet. Pathol**., v.30, p.119–129, 1993.

TÖRÖK, O.; SCHREINER, B.; SCHAFFENRATH, J.; et al. Pericytes regulate vascular immune homeostasis in the CNS. **Proc. Natl. Acad. Sci.**., v.118, n.10, p.e2016587118, 2021.

TROTTA A.; VELÁSQUEZ, L.N.; MILILLO, M.A.; et al. Platelets promote *Brucella abortus* Monocyte invasion by establishing complexes with monocytes. **Front. Immunol**., v.9, p.1000, 2018.

TROTTA, A.; MILILLO, M. A.; SERAFINO, A.; et al. *Brucella abortus*-infected platelets modulate the activation of neutrophils. **Immunol. Cell biol.**, v.98, n.9, p.743–756, 2020.

TROTTA, A.; VELÁSQUEZ, L.N.; MILILLO, M. A.; et al. Platelets Promote *Brucella abortus* Monocyte Invasion by Establishing Complexes with Monocytes. **Front. Immunol**, v.9, p.1000, 2018.

TSOLIS, R. M. Comparative genome analysis of the alpha-proteobacteria: Relationships between plant and animal pathogens and host specificity. **Proc. Natl. Acad. Sci.**, v.99, p. 12503-12505, 2002.

TSOLIS, R.M.; SESHADRI, R.; SANTOS, R.L.; et al. Genome degradation in *Brucella ovis* corresponds with narrowing of its host range and tissue tropism. **PloS One**, v.4, p. e5519, 2009.

TU, Z.; LI, Y.; SMITH, D.S.; et al. Retinal pericytes inhibit activated T cell proliferation. Invest. **Ophthalmol.** Vis. Sci., v.52; p.9005–9010, 2011.

VANLANDEWIJCK, M.; HE, L.; MÄE, M. A.; et al. A molecular atlas of cell types and zonation in the brain vasculature. **Nature,** v.560, n. 7693, p. 475-480, 2018.

VARESIO, L. M.; FIEBIG, A.; CROSSON, S. *Brucella ovis* Cysteine Biosynthesis Contributes to Peroxide Stress Survival and Fitness in the Intracellular Niche. **Infection and immunity**, v.89, n.6, p. e00808-20, 2021.

VELÁSQUEZ, L. N.; DELPINO, M. V.; IBAÑEZ, A. E. et al. *Brucella abortus* induces apoptosis of human T lymphocytes. **Microbes Infect**, v.14, n.7-8, p. 639–650, 2012.

VERDIGUEL-FERNÁNDEZ, L.; OROPEZA-NAVARRO, R.; BASURTO-ALCÁNTARA, F. J.; et al. Omp31 plays an important role on outer membrane properties and intracellular survival of *Brucella melitensis* in murine macrophages and HeLa cells. **Archives of microbiology**, v.199, n.7, p. 971–978, 2017.

VERGER, J.; GRIMONT, F.; GRIMONT, P.A.D. et al. Taxonomy of the genus *Brucella*. **Ann. Inst. Pasteur Microbiol**, v.138, p.235-238, 1987.

VERGER, J-M.; GRIMONT, F.; GRIMONT, P.A.D.; GRAYON, M.. *Brucella*, a monospecific genus as shown by deoxyribonucleic-acid hybridization. **Int. J. Syst. Evol. Microbiol**., v.35, p.292–295, 1985.

VIGLIETTI, A.I.P.; GENTILINI, M.V.; BENITEZ, A.P.C.; et al. *B. abortus* Modulates Osteoblast Function Through the Induction of Autophagy. **Front. Cell**. **Infect. Microbiol**., v.8, p.425, 2018.

VIGLIETTI, A.I.P.; GIAMBARTOLOMEI, G.H.; QUARLERI, J.; DELPINO, M.V. *Brucella abortus* infection modulates 3T3-L1 adipocyte inflammatory response and inhibits adipogenesis. **Front. Endocrinol**., v.11, p. 585923, 2020.

VINORE, S. A. Breakdown of the blood-retinal barrier. **Encyclopedia of the eye**, p. 216-222, 2010.

VITRY, M-A.; MAMBRES, D.H.; DEGHELT, M.; et al. *Brucella melitensis* invades murine erythrocytes during infection. **Infect. Immun**., v.82, p. 3927–3938, 2014.

VOISIN, M.; PROBSTL, D.; NOURSHARG, S. Venular basement membranes ubiquitously exprees matrix protein low-expressin regions. **Am. J. Pathol**., v.176, v.1, p. 482-495, 2010.

VON TELL, D.; ARMULIK, A.; BETSHOLTZ, C. Pericytes and vascular stability**. Exp. Cell Res.**, v. 312, n.5, p. 623-629, 2006.

WAKUI, S.; YOKOO, K.; MUTO, T.; et al. Localization of Ang-1, -2, Tie-2, and VEGF expression at endothelial-pericyte interdigitation in rat angiogenesis. **Lab. Invest.,** v. 86, n.11, p. 1172-1184, 2006.

WALDROP, S. G., SRIRANGANATHAN, N. Intracellular invasion and survival of *Brucella neotomae*, another possible zoonotic *Brucella* species. **PloS one**, v.14, n.4, p. e0213601, 2019.

WANG, J.; HOSHIJIMA, M.; LAM, J.; et al. Cardiomyopathy associated with microcirculation dysfunction in laminin alpha4 chain-deficient mice. **J. Biol. Chem.**, v. 281, p. 213-220, 2006.

WANG, X.; LIN, P.; YIN.; et al. 2015. *Brucella suis* vaccine strain S2-infected immortalized caprine endometrial epithelial cell lines induce non-apoptotic ER-stress. **Cell stress chaperones**, v.20, n.3, p. 399–409, 2015.

WANG, Z.; WANG, Y.; YANG, H.; et al. Doxycycline Induces Apoptosis of *Brucella Suis* S2 Strain-Infected HMC3 Microglial Cells by Activating Calreticulin-Dependent JNK/p53 Signaling Pathway. **Front. Cell. Infect. Microbiol.**, v.11, p.0640847, 2021.

WHATMORE, A.M.; DALE, E-J.; STUBBERFIELD, E.; et al. Isolation of *Brucella* from a White's tree frog (*Litoria caerulea*). **JMM. Case Reports**, 2, 1-5, 2015.

WHATMORE, A.M.; DAVISON, N.; CLOECKAERT, A.; et al. *Brucella papionis* sp. nov., isolated from baboons (*Papio* spp.). **Int. J. Syst. Evol. Microbiol**, v.64, p.4120–4128, 2014.

WILSON, C. W.; YE, W. Regulation of vascular endothelial junctions' stability and remodeling through Rap-1Rasin1 signaling. **Cell Adh. Migr.**, v.8, n.2, p. 76-83, 2014.

WINKLER, E. A., BELL, R. D.; ZLOKOVIC, B. V. Central nervous system pericytes in health and disease**. Nat. Neurosci.**, v.14, n.11, p. 1398-1405, 2011.

WONG, P. P.; MUÑOZ-FÉLIX, J. M.; HIJAZI, M.; et al. Cancer Burden Is Controlled by Mural Cell-β3-Integrin Regulated Crosstalk with Tumor Cells. **Cell**, v.181, n.6, p.1346-1363, 2020.

XAVIER, M.N.; PAIXÃO, T.A.; POESTER, F.P.; et al. Pathological, immunohistochemical and bacteriological study of tissues and milk of cows and fetuses experimentally infected with *Brucella abortus*. **J. Comp. Pathol**., v. 140, p.149-157, 2009.

Xavier, M.N.; Silva, T.M.A.; Costa, E.A.; et al. Development and evaluation of a species specific PCR assay for detection of *Brucella ovis* infection in rams. **Vet. Microbiol**, v.145, p.158–164, 2010.

XAVIER, M.N.; WINTER, M.G.; SPEES, A.M. et al. PPARγ-mediated increase in glucose availability sustains chronic *Brucella abortus* infection in alternatively activated macrophages. **Cell Host. Microbe**, v.14, p.159-170, 2013.

YANG, J.; LI, H.; WANG, Z.; YU, L.; et al. Dihydroartemisinin inhibits multiplication of *Brucella suis* vaccine strain 2 in murine microglia BV2 cells via stimulation of caspase-dependent apoptosis. **Mol. Med. Rep.**, v.20, n.5, p.4067–4072, 2019.

YOUNG, E.J. An overview of human brucellosis. **Clin. Infect. Dis**. v.21, p.283–289, 1995.

YOUNG, E.J.; GOMEZ, C.I.; YAWN, D.H.; MUSHER D.M. Comparison of *Brucella abortus* and *Brucella melitensis* infections of mice and their effect on acquired cellular resistance**. Infect. Immun**. v.26, p.680–685, 1979.

ZAVATTIERI, L.; FERRERO, M. C.; ALONSO PAIVA, I. M., S; et al. *Brucella abortus* Proliferates in Decidualized and Non-Decidualized Human Endometrial Cells Inducing a Proinflammatory Response. **Pathogens** (Basel, Switzerland), v.9, n.5, p.369., 2020.

ZEHENDER, C. M.; SEBASTIANI, A.; HUGONNET, A.; et al. Traumatic brain injury results in rapid pericyte loss followed by reactive pericytosis in the cerebral cortex. **Sci. Rep.,** v. 5, p. 134977, 2015.

ZHANG, X.; WANG, Y.; SONG, J.; et al. The endothelial basement membrane acts as a checkpoint for entry of pathogenic Tcells into the brain. **J. Exp. Med.**, v.217, p. e20191339, 2020.

ZWERDLING, A.; DELPINO, M. V.; BARRIONUEVO, P.; et al. *Brucella* lipoproteins mimic dendritic cell maturation induced by *Brucella abortus***. Microbes Infect.**, v.10, n.10-13, p.1346–1354, 2008.

ZWERDLING, A.; DELPINO, M. V.; PASQUEVICH, K. A.; et al. *Brucella abortus* activates human neutrophils. **Microbes Infect**, v.11, n.6-7, p.689–697, 2009.

Chapter II

Pericytes modulate endothelial inflammatory response during bacterial infection

Introduction

Pericytes comprise a heterogeneous population of cells that are located around blood vessels in the perivascular space in close contact with endothelial cells. Pericytes retain the capacity for proliferation and differentiation so they may be considered mesenchymal stem cells (Crisan et al., 2008; Armulik et al., 2011; Birbrair et al, 2017). Pericytes are in close contact with endothelial cells whose role in inflammation has been extensively characterized (Muller, 2016). Endothelial cells express adhesion molecules that are a key element for transendothelial migration of neutrophils towards sites of inflammation (Muller, 2016). Pericytes are also involved in this process by directly interacting with neutrophils through adhesion molecules, driving the neutrophils through gaps that facilitate neutrophil migration (Proebstl et al., 2012). However, pericytes have additional complex functions so evidences have emerged demonstrating the involvement of pericytes in many pathological conditions (Birbrair, 2019).

Pericytes and endothelial cells have physical and functional interactions through peg-socket junctions, which are considered essential for stability of blood vessels (Caruso et al., 2009; Armulik et al, 2011). Peg-socket junctions anchor these two cell types together, allowing exchanges between them through connexins, particularly connexin-43 (Cx43) (Li et al, 2011; Winkler et al, 2011). Cx-43 channels allow the transfer of ions, second messengers such as cAMP, and other small molecules between pericytes and endothelial cells (Gerhardt and Betsholtz, 2003; Armulik et al, 2005; Winkler et al, 2011; Maeda and Tsukihara, 2011).

The role of pericytes in angiogenesis and control of blood flow is well known (Hall et al., 2014; Ferland-McCollough et al., 2017; Nikolakopoulou et al., 2019). Additionally, pericytes play a role in innate immune responses. During acute inflammation induced by tumor necrosis

factor alpha (TNF-α) or lipopolysaccharide (LPS), post capillary pericytes express C-X-C Ligand 1 (CXCL1), which drives transmigration of neutrophils to the site of tissue damage (Girbl et al., 2018). Furthermore, activated precapillary and capillary pericytes express intercellular adhesion molecule 1 (ICAM-1), macrophage migration inhibitory factor (MIF), C-C motif chemokine ligand 2 (CCL2), and C-X-C motif chemokine ligand 8 (CXCL8) in order to attract and activate transmigrated neutrophils and macrophages (Stark et al., 2013). However, pericytes also have immunosuppressive properties, when these cells are co-cultured with activated T cells there is an impairment of T cell proliferation and production of interferon gamma (INF-γ) and TNF-α (Tu et al, 2011). In the retina, loss of pericytes during early stages of diabetic retinopathy results in increased leukocyte influx, hemorrhage, and microvascular lesions (Tu et al, 2011; Ogura et al, 2017), which is associated with increased production of CCL-2, IL-6, and TNF-α (Ogura et al, 2017). Pericytes also contribute to immunosuppression in the gliobastoma microenvironment *in vitro*, where pericytes negatively correlated with leukocyte recruitment and influx of $CD8^+$ T cells (Ochs et al, 2013).

During bacterial infection, invading pathogens are recognized by the host innate immune system that senses microbe-derived molecules known as pathogen-associated molecular patterns (PAMPs), which include LPS, peptidoglycans, lipoproteins, adhesins, enzymes, toxins, and nucleic acids. These molecules are recognized by Toll-like receptors (TLRs) (Kumat et al., 2011). Once PAMPs are sensed, innate immune cells trigger a pro-inflammatory response (Bonizzi and Karin, 2004). However, some pathogens can escape detection by innate immunity. For instance, LPS of *Brucella* spp., Gram-negative, facultative intracellular pathogens, has a non-canonical lipid A, making it a very weak TLR4 agonist (Moreno et al., 1981; Rasool et al., 1992; Freer et al., 1996; Lapaque et al., 2005; Lapaque et al., 2006). This feature of *Brucella* spp. makes them excellent tools to interrogate innate immune responses that are not dominated by TLR signaling. For the other side, *Listeria monocytogenes* is a Gram-positive bacteria that activated more the innate immune response, with different PAMPs, such as listeriolysin O and still can have a intracellular cycle and survival (Portnoy et al., 1988).

The role of pericytes during bacterial infections in general remains largely unknown. Based on the role of pericytes in inducing and suppressing inflammation in the context of different pathologic conditions, we aimed to test the hypothesis that pericytes modulate

inflammation during bacterial infections, using *Brucella*, *Listeria*, *Citrobacter* and *Escherichia coli* LPS.

Results

Pericyte cells are not permissive for *Brucella ovis* infection

In order to assess the influence of pericytes on endothelial-mediated inflammation, we elected to use a microbe that does not trigger strong inflammatory response. *Brucella ovis* was selected as a model organism to assess the role of pericytes in modulating inflammation due to its low intrinsic pro-inflammatory potential. Considering that *Brucella* can invade, survive, and multiply in many different cells *in vitro* and *in vivo* (Carvalho et al., 2023) first tested whether pericytes can serve as a niche for *B. ovis* infection. To this end, we inoculated cultured pericytes, endothelial cells, and macrophages with *B. ovis.* As expected, based on previous studies (Silva et al., 2011), *B. ovis* was able to invade and survive in macrophages, with an initial decrease in intracellular CFU numbers over the first 24 hours post infection (hpi), followed by intracellular multiplication from 24 to 48 hpi (Figure 2.1 A and 1B). Similarly, *B. ovis* invaded, survived, and multiplied in endothelial cells with kinetics similar to that observed in macrophages (Figure 2.1 B). However, an MOI of 1000 was required to achieve intracellular CFU numbers that were similar to those measured in macrophages infected with a MOI of 100. These results indicated that endothelial cells are permissive to *Brucella* spp. infection and intracellular survival (Ferrero et al., 2011). In contrast, *B. ovis* invaded pericytes in significantly lower numbers regardless of the MOI (either 100 or 1000). Importantly, there was no intracellular multiplication of *B. ovis* in pericytes with intracellular numbers remaining close to the limit of detection at 24 or 48 hpi (Figure 2.1A). Next, we evaluated the distribution of *B. ovis* in inoculated cultured cells. In good agreement with the intracellular CFU numbers, fluorescence microscopy demonstrated that *B. ovis* infected most of cultured macrophages and endothelial cells, but only occasionally infected pericytes (Figure 2.1 C).

Therefore, our data indicated that pericytes are significantly less permissive than endothelial cells and macrophages to internalization of *B. ovis* and are not permissive to its intracellular multiplication.

To investigated if low permissiveness of pericytes for the infection was restricted to *B. ovis* or if it can happens with other pathogens, for first tested whether pericytes can serve as a niche for *Listeria monocytogenes* infection. To this end, we inoculated cultured pericytes, endothelial cells, and macrophages with *L. monocytogenes* MOI (1:5). *L. monocytogenes* was able to invade and survive in macrophages and endothelial cells with an initial decrease in intracellular CFU numbers over 2 hpi, and increased the multiplication in 6 and 24 hpi (Figure 2.2 A). Similar what observed in *B. ovis* infection, *L. monocytogenes* invaded in significantly lower number pericytes in all times point. There results agree with previous infection with *B. ovis* and showed that pericytes are not permissive to intracellular multiplication. Besides, in Gram staining of cells infected with *L.monocytoges* agree with intracellular CFU numbers, demonstrated endothelial cells and macrophages more infected cells (Figure 2.2 C).

Although, *B. ovis* is known to have low cytotoxicity for most cells (Martín-Martín et al., 2010), considering that intracellular bacteria measured based on extracellular exposure to gentamicin may be influenced by host cell death, lactate dehydrogenase (LDH) release (as an indicator of host cell death) was measured after *B. ovis* infection. Therefore, LDH concentrations were measured in the supernatant of cultured pericytes, endothelial cells, and macrophages at 24 hpi with *B. ovis* (MOI 100). As predicted, cell death in *B. ovis*-inoculated pericytes, macrophages, and endothelial cells was very low as demonstrated by a minimum LDH release (Figure 2.2 B), indicating that intracellular CFU counts were not affected by host cell death in this study.

L. monocytogenes caused cell death due to misregulation of listeriolysion O. Due to listeriolysin O is used for the bacteria scape to the phagosome inside the cells, and this activity is cholesterol-dependet, that results in cells death (Portonoy et al., 1988). For this reason, for all cells experiments, we used a low MOI of infection. In the LDH (Figure 2.2 B) release, we demonstrated the low levels of cell death in the selected MOI, allow us to avoid cytotoxicity.

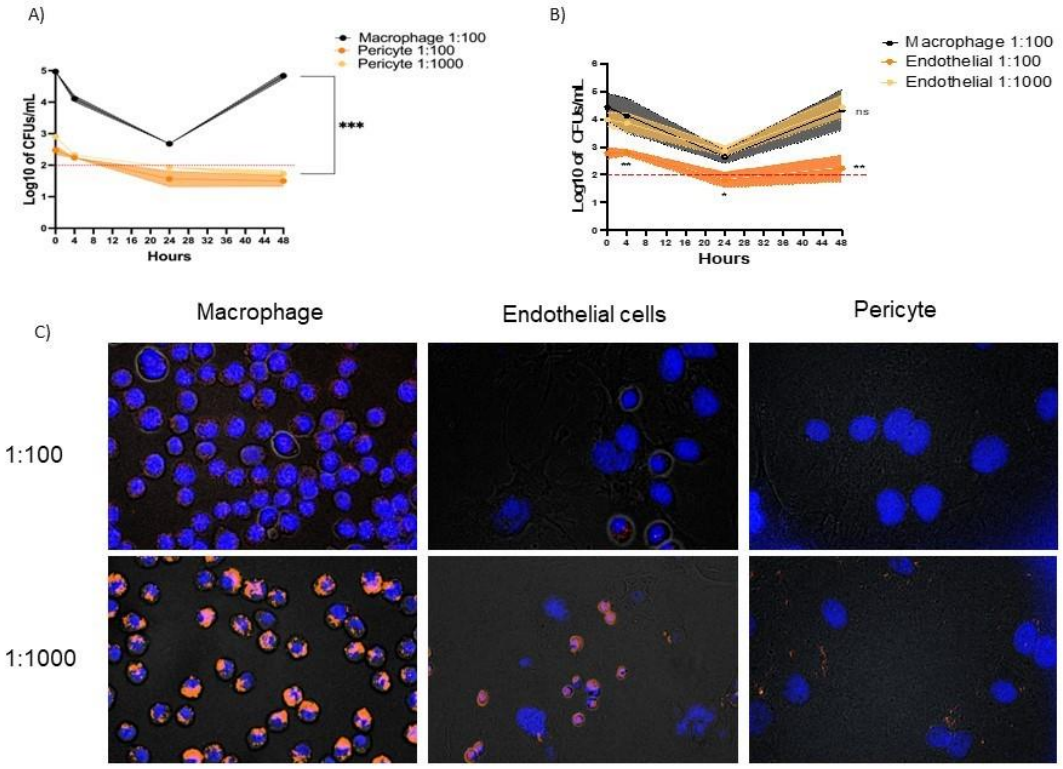

Figure 2.1 *Brucella ovis* kinetics *in vitro* curve in different types of cells. $1x10^5$ per well, pericytes (A), macrophages (A, B) or endothelial cells (B) were infected with two different MOI of *B. ovis.* Immunofluorescence of macrophages, endothelial cells and Pericytes infected with different MOI (1:100 and 1:1000) of *B. ovis mCherry* (red) and DAPI in blue. Each point represents the average of triplicate, representative of three different experiments. A LOG transformation normalized the CFU numbers. The statistical analysis was performed by ANOVA. The statistical test used was Wilcoxon test (*p<0.05; **p<0.01; ***p<0.001).

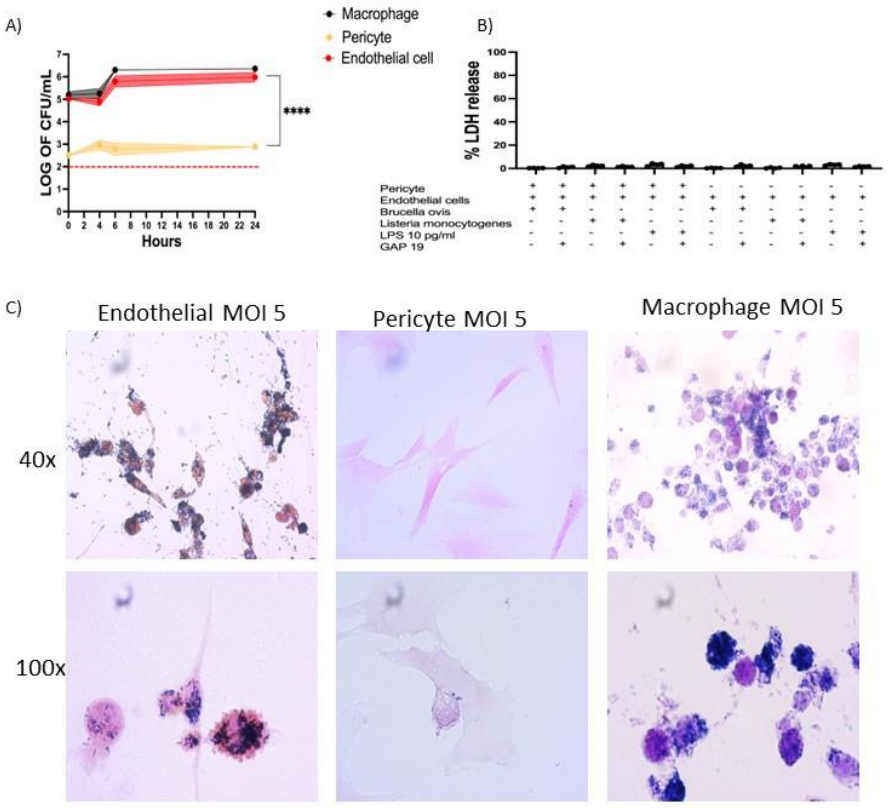

Figure 2.2 *Listeria monocytogenes* kinetics *in vitro* curve in different types of cells. $1X10^5$ per well, pericytes, macrophages and endothelial cells (A) were infected with *L. monocytogenes* (1:5). LDH assay for measure cytotoxicity (B). Gram staining for infected cells with *L. monocytogenes* with cells cytoplasm in pink and Gram-positive (*L. monocytogenes)* bacteria in blue color. Each point represents the average of triplicate, representative of 3 different experiments. A LOG transformation normalized the CFU numbers. The statistical analysis was performed by ANOVA. The statistical test used was Wilcoxon test (*p<0.05; **p<0.01; ***p<0.001).

In order to evaluate the interaction or tropism of *B. ovis* to pericytes *in vivo*, we infected nestin-GFP mice, which have nestin$^+$ pericytes that constitutively express GFP, with *B. ovis*-mCherry (1×10^6 CFU/mice), and sections of the liver and spleen were analyzed by fluorescent microscopy at six days post infection (dpi). Fluorescent *B. ovis*-mCherry was detected as clusters associated with host cells, but it did not colocalized with pericytes in any of the samples evaluated (Figure 2.3).

Together, these results support the notion that pericytes are less permissive to *B. ovis* and *L. monocytogenes* invasion and intracellular multiplication, when compared to endothelial cells and macrophages. Furthermore, there is no evidence of *B. ovis* tropism to pericytes *in vivo* in the mouse.

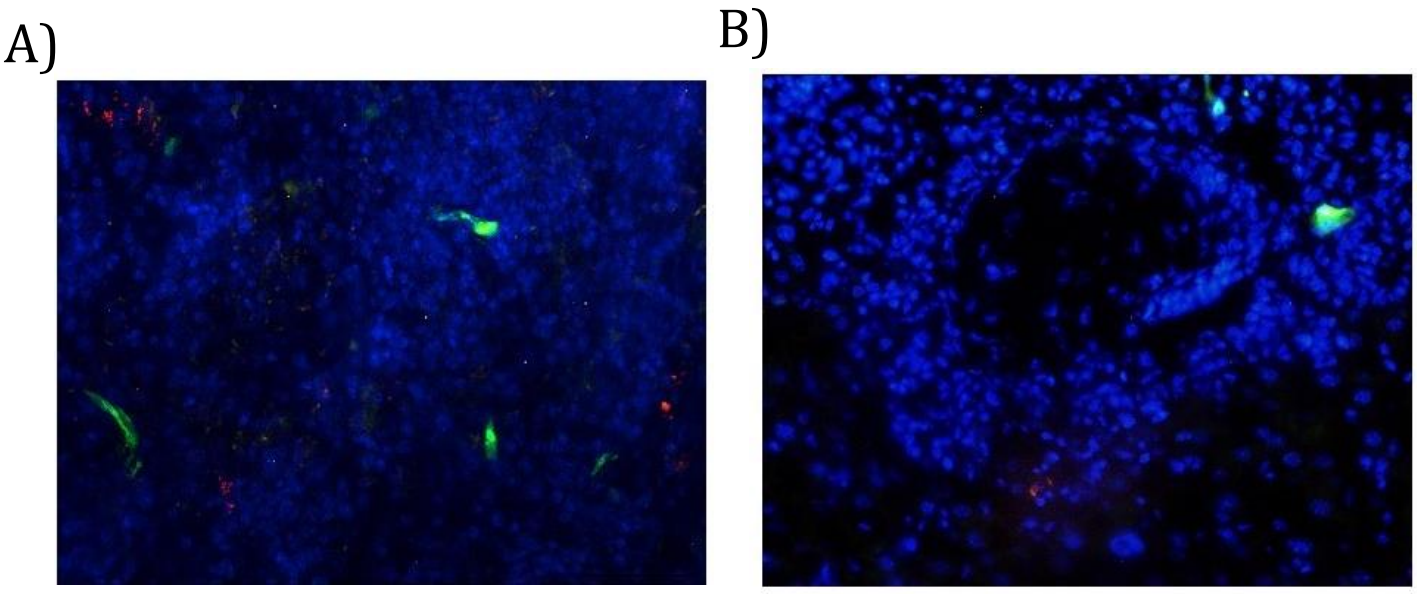

Figure 2.3 Immunofluorescence of Pericytes and *Brucella ovis mCherry*. Transgenic mice that express GFP protein (green) associated with nestin protein present in pericyte were infected with *B. ovis mCherry* (red) $1x10^6$CFU per mice via intraperitoneal route. Co-localization of pericyte (green) and *B. ovis* was analyzed in liver (A)and spleen (B).

Pericytes downregulate expression of inflammatory mediators and adhesion molecules in endothelial cells stimulated with *B. ovis*

Considering the role of pericytes controlling leukocyte migration though the vascular wall (Ogura et al, 2017; Torok et al 2021), and the expression of Ig-like cell adhesion molecules (CAMs), namely ICAM-1/CD54, ICAM-2/CD102, VCAM-1/CD106, and PECAM-1/CD31 (Schnoor et al., 2015; Timmerman et al, 2016) by endothelial cells, which is a key step during the initial phase of acute inflammation, we assessed whether pericytes influence expression of

adhesion molecules by endothelial cells during infection with *B. ovis* (MOI 100). Transcriptional levels of *Icam1* (also known as CD54) and *Pecam1* (also known as CD31) were determined at 24 hpi. When endothelial cells were co-cultured with pericytes there was downregulation of *Icam1* and *Pecam-1* when compared with endothelial cells alone with reductions of 39.21 and 129.64 folds in mRNA levels of *Icam1* and *Pecam1* at 24 hpi, respectively (Fig. 2.4 A and 2.4 B). These results suggest that pericytes downregulate transcription levels of *Icam1* and *Pecam1* in endothelial cells. To further characterize reduction of adhesion molecules when endothelial cells are in contact with pericytes, we performed immunofluorescencent detection of PECAM-1. Endothelial cells alone had marked expression of PECAM-1 when inoculated with *B. ovis* (Fig. 2.4 C), whereas expression of PECAM-1 was markedly suppressed when endothelial cells were co-cultured with pericytes (Fig. 2.4 C).

In addition to expression of adhesion molecules, endothelial cells enhance the inflammatory response by triggering expression of proinflammatory genes such as *Tnfα, Il6* and *Ccl2* when exposed to PAMPs (Ferrero et al., 2011; Luyendyk et al., 2019). Therefore, transcription levels of *Tnfα, Il6*, and *Ccl2* were measured in endothelial cells alone or endothelial cells co-cultured with pericytes at 24 hpi with *B. ovis* (Figure 2.5A and 2.5 B). *Tnfα Il6*, and *Ccl2* were upregulated in endothelial cells infected with *B. ovis* with increases of 437.84, 2,365.82 and, 343.39 fold changes in mRNA levels at 24 hpi, respectively. These results indicate that pericytes suppress expression of adhesion molecules and inflammatory mediators by cultured endothelial cells during the course of *B. ovis* infection.

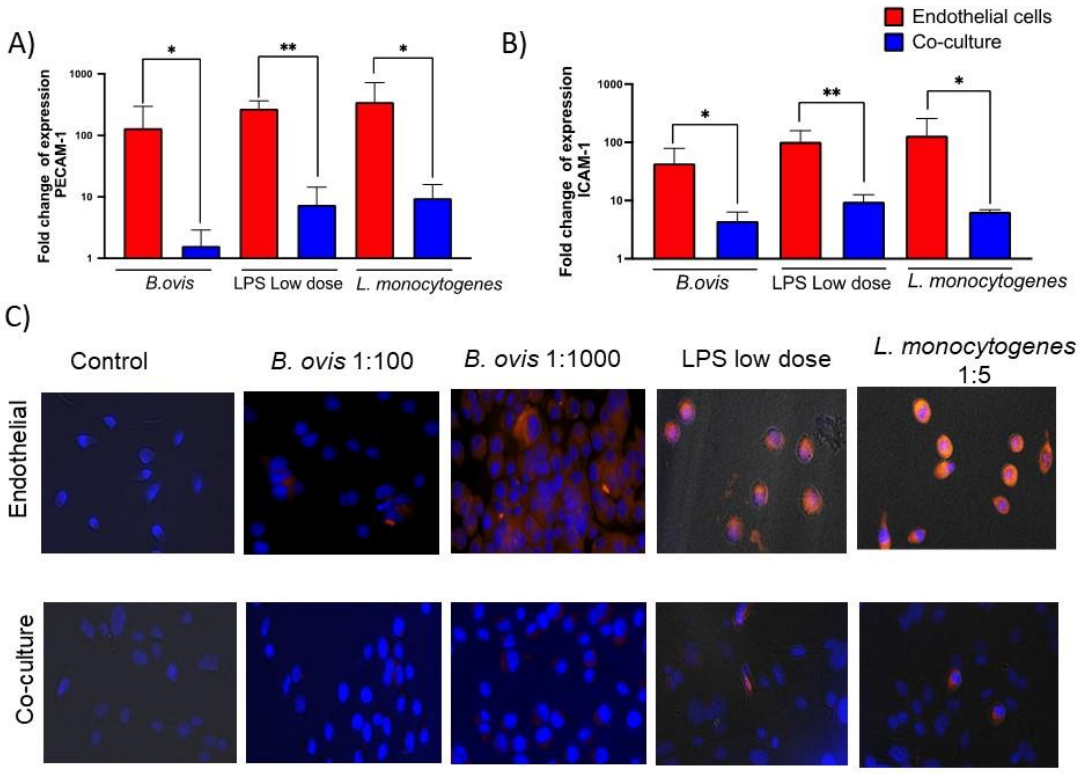

Figure 2.4 Expression of adhesion molecules' profile in culture co-culture of pericytes and endothelial cells challenge with different bacterial stimuli. Transcriptional profile of co-cultured of endothelial cells and pericytes (2:1) or endothelial cells alone infected or not infected with *Brucella ovis* (MOI 1:100), *Listeria monocytogenes* (MOI 1:5) and *E. coli* LPS in low dose at 24 hour after stimulation (A) *Pecam1* and (B) *Icam1* as fold change in comparison to uninfected controls. Bars represent mean and standard deviations of triplicate. The statistical analysis was performed by ANOVA. The statistical test used was Wilcoxon test (*$p<0.05$; **$p<0.01$). PECAM-1 (red) expression in the immunofluorescence of the same *in vitro* condictions,

Pericyte modulation of endothelial inflammatory response is conserved in response to various bacterial pathogens

In order to evaluate whether the modulation of expression of adhesion molecules and inflammatory mediators was specific to *B. ovis*, different stimuli were employed: *L. monocytogenes* (MOI 5), and purified *Escherichia coli* LPS (10 pg/mL). Considering the possibility of cytotoxicity, LDH was measured in the supernatant of cultures exposed to these stimuli. Under the same experimental conditions of endothelial cells alone or co-cultured with pericytes stimulated with *E. coli* LPS or inoculated with *L. monocytogenes* exhibited minimum LDH release (~less that 10%) (Figure 2.2 B).

Similar to our previous results during the infection with *B. ovis*, both *L. monocytogenes* and *E. coli* LPS triggered expression of adhesion molecules (ICAM-1 and PECAM-1) (Figure 2.4 A) and in pro-inflammatory genes (*Tnfα, Il6*, and *Ccl2*) as demonstrated by mRNA levels (Figure 2.5 A and B). In contrast, when endothelial cells were co-cultured with pericytes, there was down-regulation of adhesion molecules and inflammatory mediators when exposed to *E. coli* LPS or *L. monocytogenes* under the same experimental conditions (Figure 2.2 B). These results indicate that the modulation of endothelial cells inflammatory response by pericytes is not specific for *B. ovis*, occurring in response to various inflammatory stimuli such as a Gram-positive pathogen (*L. monocytogenes*) or a strong TLR4 agonist (*E. coli* LPS).

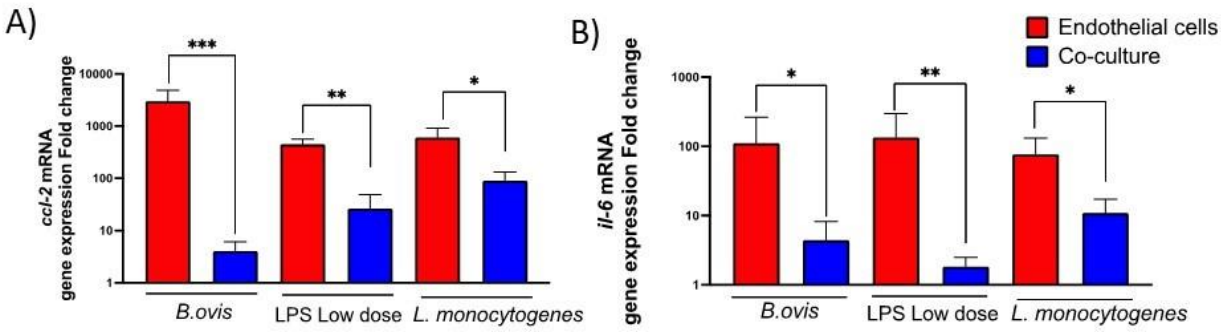

Figure 2.5 Transcriptional inflammatory profile in cell culture co-culture of pericytes and endothelial cells challenge with different bacterial stimulus. Transcriptional profile of co-cultured of endothelial cells and pericytes (2:1) or endothelial cells alone infected or not infected with *Brucella ovis* (MOI 1:100), *Listeria monocytogenes* (MOI 1:5) and *E. coli* LPS in low dose at 24 hours after stimulation (A) *Ccl2* (B), *Il6 a*s fold change in comparison to uninfected controls. Bars represent mean and standard deviations of triplicate of one experiment representative of in three repetitions. The statistical analysis was performed by ANOVA. The statistical test used was Wilcoxon test (*p<0.05; **p<0.01; ***p<0.001).

The stealthy pathogen *Brucella ovis* induces marked acute inflammation *in vivo* in pericyte-depleted mice

The neuron-glial antigen 2 proteoglycan (NG2) is one of the most reliable known markers for arteriolar and capillary pericytes (Navarro et al., 2016; Yamazaki and Mukouyama, 2018). The NG2 glycoprotein, also known as chondroitin sulfate proteoglycan-4 (CSPG-4), is a cell surface component that plays an essential role in pericyte maturation, inducing proliferation and motility, favoring tissue remodeling and neovascularization (Ozerdem et al, 2001; Ozerdem et al, 2002; Ozerdem et al, 2003; Couchman, 2003; Gibby et al, 2012). To investigate the role of pericytes in modulating acute inflammation *in vivo*, we used double-transgenic mice (NG2creER™ x iDTR), in which NG2-expressing pericytes can be induced to express diphtheria toxin receptor (DTR) after treatment with tamoxifen (Figure 2.6 A). This allows for selective depletion of NG2-expressing pericytes upon treatment of transgenic mice with tamoxifen

followed by diphtheria toxin. Isogenic iDTR C57BL/6 mice (without depletion of pericytes, but subjected to the same treatment protocol) were used as controls. Mice were infected intraperitoneally (IP) with 10^6 CFU of *B. ovis*, and were sampled at 1, 5, and 15 dpi (Figure 2.6 B). Depletion of $NG2^+$ pericytes was confirmed by immunohistochemistry using a monoclonal antibody targeting the NG2 glycoprotein on liver samples (Fig. 2.6 C). In non-depleted mice, $NG2^+$ immunostained cells were located in the space of Disse positioned around the sinusoids, similar to previous reports (Sato et al., 2003). In contrast livers of pericyte-depleted mice exhibited a marked reduction in $NG2^+$ immunostaining (Fig. 2.6 C).

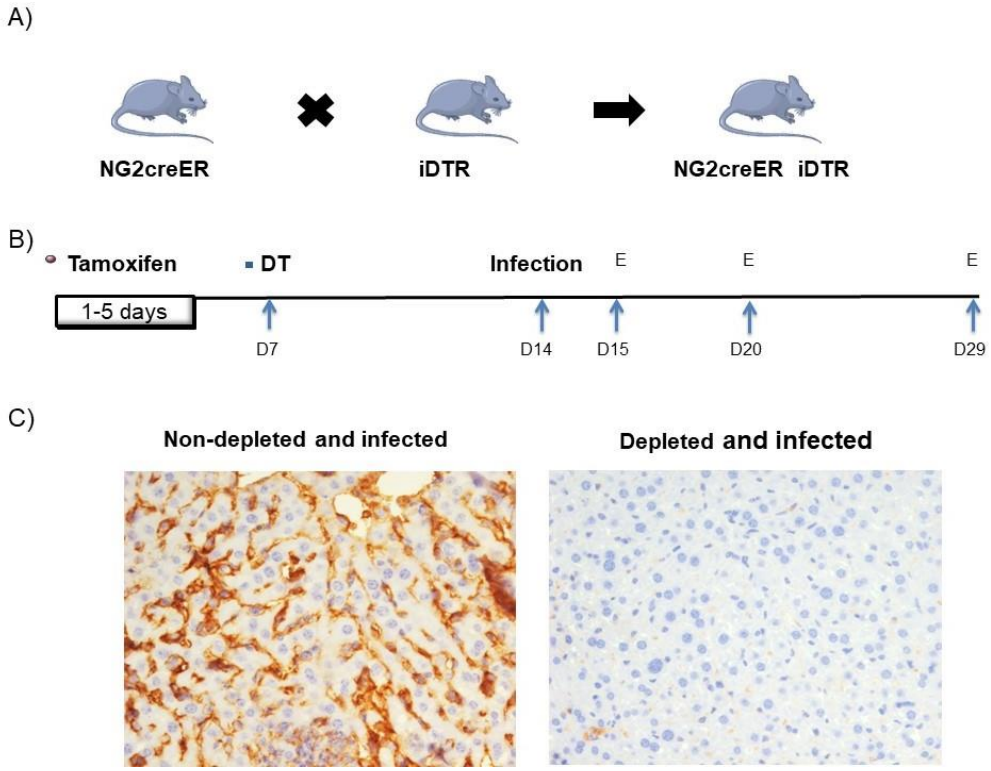

Figure 2.6 Mouse model used for the depletion of Pericyte. Breeding pairs for generated of experimental animals (A). The depletion process and time of infection and end point (represented by "E") (B). Immunohistochemistry for NG2 (pericyte) for confirming the depletion (C).

We next determined the effect of pericyte depletion on *B. ovis* infection. Based on previous studies, we did not expect *B. ovis* to cause lethal infections in mice (Silva et al., 2011), which was confirmed in our control mice, that exhibited no clinical signs of infection. In contrast, 5 out of 10 pericyte-depleted mice developed clinical signs starting at 4 dpi. These mice had lethargy, curved backs, bristly pelts, shaking, and abdominal rigidity, with unexpected lethal outcomes in 30% (3/10) of mice (Figure 2.7 A). In addition, infected mice were sampled at 1, 5, and 15 dpi, allowing an assessment of pathologic changes during the course of infection. At 1 dpi none of the mice had gross changes, but at 6 or 15 dpi all pericyte-depleted mice infected with *B. ovis* developed acute fibrinous peritonitis. In contrast, none of the infected non-depleted mice or uninfected, pericyte-depleted controls developed any gross lesions in the peritoneal cavity (Fig. 2.7 B). The abdominal cavities of pericyte-depleted mice infected with *B. ovis* contained large amounts of fibrin adhered to the surface of the liver, spleen and other abdominal organs characterizing a severe diffuse fibrinous peritonitis (Fig. 2.7 B). In contrast, neither control (non-depleted) infected mice nor mock-infected, pericyte-depleted mice developed peritonitis. All infected mice (pericyte-depleted or non depleted) developed splenomegaly with multifocal white-yellow areas in the liver and spleen. Microscopic analysis confirmed the diagnosis of fibrinous peritonitis in pericyte-depleted mice infected with *B. ovis*. The hepatic parenchyma adjacent to the capsule had marked hepatocellular degeneration (cytoplasmic vacuolation and nuclear pycnosis), with mild to moderate neutrophilic and histiocytic peri-hepatitis, which was interpreted as degenerative process secondary to peritonitis. None of these changes were observed in non depleted and infected mice.

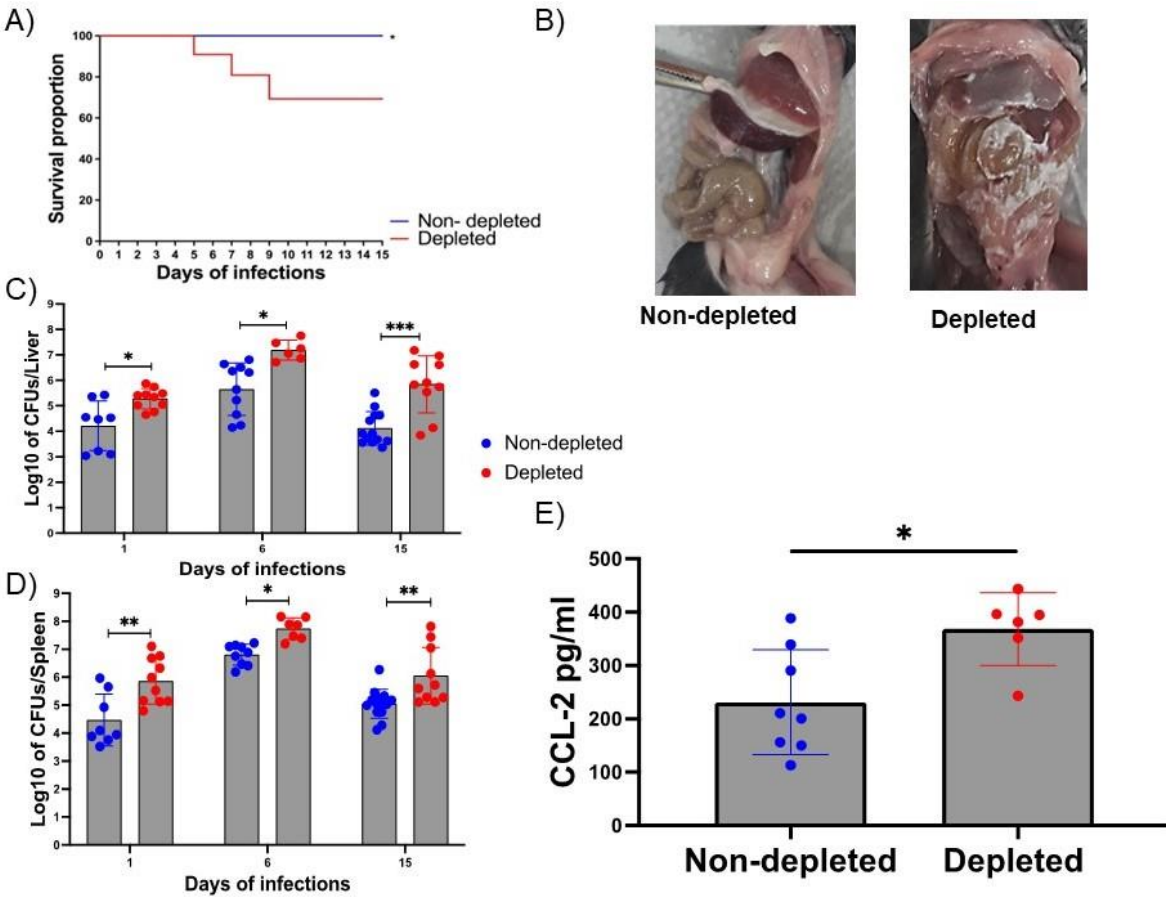

Figure 2.7 Effects of depletion of pericyte in *Brucella ovis* infection. Transgenic mice with depletion of pericyte were infected with $1x10^{6}$ CFU of *B. ovis* intraperitoneal. Transgenic mice for pericyte depletion or non-depleted mice were infected with $1x10^{6}$ CFU of *B. ovis* per animal. Gross change in the peritoneal cavity of mice pericyte depleted or not infected with *B. ovis* (A). Survival curve of mice (B). Bacteriology of the liver (C) and spleen (D) were collected for bacteriology analysis. ELISA was used to measure CCL-2 in each animal's serum (E). A LOG transformation normalized the CFU numbers. Each point represents the mouse value, while the bars represent the mean of each group and the standard difference. The statistical analysis was performed by ANOVA. The statistical test used was Wilcoxon test (*p<0.05; **p<0.01; ***p<0.001).

We next determined the effect of pericyte depletion on other bacterial model, such as *L. monocytogenes* infection. Both infected groups, depleted and non-depleted showed weight loss and clinical signals (Figure 2.8 A). Both groups showed lethargy, shivers, conjunctivitis and diarrhea. However, the depleted and infected mice showed more clinical manifestation (Figure 2.8 B). All pericyte-depleted mice infected with *L. monocytogenes* developed acute fibrinous peritonitis. In contrast, none of the infected non-depleted mice or uninfected, pericyte-depleted controls developed any gross lesions in the peritoneal cavity (Fig. 2.8 C), such we observed in the previous experiment. The bacteria recovery in the liver and spleen was higher in depleted mice (Figure 2.8 D and E). Besides, depleted group and infected with *L.monocytogenes* showed more CCL-2 in serum (Figure 2.8 E).

To ensure that peritonitis in pericyte-depleted mice were not due to other opportunistic pathogens, abdominal contents from pericyte-depleted and infected mice (with peritonitis) as well as from non-depleted and infected mice or uninfected controls were cultured for bacterial isolation. No pathogenic or opportunistic microorganism other than *B. ovis* or *L. monocytogenes* in the case of infected mice, were cultured from the abdominal cavity, demonstrating that the peritonitis in infected pericyte-depleted mice was caused by *B. ovis* and *L. monocytogenes* infection.

Together these results indicate that, as demonstrated in cultured cells, pericytes restrain the acute inflammatory response *in vivo* since *L. monocytogenes* or even *B. ovis*, which is a stealthy pathogen that does not trigger inflammation when inoculated intraperitoneally in mice, is capable of inducing an acute severe inflammatory response in the abdominal cavity in the absence of pericytes.

Live virulent *Brucella ovis* is required for eliciting inflammation in pericyte-depleted mice

Fibrinous peritonitis was a consistent finding in pericyte-depleted mice intraperitoneally infected with *B. ovis*. *Brucella* sp. as well as other intracellular bacteria developed strategies for intracellular survival and multiplication. The *virB* operon-encoded type IV secretion system (T4SS) is required for intracellular survival of *Brucella* spp. (Celli, 2019) Indeed, strains lacking a functional T4SS are not capable of evading lysosomal degradation, and neither replicate nor survive in host cells. In this context we investigated whether a mutant *B. ovis* strain lacking a functional T4SS or inactivated *B. ovis* (gamma irradiated) could induce peritonitis in pericyte-depleted mice. At 6 dpi, consistent with our previous experiments, all pericyte-depleted mice that were infected with wild type *B. ovis* developed peritonitis (based on both gross and histologic findings), whereas none of the pericyte-depleted mice infected with *B. ovis* Δ*virB2* (strain lacking a functional T4SS) or inoculated with inactivated, but structurally intact gamma irradiated *B. ovis* developed peritonitis (Table 1).

Table 1. Peritoneal changes in the abdominal cavity with different bacterial inoculum of *Brucella ovis*

Group	**N**	**Infection**	**Fibrinous peritonitis**
Non depleted and infected with WT *B. ovis*	5	$1x10^6$ *B. ovis* ATCC	Absent
Depleted and infected with WT *B. ovis*	4	$1x10^6$ *B. ovis* ATCC	Present*
Non depleted and infected Δ*virB2 B. ovis*	5	$1x10^6$ *B. ovis virB*2	Absent
Depleted and infected Δ*virB2 B. ovis*	5	$1x10^6$ *B. ovis virB*2	Absent
Non depleted and inoculated with γ-irradiated *B. ovis*	3	$1x10^6$ *B. ovis* γ-irradiated	Absent
Depleted and inoculated with γ-irradiated *B. ovis*	4	$1x10^6$ *B. ovis* γ-irradiated	Absent

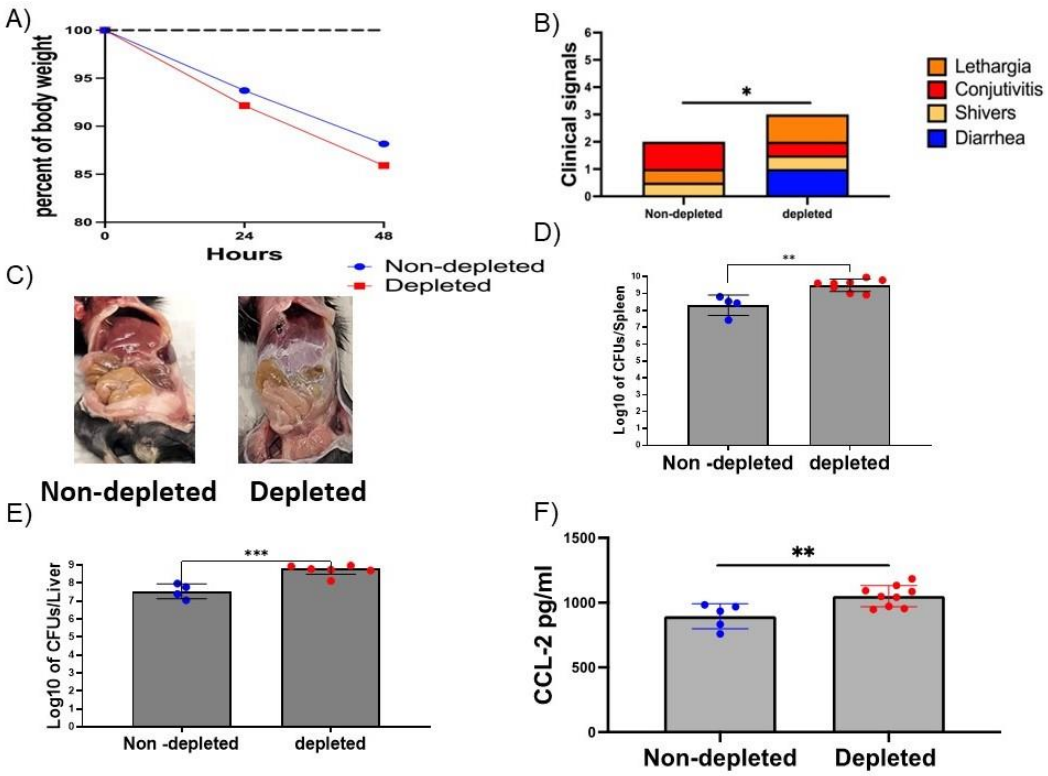

Figure 2.8 Effects of depletion of pericyte in *Listeria monocytogenes* infection. Transgenic mice with depletion of pericyte were infected with $5x10^4$ CFU of *L. monocytogenes* intraperitoneal. Clinical changes after *L. monocytogenes* infection in non-depleted and depleted mice. Transgenic mice for pericyte depletion or non-depleted mice were infected with *L. monocytogenes* $5x10^4$ CFU per mice. The weight was measured every day starting the day before infection until the end point (A). The percentage of weight was calculated as 100% before infection. In 48 hours post infection animals showed different clinical signs in both groups (B). Gross change in the peritoneal cavity of mice pericyte depleted or not infected with *L. monocytogenes* (C). After 48 hours post infection the liver (D) and spleen (E) were collected for bacteriology analysis. ELISA was used to measure CCL-2 in the serum of each mouse (F). A Log transformation normalized the CFU numbers. Each point represents the mouse value, while the bars represent the mean of each group and the standard difference. The statistical analysis was performed by ANOVA. The statistical test used was Wilcoxon test (*$p<0.05$; **$p<0.01$).

Pericyte depletion increased systemic *Brucella ovis* and *Listeria monocytogenes* dissemination in mice

To determine whether pericytes limit bacterial dissemination from the site of infection, we determined bacterial loads in the liver and spleen of control and pericyte-depleted mice. At 1 dpi, pericyte-depleted mice had approximately tenfold more bacteria in the liver and spleen in *B. ovis* (Figure 2.7 C and 2.7 D) and *L. monocytogenes* (Figure 2.8 D and 2.8 E), suggesting that pericytes contribute to controlling dissemination of bacterial infection. Additionally, we measure the CCL-2 in the serum of the mice infected depleted or not. The CCL-2 levels are increased in the depleted and infected mice with *B. ovis* (Figure 2.7 E) and *L. monocytogenes* (Figure 2.8 F) in agreement with what we found previously in our co-culture model. Also, in agreement with our co-culture model, it was demonstrated the presence of more amount of mRNA of *Pecam-1* per in situ hybridization on the liver of depleted mice infected with *B. ovis* (Figure 2.9).

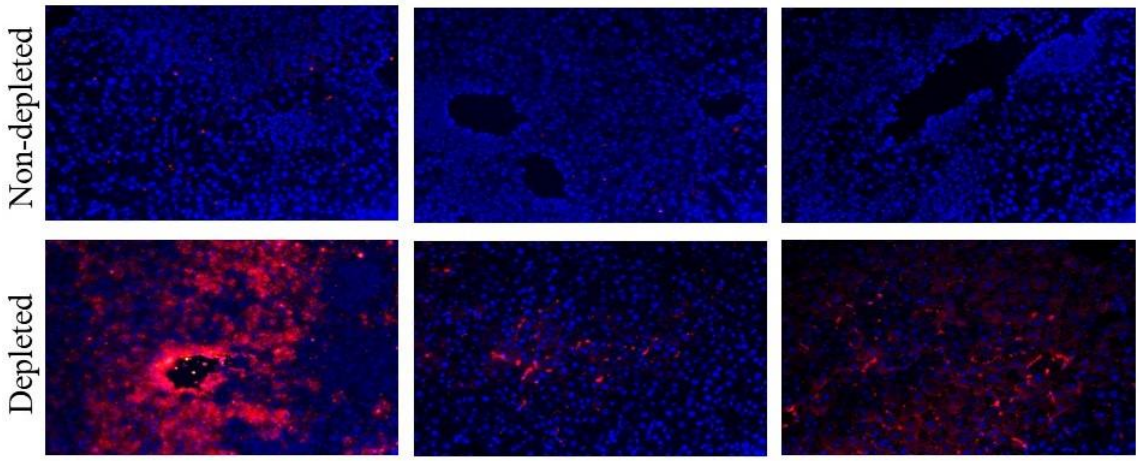

Figure 2.9 In situ hybridization for *Pecam1* in the mice depleted or not for pericyte and infected with *Brucella ovis.* ISH signals are in red, and the nucleus were marked with DAPI (blue) in the liver. Each picture represents one animal, and they are representative for the group.

The difference of colonization persisted at 6 dpi, and increased by 15 dpi when it reached approximately 10 or 100-fold difference in the spleen or liver, respectively. Interestingly, the attenuated *B. ovis* Δ*virB2* strain, which is deficient in its T4SS, was also recovered in

approximately tenfold higher numbers from the livers and spleens of pericyte-depleted mice compared to control mice (Fig. 2.10 A and 2.10 B). Thus, the absence of pericytes did not enable the *B. ovis* T4SS mutant to replicate at wild type levels in tissue (Fig. 2.10 A and 2.10 B), but rather permitted it to disseminate from the inoculation site to liver and spleen. Pericyte-depleted mice had significantly lower numbers of *B. ovis* Δ*virB2* in the liver and spleen, when compared to the wild type strain, indicating that pericyte-depleted mice were still able to largely control *B. ovis* Δ*virB2.*

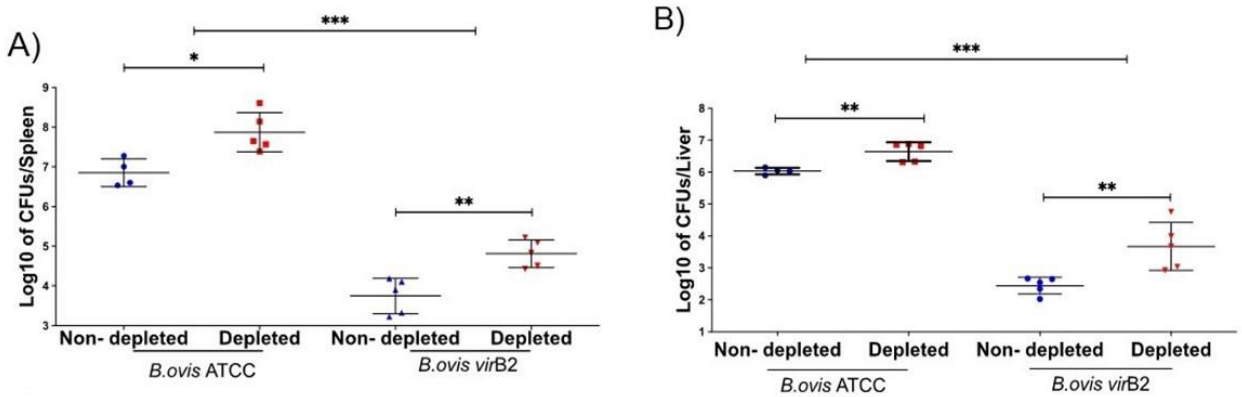

Figure 2.10 Effects of depletion of pericyte in infection with *Brucella ovis* Δ*virB2* infection. Transgenic mice with depletion of pericyte were infected with $1x10^6$ CFU of *B. ovis* Δ*virB2* or *B. ovis* wt intraperitoneal. Bacteriology analysis of spleen (A) and liver (B). A LOG transformation normalized the CFU numbers. Each point represents the mouse value, while the bars represent the mean of each group and the standard difference. The statistical analysis was performed by ANOVA. The statistical test used was Wilcoxon test (*$p<0.05$; **$p<0.01$).

One possible explanation for the increased inflammatory pathology in the pericyte-depleted mice is the increased bacterial infection levels in tissue. To explore this possible mechanism, C57BL/6 mice were intraperitoneally infected with 10^7, 10^8, or 10^9 CFU of wild type *B. ovis* and euthanized at 1, 3, or 7 dpi for assessment of inflammatory responses (Figure 2.11 A).

None of the challenge doses at any of the time points elicited gross or microscopic changes in the peritoneal cavity. These results indicated that the *B. ovis*-induced peritonitis is pericyte-depleted mice is due to absence of pericytes, not to higher bacterial loads (Figure 2.11 B). As expected, *B. ovis* CFU numbers in the spleen and liver were higher in mice subjected to higher challenge doses (Figure 2.11 C-D), indicating that systemic colonization in mice is dose-dependent under these experimental conditions. Importantly, even with similar *B. ovis* CFU numbers in tissues comparing wild type mice infected with the highest challenge dose and pericyte-depleted mice (between 10^7 and 10^8 in the spleen), there were neither gross nor histological signs of peritonitis.

Microscopic lesions were similar in all wild type *B. ovis* infected mice, but pericyte-depleted mice developed more severe lesions when compared to infected non depleted mice at 6 dpi (Fig. 2.12 and 2.13). However, fibrinous peritonitis was observed only in infected pericyte-depleted mice. Infected mice had moderate to severe multifocal randomly distributed inflammatory infiltrates in the liver and spleen, composed of epithelioid macrophages, neutrophils and lymphocytes, associated with moderate multifocal necrosis and thrombosis in the liver. Immunohistochemistry demonstrated intralesional *B. ovis* in hepatic and splenic lesions of all infected mice, confirming that the inflammatory lesions were due to *B. ovis* infection. Immunostained *B. ovis* was mostly associated with macrophages and neutrophils. Although intralesional *B. ovis* was detected in all infected mice, immunostaining was more intense in the liver and spleen from pericyte-depleted mice compared to non-depleted mice. Importantly, immunostained *B. ovis* was associated with fibrin deposits in the peritoneum of pericyte-depleted mice.

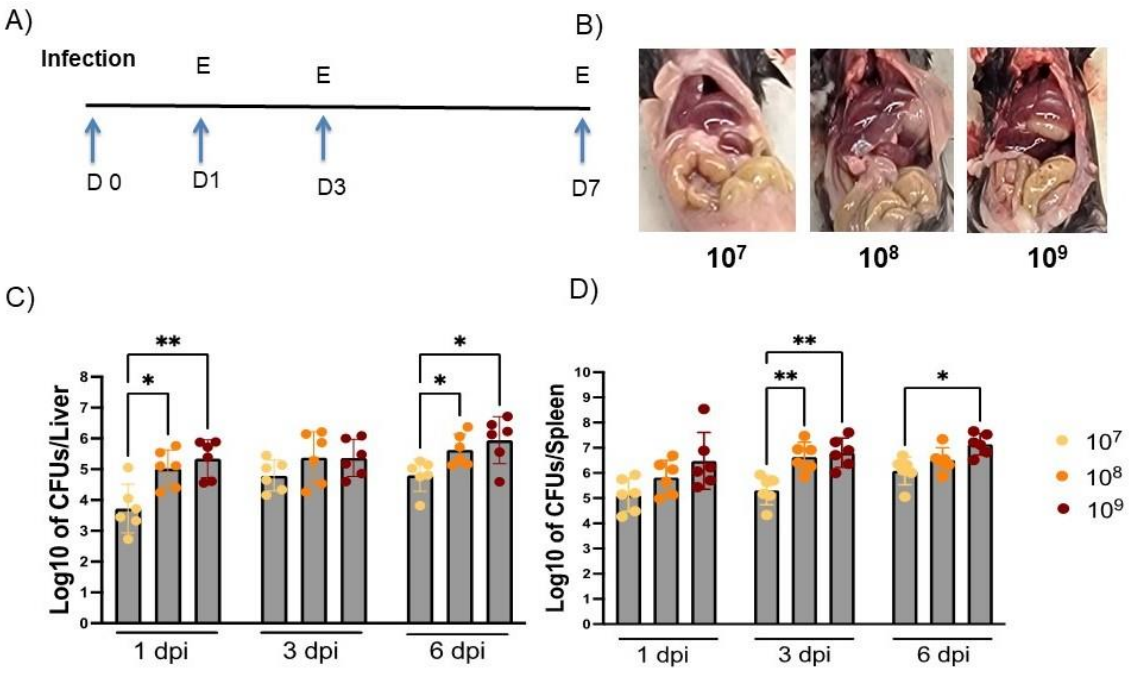

Figure 2. 11 High dose challenge with *Brucella ovis*. Squematic drawing of the experimental challenge with C57bl 6 mice were infected with $1x10^7$, $1x10^8$ or $1x10^9$ *B. ovis* intraperitoneal injections and euthanasia was performed 1, 3 and 6 days after infection (A). No significant peritoneal gross was observed in any of the groups (B). The bacteriology of the liver (C) and spleen (D) was performed at each time point. A LOG transformation normalized the CFU numbers. Each point represents the mouse value, while the bars represent the mean of each group and the standard difference. ANOVA performed the statistical analysis. (*p<0.05; **p<0.01).

Besides, the microgranuloma lesion in the liver, under the hepatic capsule, the hepatocyte cytoplasm contained multiple, colorless, well-defined vacuoles associated with nuclear pycnosis. Moreover, mild to moderate infiltration of neutrophils and macrophages caused degeneration on the hepatic capsule and neutrophilic-histiocytic perihepatitis in the areas that showed depletion of pericyte (Supplementary Figure 1 A and B). The vacuoles were PAS negative (Supplementary Figure 1 C). None of such alterations were found in livers of infected non-depleted mice. Besides, we so a accumulation of mRNA of *Pecam1* in the ISH in the areas of these lesions. We still do not know the cause of this histologic lesion in the depleted animals.

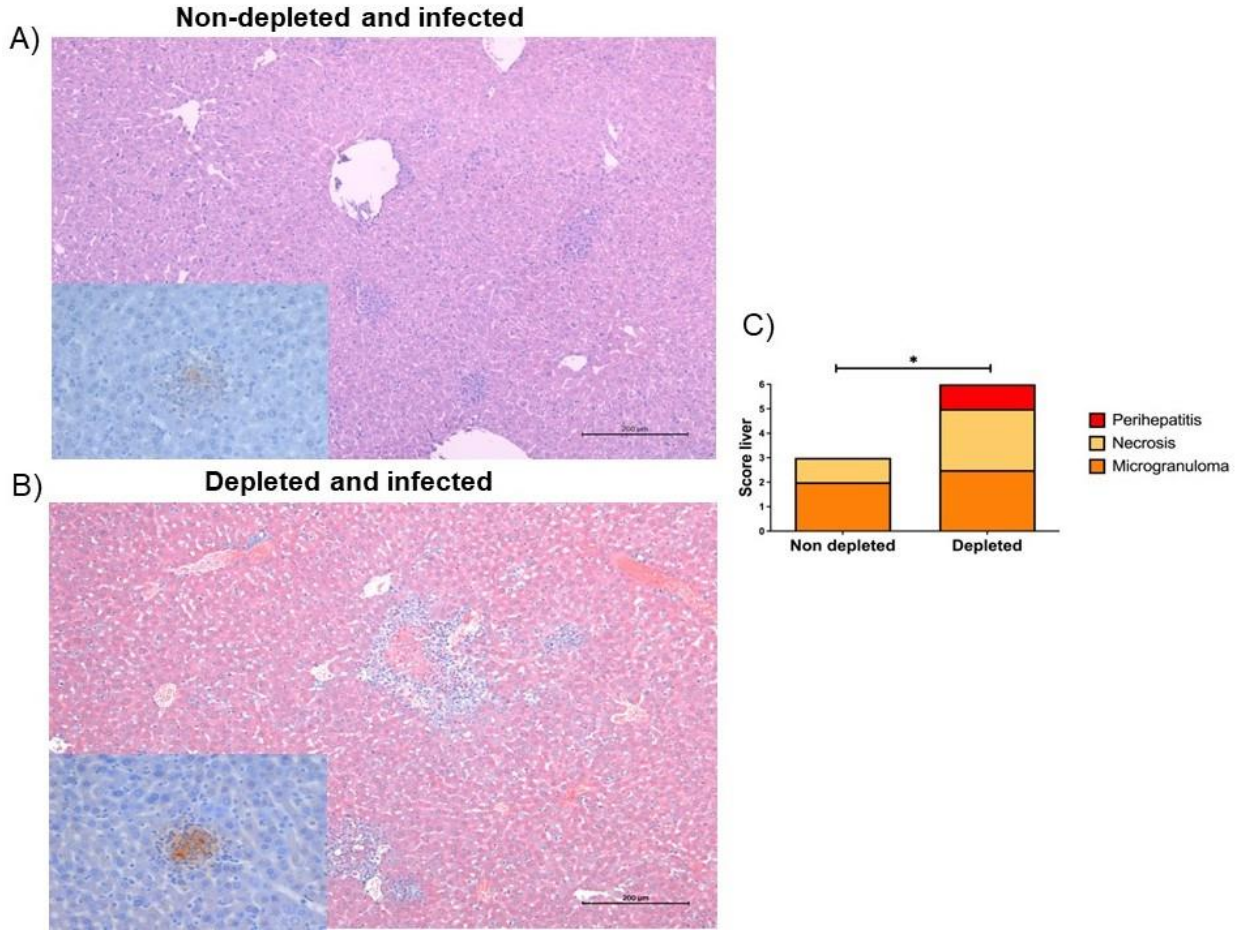

Figure 2.12 Microscopic changes in the liver of pericyte depleted animals infected with *Brucella ovis*. Liver of infected mice non-depleted (A) and pericyte depleted (B). In both groups showed microganulomas associated with necrosis, with immunolabeled intralesional *Brucella ovis*. Score of liver lesion of experimental mice (C). Bar represented the median of groups. The groups were compared with Kruskal Wallys (*$p<0.05$)

These results suggest pericytes partially prevent systemic dissemination and colonization of *B. ovis* in experimentally infected mice, and pericyte-deplete mice develop more severe lesions associated Brucella infection with abundant intralesional *B. ovis*.

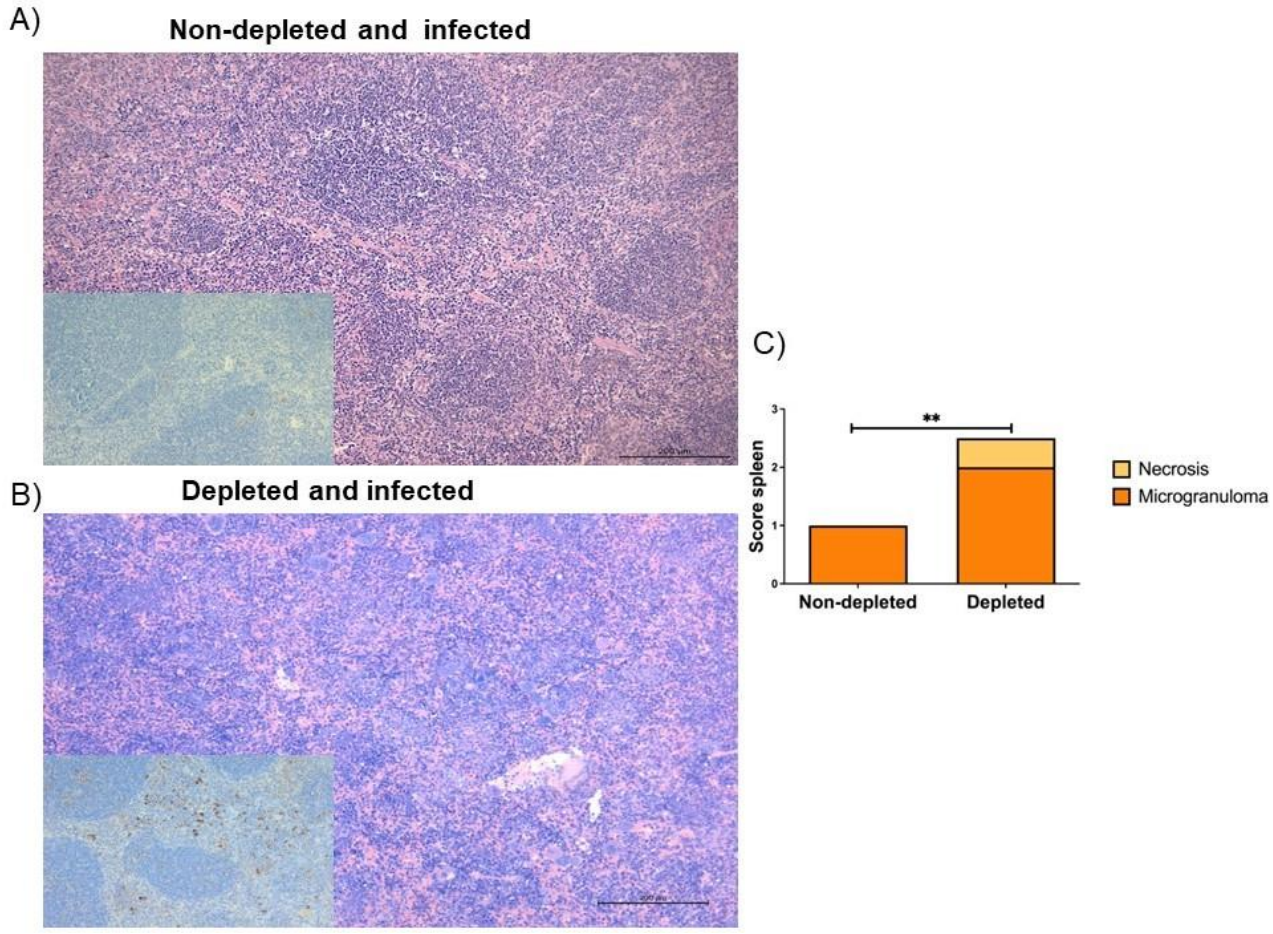

Figure 2.13 Microscopic changes in the spleen of pericyte depleted animals infected with *Brucella ovis*. spleen of infected mice non-depleted (A) and pericyte depleted (B). In both groups there were microganulomas with intralesional *Brucella ovis*. Score of spleen lesion of experimental mice (C). Bar represented the median of groups. The groups were compared with Kruskal Wallis (**p<0.01)

A Natural pathogens of mice *Citrobacter rodentium* trigers increased inflammatory lesions in pericytes depleted mice

Our previous results showed fibrinous peritonitis in mice depleted of pericytes for two different pathogens. In the both infections model we used bacterial that are not naturally found in the mice, and the host is used for the study of the agent. Furthermore, both pathogens are studied using experimental routes of infection. For seeing the effects of the pericytes depletion on natural pathogens in a natural route of infection. We infected non-depleted or pericyte depleted mice with *Citrobacter rodentium* (*C. rodentium*). Besides, *C. rodentium* is a Gram-negative bacteria that has the capacity to cause diseases in mice. These agents provoke colonic hyperplasia without or in low levels of inflammation in the intestine (Barthold et al., 1978; Schauer and Falkow, 1993; Schauer et al., 1995). We plated fecal contents before and after the depletion process, and no bacterial growth was observed. According to these findings, the experimental mice were free of Enterobactereaceaes during all stages of the infection process before they were infected.

We measured the amount of bacterial in the fecal contents daily after the infection. The groups pericyte depleted and non-depleted showed similar levels of bacterial colonization after the infection (Figure 2.14 A). Both groups showed equally lost of body wiegth after the infection (Figure 2.14 B). After 6 dpi, we performaded the euthanasia. Three (3/6) pericyte-depleted mice showed in the cecum moderate decreased of volume and more the cecum's wall white when compare to the non-depleted group, compatible with typhlitis. We measure the colon length and the depleted mice showed a decreased of colon lenghth (Figure 2.14 C) The bacteria recovery in the colon contents, cecum contents, and cecum (Figure 2.14 D, E, and G) were higher in the pericyte-depleted mice. In the colon, mesenteric lymph node, liver and spleen were similar in both experimental groups (Figure 2.14 F, H, I and J). These finds showed that pericyte per natural route and natural pathogens also affects the bacterial colonization (in the colon contents, cecum contents and cecum) and increased inflammatory lesions in the large intestine. However, for the natural route, the systemic dissemination for these agent was not affected in the depleted mice.

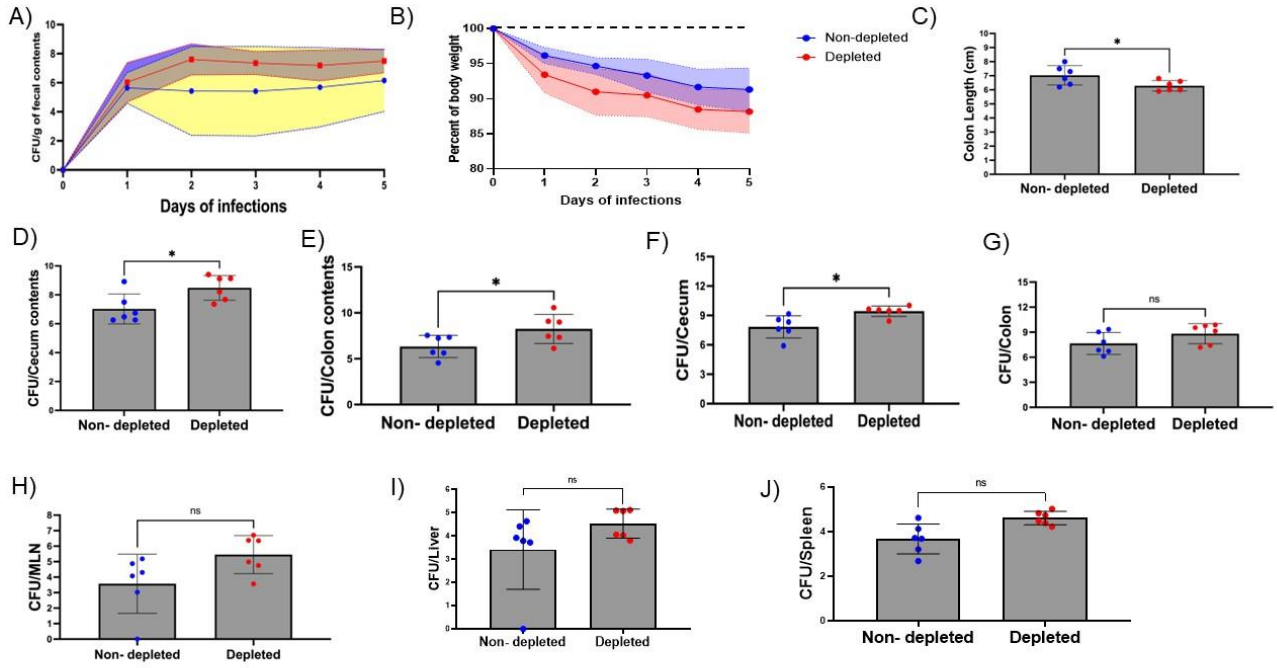

Figure 2.14 Effects of depletion of pericyte in *Citrobacter rodentium* infection by oral gavage. Transgenic mice with depletion of pericyte were infected with $5x10^9$ CFU of *C. rodentium* oral gavage. The fecal content bacterial was measure daily (A).. The weight was measured every day starting the day before infection until the end point (B). The percentage of weight was calculated as 100% before infection (B). Colon length of both groups in measure in cm (C). After 6 days post infection the cecum contents (D), colon contents (E), cecum (F), colon (G) mesenteric lymph node (H), liver (I) and spleen (J) were collected for bacteriology analysis. A LOG transformation normalized the CFU numbers. Each point represents the mouse value, while the bars represent the mean of each group and the standard difference. The statistical analysis was performed by ANOVA. The statistical test used was Wilcoxon test (*$p<0.05$; **$p<0.01$).

Microscopic lesions in the cecum section were distint to the experimental groups. Both non-depleted and depleted showed an ephitelial hyperplasia in the mucosa layer of cecum and submucosa edema, in the non-depleted the severity range was to abscent to moderate. And in the pericyte-depleted mice mild to several. Besides these lesions found in both groups,in the depleted mice was observed a infiltration mild-to moderate of neutrophils in the mucosa and submucosa and a neutrophilic exsudate in the lumen of the cecum (Figure 2.15 A). In general, the lesion score of the cecum was higher in the pericyte-depleted animals (Figure 2.15 B). This way, in the pericyte depleted mice showed an increased in inflammatory response in the cecum with a increased of bacteria in the lumen and content but in the systemic spread showed the same level in pericyte-depleted and non-depleted group.

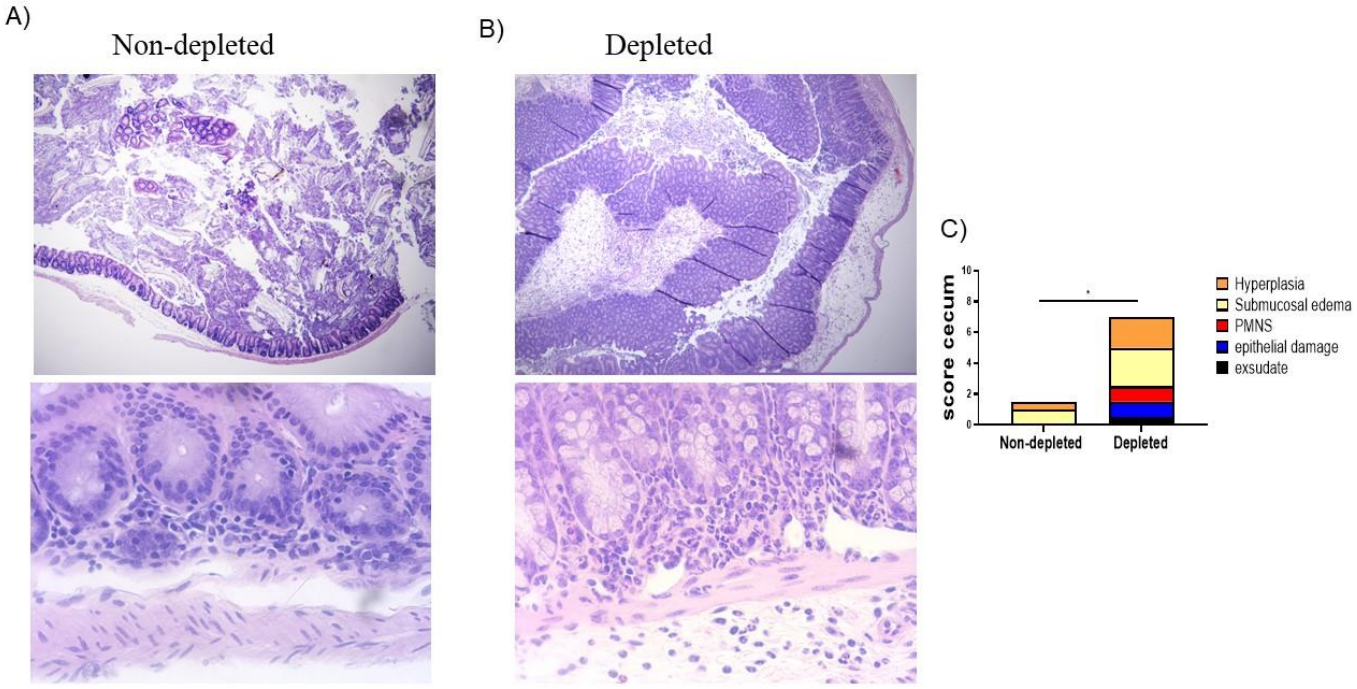

Figure 2.15 Microscopic changes in the cecum of pericyte depleted animals infected with *Citrobacter rodentium*. Cecum of infected mice non-depleted (A) and pericyte depleted (B). In both showed hyperplasia of epithelial layer. Score of cecum lesion of experimental mice (C). Bar represented the median of groups. The groups were compared with Kruskal Wallis (*p<0.05).

Modulation of endothelial inflammatory response by pericytes is mediated by connexin 43

Pericytes and endothelial cells interact with each other through peg-socket junctions (Caruso et al., 2009), which are rich in gap junctions and hemichannels composed of transmembrane connexins (Cx), particularly Cx43 (Li et al., 2011; Winkler et al, 2011; Ivanova et al., 2019; Payne et al., 2022), although there are reports that pericytes may also express Cx30.2 (Manasson et al., 2013) Cx37, and Cx40 (Ivanova et al., 2019). Therefore, we first assessed constitutive transcription of Cx43, Cx37, Cx30.2, and Cx40 by endothelial cells, pericytes and co-cultured endothelial cells and pericytes. Transcription of Cx43 was relatively abundant and similar among the individual cultures or co-cultured endothelial cells and pericytes, and it was not

affected by inoculation with *B. ovis* (Figure 2.16 A). In contrast, transcripts for Cx37, Cx30.2, and Cx40 were either scarce or absent under all experimental conditions (Figure 2.16 B-D).

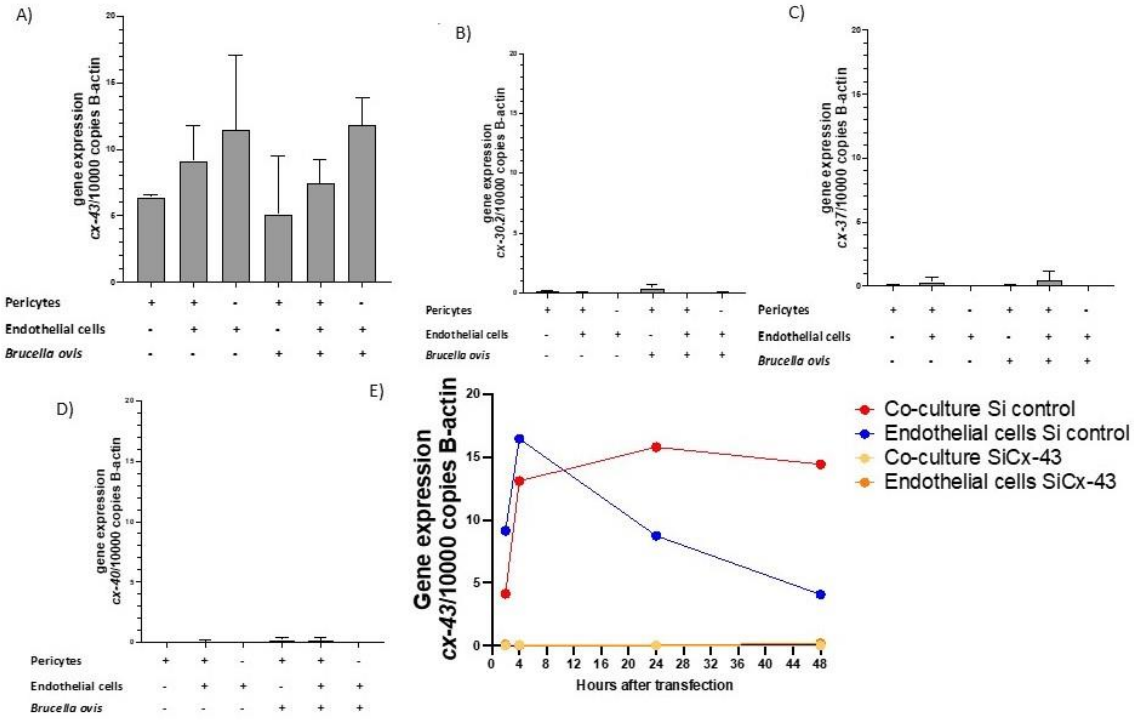

Figure 2.16 Connexin profile in co-culture model and endothelial cells alone. Transcriptional profile of co-cultured of endothelial cells and pericytes (2:1) or endothelial cells alone infected or not infected with *Brucella ovis* (MOI 1:100) for connexins. A) *Connexin 43* (B), *Connexin 30.2* (C), *Connexin 37* (D), *Connexin 40* and (E) kinectics of connexin -43 after siRNA for Connexin 43 or siRNA control transfection as gene expression for 1000 copies of *β*-

Gap19 is a peptide that blocks gap junctions (Ponsaerts et al., 2010). In order to test the hypothesis that gap junctions, particularly those formed by Cx43, are involved in the cross-talking between endothelial cells and pericytes, co-cultured pericytes and endothelial cells or endothelial cells alone were treated with Gap19 for 24 hours, and then subjected to various

inflammatory stimuli, including *B. ovis* (MOI 100), *L. monocytogenes* (MOI 5), and *E. coli* LPS (10 pg/mL), or sterile RPMI-control. Preliminarily, we measure the LDH release by cells treated with Gap19 to ensure that this peptide does not have a cytotoxic effect. LDH levels in culture treated with Gap19 were less of 10% of those measured in negative control cultures (Figure 2.2 B). We then demonstrated that Gap19 treatment prevented the pericyte-induced downregulation of expression of adhesion molecules (PECAM-1 and ICAM-1) after inflammatory stimuli as measured by mRNA and protein expression at 24 hpi (Figure 2.17 A-C). A similar result was obtained when measuring transcription of pro-inflammatory genes (*Ccl2, Il6*) (Figure 2.18 A and B). Therefore, co-cultured endothelial cells and pericytes treated with Gap19 expressed PECAM-1 in similar levels when compared to endothelial cells alone subjected to various inflammatory stimuli: *B. ovis* (MOI 100), *L. monocytogenes* (MOI 5), or LPS (10 pg/mL) at 24 hpi. Conversely, as observed in our previous experiments, endothelial cells co-cultured with pericytes in the absence of Gap19 did not express high levels of PECAM-1 in response to these stimuli.

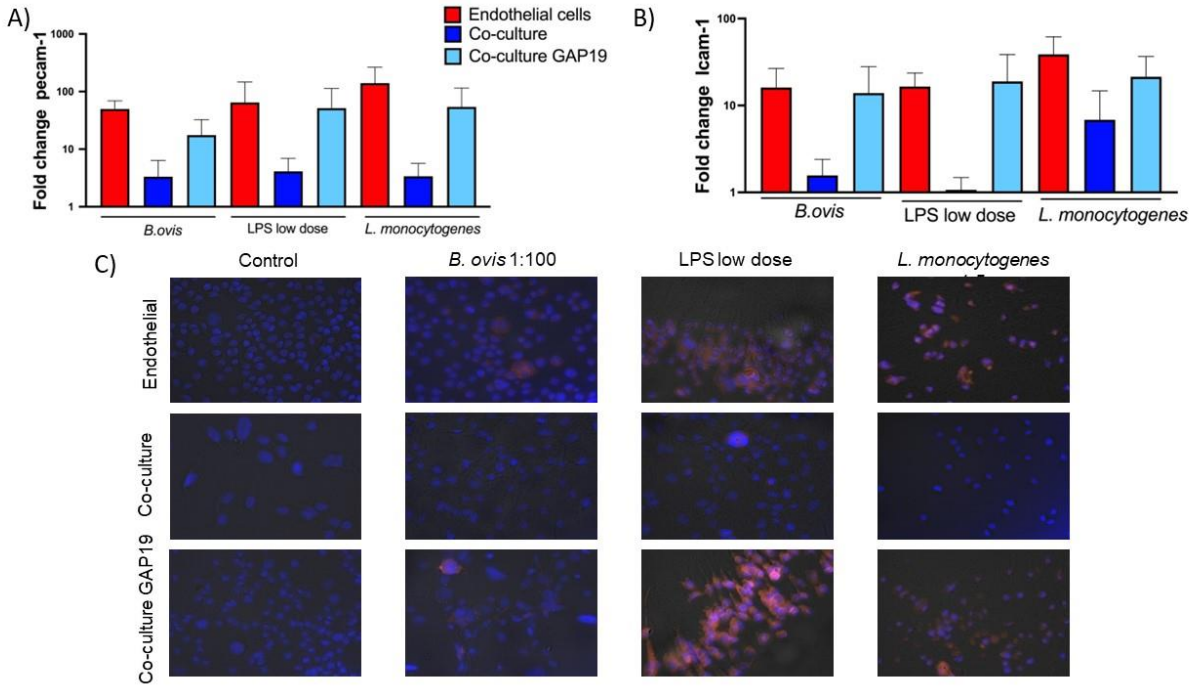

Figure 2.17 Effect of the block of connexin 43 in the profile of adhesion molecules of endothelial cells culture or co-culture of endothelial cells/pericytes and challenge with different bacterial stimulus. Transcriptional profile of co-cultured of endothelial cells and pericytes (2:1) or endothelial cells alone treated with 100 μM 24 hours before infection and after daily. The cells were infected or not infected with *Brucella ovis* (MOI 1:100), *Listeria monocytogenes* (MOI 1:5) and LPS in low dose at 24 hour after stimulation (A) *Pecam-1* and (B) *Icam-1* as fold change in comparison to uninfected controls. Bars represent mean and standard deviations of triplicate. PECAM-1 (red) expression in the immunofluorescence of the same *in vitro* condictions, showed the increased of expression of PECAM-1 in endothelial cells in all stimulus. Magnification of 40x.

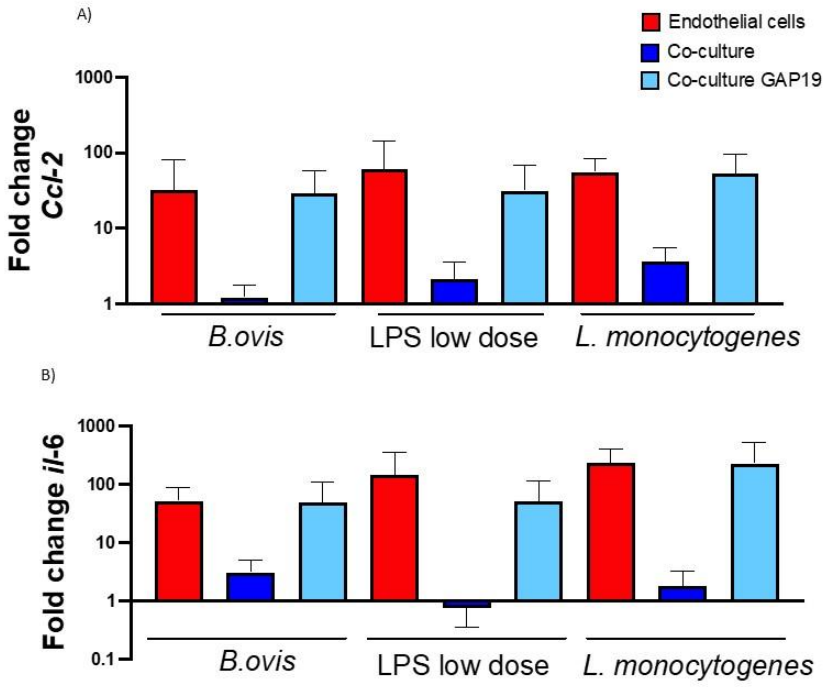

Figure 2.18 Effects of connexin 43 block (GAP19) in cell culture co-culture of pericytes and endothelial cells challenge with different bacterial stimulus. Transcriptional profile of co-cultured of endothelial cells and pericytes (2:1) or endothelial cells alone infected or not infected with *Brucella ovis* (MOI 1:100), *Listeria monocytogenes* (MOI 1:5) and LPS in low dose at 24 hour after stimulation treatead with 100 μM of GAP or culture media (A) *Ccl2* (B), *Il6* (B) as fold change in comparison to uninfected controls. Bars represent mean and standard deviations of triplicate.

To demonstrate that the modulation of endothelial inflammatory responses by pericytes is specifically mediated by Cx43, we used a siRNA for suppressing expression of Cx43, which resulted in marked decrease of Cx43 transcripts in endothelial cells and pericytes either alone or in co-culture (Figure 2.16 E). Then, co-cultured endothelial cells and pericytes or endothelial cells alone were subjected to pro-inflammatory stimuli: *B. ovis* (MOI 100), *L. monocytogenes* (MOI 5), *E. coli* LPS (10 pg/mL), or sterile RPMI-control. Silencing of Cx43 expression result in

decreased of adhesion molecule (*Ccl2, Il6)* and adhesion molecules (*Pecam1, Icam1)* (Figure 2.19).

Together these results indicate that the modulation of endothelial inflammatory responses by pericytes is mediated by Cx43.

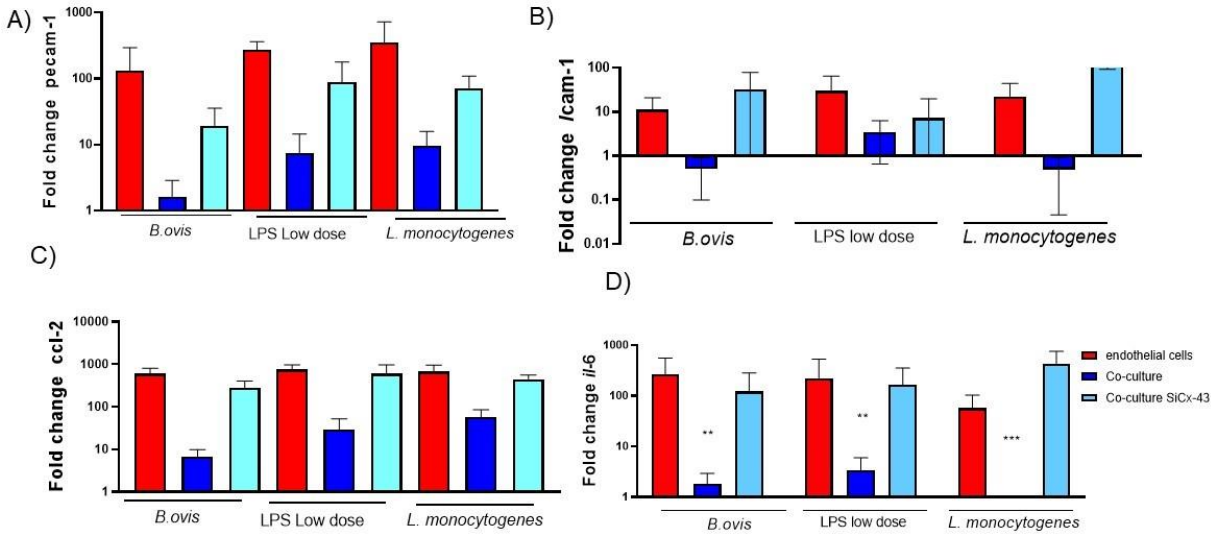

Figure 2.19 Effects of SiRNA of connexin 43 in the production of inflammatory molecules and adhesion molecules. Co-culture showing the effects of Si RNA for connexin 43 in the transcriptional levels for *Pecam1* (A), *Icam1* (B), *Ccl2* (C), and *Il6* (D).

Blocking connexin-43 *in vivo* increased the bacterial colonization and inflammation

For investigated the effects of block of connexin 43, we administrated GAP19 25 mg/kg or PBS one hour before the infection and daily for 3 days of infection (Figure 2.20 A). The GAP19 administrated in the infected mice with *B. ovis* and blocker of connexin 43 showed an increased of bacterial colonization in the liver and spleen (Figure 2.17 C and D). However, we do not observed peritoneal gross change such peritoniteal cavity (Figure 2.20 B), that we

demonstrated in the depleted group challenge with the same pathogen. To investigated the inflammatory response, we measure the CCL-2 expression in the serum of the mice treated with GAP19. The serum of animals treated and infected showed high dose of CCL-2 in the serum.

Together these results showed that the connexin-43 increased the bacterial colonization and the levels of CCL-2 in the blood.

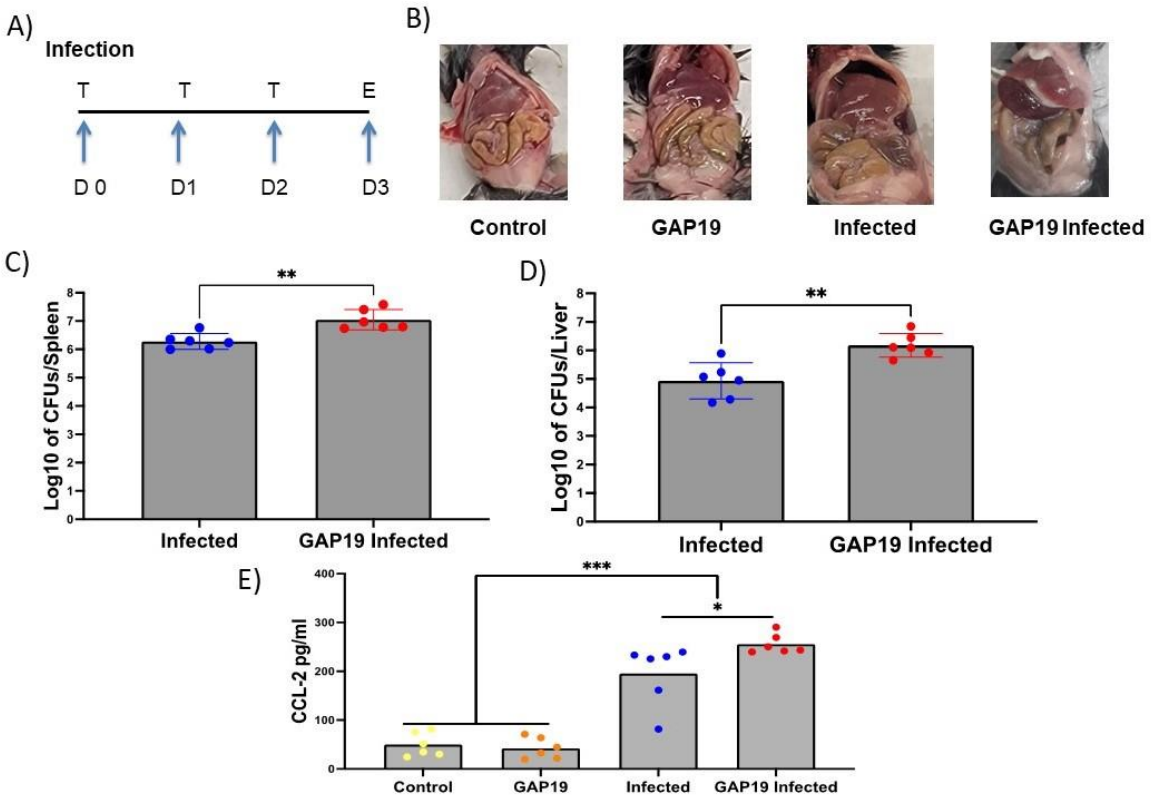

Figure 2.20 Effects of connexin 43 block (Gap junction channels) systemically in *Brucella ovis* infection colonization of liver and spleen. Squematic drawing of the experimental challenge with C57bl 6 mice treated with 25 mg/kg of GAP19 daily. In the first day of the experiment, after 1 hour of the first dose of GAP19 the mice were infected with 10^6 CFU of *B. ovis*. The eutanazia was made after 3 days of infection (A). Gross change in the peritoneal cavity of experimental mice without any significant lesion

Discussion

In this study, we demonstrated a previously unknown function of pericytes modulating endothelial inflammatory responses to bacterial infections *in vitro* and *in vivo*, diminishing bacterial-elicited inflammation. In the absence of pericytes endothelial cells displayed a much stronger pro-inflammatory response to bacterial stimuli, as demonstrated by higher expression of adhesion molecules and pro-inflammatory cytokines and chemokines. Furthermore, we demonstrated that interaction of pericytes and endothelial cells in this context is mediated by Cx43. This mechanism is likely relevant for preventing excessive tissue damage induced by inflammation, indirectly contributing to restoration of host homeostasis (Figure 2.21). Importantly, pathogenic bacteria cause damage not only through their virulence factors but also by inducing inflammatory responses. The blood vessels play a key role during the host inflammatory response by transporting leukocytes and soluble inflammatory mediators (Chousterman et al., 2017). In addition, endothelial cells are a source of several cytokines, chemokines and other molecules that are required for the innate immune response (Schmeck et al., 2006; Ferrero et al., 2011). However, a "cytokine storm" may drastically impact morbidity and mortality due to severe clinical manifestations for example, in cases of sepsis (Chousterman et al., 2017). This study demonstrated that pericytes may be essential to prevent exacerbated and potentially deleterious endothelial cells-mediated pro-inflammatory mechanisms.

We initially demonstrated pericyte modulation of endothelial cells inflammatory response against *B. ovis* infection. *Brucella* spp. are considered stealthy pathogens that usually do not trigger a detectable inflammatory response during the acute phase of infection (Grilló et al., 2012). Thus, *B. ovis* was elected as a model organism to assess the role of pericytes in inflammation due to its low intrinsic pro-inflammatory potential. Although *B. abortus* invades and survives within cultured endothelial cells infected *in vitro* (Ferrero et al., 2011), there are no previous studies on the interaction of *Brucella* spp. and pericytes. Furthermore, in this study we also employed *L. monocytogenes,* a Gram-positive facultative intracellular bacterial pathogen (Yin et al., 2019), and purified *E. coli* LPS, which is a strong TLR4 agonist (Lapaque et al., 2006). Therefore, we demonstrated that this mechanism was not restricted to one specific bacterial agent since stimulation with *B. ovis, L. monocytogenes,* and *E. coli* LPS induced upregulation of adhesion molecules (ICAM and PECAM) and pro-inflammatory genes (*Il-6, Ccl-2, Tnf-α*) in endothelial cells, but when endothelial cells were co-cultured with pericytes these

responses were markedly diminished. endothelial cells are involved in several physiologic functions and pathologic responses, including metabolic homeostasis, vascular hemodynamics, vascular permeability, coagulation, and cell extravasation (leukocytes trafficking) (Armulik, 2011). Inflammatory mechanisms specifically performed by endothelial cells are critical in many diseases such as septic shock (Vallet, 2003) and thrombosis (Wu et al., 1988). Inflammatory signals from exogenous or endogenous sources may stimulate endothelial cells to escalate inflammation through the production of cytokines /chemokines (such as, IL-6, MCP1, and TNF-α) and adhesion molecules (ICAM-1, VCAM-1, PECAM-1, and E-selectin) (Yamagami et al., 2003). Our *in vitro* results are in good agreement with a previous study, which demonstrated that pericyte loss in the retina increases leukocytes infiltration, and upregulates expression of inflammatory genes and adhesion molecules by retinal endothelial cells (Ogura et al., 2017).

Intraperitoneal infection of pericyte-depleted mice with wild type *B. ovis*, a stealthy pathogen, resulted in development of clinical signs, fibrous peritonitis, and mortality. These results unequivocally demonstrate a relevant role of pericytes in regulating inflammation *in vivo*. Clinical signs and mortality did not occur in wild type mice experimentally infected with high doses of *B. ovis* (10^7, 10^8, or 10^9 CFU/ animal), which was expected in *Brucella* spp.-infected mice (Grilló et al., 2012). Importantly, even after these very high challenge doses *B. ovis* was not capable of inducing peritonitis in wild type mice with an intact population of pericytes. Furthermore, although high challenge doses of wild type *B. abortus* or *B. microti*, a highly pathogenic species to mice, may result in lethal infections (Barqueiro-Calvo et al., 2007; Jiménez de Bagués et al., 2010), even under those conditions there are no previous reports of any gross or histological changes in the peritoneal cavity or peritonitis. Therefore, the interpretation of our results point to the fact that a reduction in the pericyte population rendered mice more sensitive to *B. ovis*-elicited inflammation. However, this is not a species-specific phenomenon since another intracellular bacterial pathogen, as the Gram-positive *L. monocytogenes* that usually does not trigger a detectable inflammatory response in the abdominal cavity, induced peritonitis in pericyte-depleted mice. Thus, the modulation of endothelial cells inflammatory responses demonstrated in our initial experiments in cultured cells correlated very well with the outcome of infection *in vivo* and *in vitro*. Conversely, a pro-inflammatory response obviously plays a positive role for controlling pathogens, such as *L. monocytogenes* (Zenewick and Shen, 2007), but in spite

of a stronger local inflammatory response, there were higher bacterial loads at systemic sites of infection, indicating that the absence of pericytes results in more systemic dissemination of these pathogens, which is somewhat expected since pericytes directly maintain vascular integrity (Pieper et al., 2013). Futhermore, natural pathogen infected per the natural via, *C. rodentium* provoked more histologic lesions in the cecum of pericyte-depleted mice. *C. rodentium* in mouse caused a mild enteritis associated with epithelial hyperplasia (Schauer and Falkow, 1993), but is not associated with exacerbated inflammation, as we found in the pericyte-depleted mice. This highlty the importance of pericyte even in the natural via of infection of one self limiting pathogen infection, such *C. rodentium*.

In this study, absence of pericytes increased expression of adhesion molecules (ICAM-1 and PECAM-1) by endothelial cells in response to bacterial stimuli. During the inflammatory process, leukocytes cross the endothelial layer by anchoring themselves through adhesion molecules such as PECAM-1 and ICAM-1 (Nourshargh et al., 2016). *In vivo* infection of pericyte-depleted mice with wild type *B. ovis* by the IP s route resulted in fibrous peritonitis and infiltration of macrophages and neutrophils. Importantly, as a stealthy pathogen, *B. ovis* does not elicit a detectable inflammatory response in the abdominal cavity when inoculated intraperitoneally (Grilló et al., 2012). Recruitment of leukocytes from the bloodstream and the sequence of adhesive contacts of these cells with endothelial cells that will ultimately allow leukocytes to migrate to the site of injury are essential steps for host defense. This innate immune reaction must be well orchestrated to avoid migration of excessive numbers of inflammatory cells and consequently tissue damage (Nourshargh et al., 2016). In extreme cases, an overwhelming pro-inflammatory response may result in devastating consequences such as in sepsis (Bathia and Moochhala, 2004). Our findings are also in good agreement with previous studies (Ogura et al., 2017) that indicated that pericyte depletion may favor macrophages and neutrophils infiltration in tissues. Therefore, increased expression of adhesion molecules by endothelial cells in the absence of pericytes likely had a relevant role for the development of peritonitis in our *in vivo* model of infection.

In addition to their structural and the physiological functions, pericytes have been implicated in disease development and recrudescence, including neurological disorders, cancer, and diabetic-related conditions (Hall et al., 2014; Ferland-McCollough et al., 2017;

Nikolakopoulou et al., 2019). There are also evidences that pericytes may be implicated in human cytomegalovirus infection (Wilkerson et al., 2015; Aronoff et al., 2017). This study demonstrated that pericytes are not preferential target cells for *B. ovis* infection. Our experimental evidence indicates that pericytes are rarely infected and are not permissive to either *B. ovis* or *L. monocytogenes* intracellular growth. In contrast, pericytes are susceptible to infection by *Bartonella henselae*. Cultured human pericytes are permissive to invasion by *B. henselae*, which induces pathological angiogenesis resulting in a condition known as angiomatosis. *B. henselae*-infected pericytes produce higher levels of vascular endothelial growth factor (VEGF), which may be responsible for the abnormal angiogenesis induced by this pathogen (Varanat et al., 2013). In contrast, *B. ovis* can invade and replicate in endothelial cells, which is in agreement with a previous study that demonstrated infection of human endothelial cells with *B. abortus* (Ferrero et al., 2011). Therefore, the modulation of endothelial cells inflammatory responses by pericytes is likely to be a steady state mechanism that prevents unwanted or exacerbated inflammation driven by endothelial cells. In other words, under these conditions, pericytes do not necessarily need to sense invading bacteria to exert their modulatory function. Importantly, we demonstrated that Cx43, presumably in gap junctions, is responsible for the cross-talk between pericytes and endothelial cells, which is compatible with a steady state modulation by pericytes. During inflammation, the crosstalk between endothelial cells and pericytes maintain the inflammatory process tightly regulated. Indeed, disturbances of this mechanism of cell-to-cell communication may cause microvascular dysfunction, such micro hemorrhages (Ogura et al., 2017). For instance, decreased pericyte coverage over blood vessels of the subcortical white matter of Alzheimer's disease patients was related to changes in vascular density and high accumulation of blood-derived extravascular fibrin deposits (Montagne et al., 2017). Furthermore, expression of adhesion molecules by endothelial cells is critical for recruitment, activation, and influx of leukocytes in the site of inflammation, representing a key step for an effective innate immune response (Smiley et al., 2001; Luyendyk et al., 2019). Importantly, endothelial cells are capable of triggering a pro-inflammatory response to stimulation with PAMPs (Schmeck et al., 2006; Ferrero et al., 2011) since endothelial cells are known to express TLR-4 and TLR-2 (Fan et al., 2003). In this study, pericyte depletion with bacterial infection triggered a severe inflammatory process that resulted in fibrin deposition and intense inflammatory cell infiltration at the site of infection.

In conclusion, this study demonstrated that pericytes play a role controlling endothelial cells-mediated inflammatory mechanisms both *in vivo* and *in vitro* in response to bacterial stimuli. Our results also support the notion that the modulation of endothelial cells inflammatory response by pericytes is mediated by Cx43. Therefore, we hypothesize that pericytes promotes a steady state modulation of endothelial cells inflammatory threshold, which may be critical for preventing exacerbated innate immune reactions that may cause tissue damage, due to an overwhelming production of proinflammatory cytokines and chemokines and increased infiltration and activation of leukocytes.

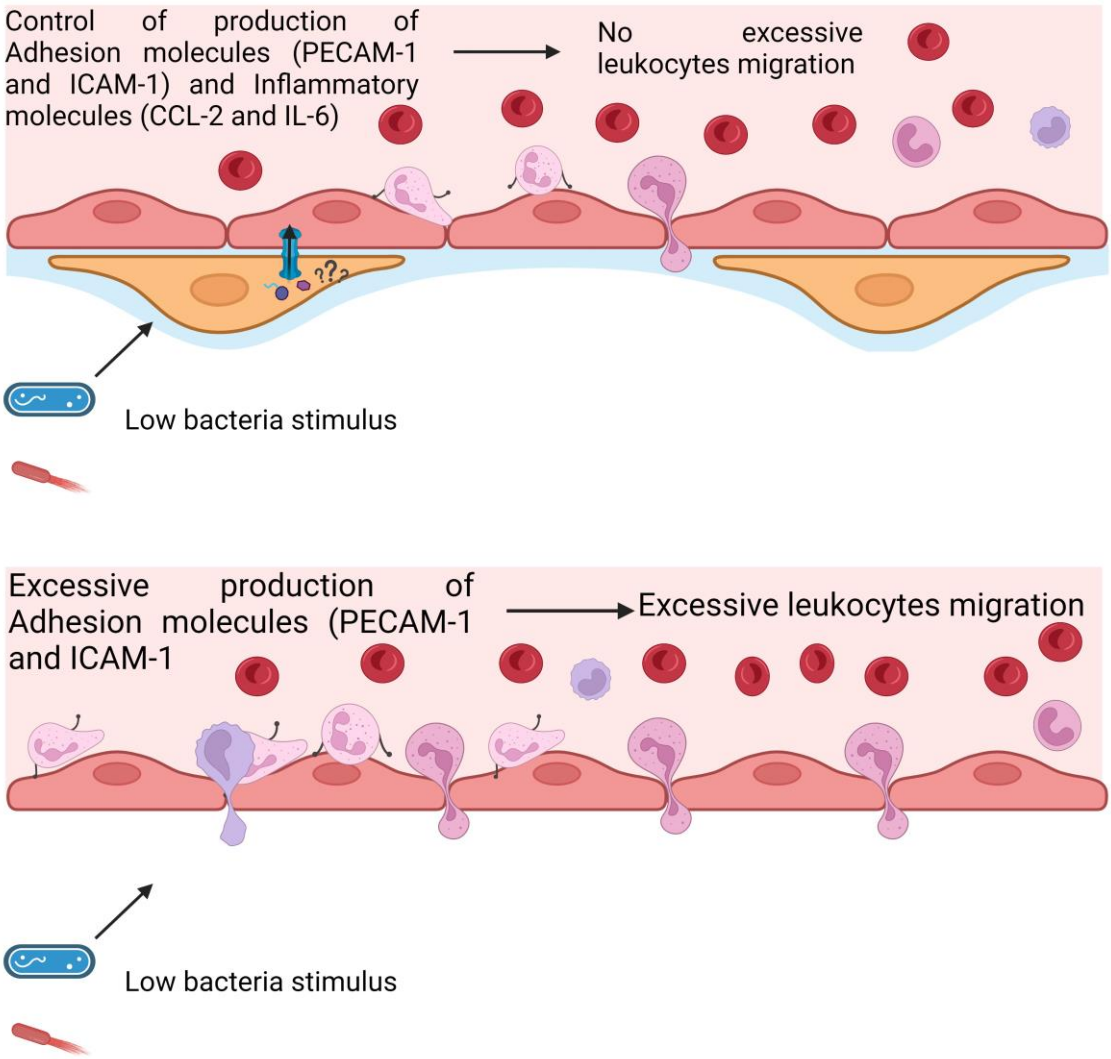

Figure 2.21 Illustration of Influence of pericyte in endothelial cells in bacterial challenge. Created with BioRender

Material and methods

Bacterial strains and culture conditions

Wild type *B. ovis* ATCC 25840, *B. ovis* Δ*virB2* (Macedo et al., 2015), *B. ovis* expressing *mCherry* fluorescent protein (*B. ovis* mCherry), and wild type *L. monocytogenes* 10403s were used in this study. *B. ovis* strains were grown on tryptose soy agar supplemented with 1% hemoglobin (hTSA) (Becton Dickinson, Brazil) in a humidified incubator at 37°C with 5% CO_2 for 3 days. *L. monocytogenes* were grown on brain heart broth (BHI) agar plates or broth. Inocula were prepared by suspending the colonies harvested from plates in sterile PBS (Phosphate Buffer Saline, pH 7.4, Sigma-Aldrich) or BHI broth. The quantity of colony-forming units (CFU)/mL of inoculum was estimated by spectrophotometry at 600 nm (SmartSpec Plus Bio-Rad, US) and confirmed by counting individual colonies grown on plate after incubation of 10-fold serial dilutions.

Bacterial suspensions of inactivated *B. ovis* ATCC 25840 were prepared by irradiating a PBS suspension containing 1 x 10^9 CFU/mL of bacteria with 15 Kgray of gamma radiation for 12 hours (Laboratory of Gamma Irradiation at the Center for Development of Nuclear Technology – CDTN-UFMG). Bacterial inactivity was confirmed by plating aliquots of gamma-irradiated bacteria onto hTSA.

Ethics statement, genetic background of mice and genotyping

The Ethics Committee on Animal Experimentation at the Universidade Federal de Minas Gerais (CEUA-UFMG protocols 268/2018, 330/2018) and University of California Davis (IACU protocol # 23006) approved the procedures and handling performed on animals in this study.

The NG2creER™, iDTR (inducible DTR) and Nes-GFP (Nestin expressing GFP) C57BL/6 transgenic mice were kindly provided by Dr. A. Birbrair from the Institute of Biological Science (ICB) at UFMG or purchased from Jackson Laboratory. Wild type C57BL/6 mice were purchased from Jackson Laboratory. By crossbreeding homozygotes iDTR and heterozygotes NG2creER™ C57BL/6, the double transgenic lineage NG2creER™ x iDTR was obtained, whereas the CRE-negative C57BL/6 mice (iDTR mice) were used as negative controls. Mice were maintained at cages under controlled temperature and humidity (25°C, 70%), and had free access to filtered water and commercial feed.

The genetic background of the crossbred animals was checked by PCR using the CRE primers described by Liu et al. (2003). DNA samples were extracted as described (Pitcher et al., 1989) from samples of the ear tip. PCR mixture contained 15.0 µL of PCR Supermix (Thermo Fisher Scientific, US), 1.0 µM of each primer, 4.0 µL of DNA and supplementation with 1.0 U of Taq DNA polymerase recombinant (Thermo Fisher Scientific, US). PCR reaction was set up as follows: 94°C for a 5 min, 35 cycles at 94°C for 30 s, 55°C for 30 s, 72°C for 1 min, and a 7 min final elongation step at 72°C. A 412-bp amplicon was expected from positive DNA on a 1.5% agarose gel.

Cell lines, culture and co-culture conditions

Mouse brain vascular pericyte primary cells (iXCells), mouse endothelial cell line EOMA (ATCC), and mouse macrophage cell line J774 (ATCC) were maintained in RPMI supplemented with 10% fetal bovine serum (FBS) or pericyte media (iXCells) supplemented with 10% FBS, and incubated at 37ºC with 5% CO_2. For co-culture experiments, endothelial cells and pericytes were co-cultured in the proportion of 2:1 (endothelial cells: pericytes) for 24 hours prior to the experimental treatments.

Cells were seed (1×10^5 cells/well) in 96 well plates and infected with *B. ovis* with a multiplicity of infection (MOI) of 100 or 1000. For co-cultures, endothelial cells and pericytes were seed at 1×10^5 cells/well and 5×10^4 cells/well, respectively, in a 24-well plate, and inoculated with *B. ovis* (MOI 100), *L. monocytogenes* (MOI 5), or stimulated with 10 pg/mL of purified *E. coli* LPS (eBioscience). Sterile RPMI was used as negative control. endothelial cells and co-cultures treated with the gap junction blocker Gap19 (Tocris), 100 µM in each well, or sterile RPMI as negative control.

NG2 cell depletion and mouse infection

NG2 cell depletion was performed as described (Kunisaki et al., 2013). Briefly, 4 to 6-week-old mice received 1 mg of tamoxifen (Sigma -Aldrich) IP twice a day (12-hour intervals) for five consecutive days. Two days later (7^{th} day of the protocol), diphtheria toxin (DT), which triggers NG2cre cell depletion, was intraperitoneally injected at a single dose of 100 µg/Kg of body weight. Seven days later (14^{th} day of the protocol), mice were 6 to 8-week-old and used for experimental infections. NG2+ pericyte-depleted C57BL/6 mice (n = 10) and iDTR C57BL/6 mice (n = 14) were IP injected with 100 µL of a suspension containing 1 x 10^7 CFU/mL of *B. ovis*,or *L. monocytogenes* 1x10^5CFU/ml. And for oral gavage *C. rodentium* 1x10^{10} CFU/ml. Mice were subjected to euthanasia at 1, 3, and 15 dpi. Liver and spleen were sampled for bacteriology and histopathology. For *Citrobacter* bacteriology after 6 dpi was colleted fecal contents, cecum contents, colon contents, colon, cecum, liver, spleen and mesenteric Lymph.

Six to 8-week-old *Nes*-GFP C57BL mice (n = 7) were inoculated IP with 100 µL of a suspension containing 1 x 10^7 CFU/mL of *B. ovis mCherry*. At 24 hpi (n = 3) and 3 dpi (n = 4) were euthanized and sampled as described above.

For experiments with higher infectious doses, C57BL/6 were inoculated with 100 µL of a suspension containing 1 x 10^8, 1 x 10^9, or 1 x 10^{10} CFU/mL of wild type *B. ovis*, and subjected to euthanasia and sampling at 1, 3, and 7 dpi.

Bacteriologic cultures

Tissue samples were placed in sterile PBS (pH 7.4), and maintained on until they were macerated and serially diluted (10-fold dilutions) in PBS. One hundred µL of each dilution were plated on hTSA, Mcokey or LB, in duplicates. Plates were incubated at 37ºC in a humidified incubator supplemented with 5% CO_2 for 1 to 5 days, when colonies were counted.

RNA isolation and RT-qPCR

Total RNA was extracted from cell cultures or tissue samples by Trizol (TermoFisher) following the manufacturer's instructions. One μg of total RNA was used for cDNA synthesis using a RT master Mix, and qPCR was performed using a Fast SYBR-Green Master Mix (Applied Biosystems) detected by StepOnePlus real-time PCR system (Applied Biosystems). Primer sequences used in this study are described in Supplementary Table 1. After 40 cycles, the Ct values were determined and normalized based on β-actin mRNA. Fold changes in expression between control, and stimulated groups were determined by the ΔΔct method (Livak et al., 2001).

Cytotoxicity assay

LDH release was measure in cell culture supernatants using the Cytotox96 non radioactive cytotoxicity assay (Promega), as previously described (Jiménez de Bagüés et al., 2010). Cell death was estimated as the percentage of LDH release, which was calculated using the following formula proposed by the manufacturer:

percentage of LDH release = 100 x (test LDH release – spontaneous release)/(maximum release-spontaneous release)

siRNA transfection

Transfections with Xfect™ were performed according to the manufacturer's instructions within the recommended reagent/RNA or reagent/siRNA ratio range. For transfections cells were plated at constant density 1 x 10^5 cells of endothelial cells alone or with 5x 10^4 cell/well in 24 well-plates one day prior to transfection. SiRNA connexin-43 after transfections cells were stimulated with *B. ovis*, *Listeria monocytogenes* or LPS low dose.

***In situ* hybridization**

Slices were submitted for *In situ* hybridization for murine PECAM-1 mRNA in the liver and spleen of experimental mice using *ISH* RNAview (Introgen) and followed the manufacturer's instructions.

Histopathology

Liver and spleen were sampled, fixed by immersion in 10% buffered formalin for 24 hours, and embedded in paraffin. Tissue sections (3-4 μm-thick) were stained with hematoxylin and eosin. Lesions in the liver and spleen (inflammation and necrosis) were scored as 0 to 3, being 0 = absent, 1 = mild, 2 = moderate, and 3 = severe, with a total score ranging from 0 to 6. In the liver, perihepatitis, thrombosis and hepatocyte degeneration were scored as 0 or 1, being 0 = absent and 1 = present.

Immunohistochemistry and immunofluorescence

Tissue sections (3-4 μm-thick) were deparaffinized in xylene and hydrated in decreasing ethanol concentrations. Only NG2 epitopes needed antigen retrieval, which was performed by heating the tissue fragments immersed in high pH solution (EnVision FLEX – Dako, US) for 10 min in a pressure cooker. Tissue sections were incubated with 3% hydrogen peroxide for 1 hour and treated with 3% skimmed milk for 1 hour. A primary anti-*Brucella* rabbit polyclonal antibody (1:1,000 dilution) was incubated with the tissue sections at room temperature for 1 hour, whereas a primary anti-NG2 rabbit polyclonal antibody (Chemicon - AB5320, Sigma-Aldrich, US) was incubated (1:250 dilution) with the tissue sections at 6^{o}C overnight. Samples were then incubated with a secondary antibody (EnVision FLEX - Dako, US) for 1 hour at room temperature. The

chromogen was 3,3'-diaminobenzidine tetrahydrochloride (DAB) used according to the manufacturer's instructions (EnVision FLEX - Dako, US). Tissue sections were counterstained with Harris hematoxylin, dehydrated and assembled for analysis.

Liver and spleen of infected of *B. ovis mCherry*-of *Nestin*-GFP mice were fixed by IV perfusion with 4% paraformaldehyde and post-fixed for 24 hours in 4% paraformaldehyde, incubated in 40% sucrose solution for 48 hours, embedded in OCT (Sigma), and storage at -20°C. Frozen of 5 to 6 µm-thick tissue sections were obtained using a cryostat (Easy Path). Then cell nuclei were stained with DAPI (Sigma). Images were acquired using as optical microscope (Leica DM3000, US).

Cultured cells were fixed with 4% of paraformaldehyde for 10 min and incubated with the primary monoclonal anti-PECAM-1 (Santa Cruz, 1:500 dilution) for 1 hour at room temperature protected from light. The secondary antibody IgG anti-mouse with Alexa fluor 560 (ThermoFisher, 1:400) was incubated for 2 hours at room temperature, after washing DAPI (Sigma, 1:1000) was incubated for 30 minutes at room temperature.

Statistical analyses

Statistical analyses were performed using the GraphPad Prism for Windows, version 8.4.2. Data were submitted to the Anderson-Darling test of normality. Prior to statistical analysis, bacterial counts were logarithmically transformed and compared by ANOVA followed by Tukey's post-hoc test. The averaged log numbers were used for index calculation as follows: the mean log number from treated animals (pericyte-depleted mice) was subtracted from the mean log number from untreated animals (control mice) for each analyzed organ.

Histopathological scores were analyzed as non-parametrical data by means of Mann-Whitney test, while quantifications on $NG2^+$ cells were analyzed by means of Kruskal-Whalis

tests followed by Dunn's post-hoc test. The frequency of peritonitis among experimental groups was analyzed by Fisher’s exact test.

This masnuscript was formatted for a future submission in Cells Host and Microbe

References

1. A. Armulik, A. Abramsson, C. Betsholtz. Endothelial/pericyte interactions. *Circ. Res.* **97**, 512-523 (2005).

2. A. Armulik, G. Genove, C. Betsholtz, Pericytes: developmental, physiological, and pathological perspectives, problems, and promises. *Dev. Cell.* **21**, 193-215 (2011).

3. D. M. Aronoff, H. Correa, L. M. Rogers, R. Arav-Boger, D. J. Alcendor, Placental pericytes and cytomegalovirus infectivity: Implications for HCMV placental pathology and congenital disease. *Am. J. Reprod. Immunol.* **78**, 10.1111/aji.12728 (2017).

4. E. Barquero-Calvo *et al.*, *Brucella abortus* uses a stealthy strategy to avoid activation of the innate immune system during the onset of infection. *PLoS One.***2**, e631 (2007).

5. M. Bhatia, S. Moochhala, Role of inflammatory mediators in the pathophysiology of acute respiratory distress syndrome. *J. Pathol.* **202**, 145-156 (2004).

6. A. Birbrair *et al.*, How plastic are pericytes? *Stem Cells Dev.* **15**, 1013-1019 (2017).

7. A. Birbrair, Pericyte biology: development, homeostasis, and disease. *Adv Exp Med Biol.* **1147**, 1-344 (2019).

8. G. Bonizzi, M. Karin, The two NF-kappaB activation pathways and their role in innate and adaptative immunity. *Trends Immunol.* **25**, 280-288 (2004).

9. R. A. Caruso *et al.*, Ultrastrutural description of pericyte/endothelium peg-socket interdigitations in the microvasculalature of human gastric carcinmas. *Anticancer Res.* **29**, 449-453 (2009).

10. J. Celli, The Intracellular Life Cycle of *Brucella* spp. *Microbiol. Spectr.* **7**, 10.1128/microbiolspec.BAI-0006-2019 (2019).

11. B. G. Chousterman, F. K. Swirski, G. F. Weber. Cytokine storm and sepsis disease pathogenesis. *Semin. Immunopathol.* **39**, 517-528 (2017).

12. J. R. Couchman, Syndecans: proteoglicans regulators of cell-surface microdomains? *Nat. Rev. Mol. Cell. Biol.* **4**, 926-938 (2003).

13. M. Crisan *et al.*, A perivascular origin for mesenchymal stem cells in multiple human organs. *Cell Stem Cell*. **3**, 301-313 (2008).

14. J. Fan, R. S. Frey, A. B. Malik, TLR4 signaling induces TLR2 expression in endothelial cells via neutrophil NADPH oxidase. *J. Clin. Invest.* **112**, 1234-1243 (2003).

15. D. Ferland-McCollough, S. Slater, J. Richard, C. Reni, G. Mangialardi, Pericytes, an overlooked player in vascular pathobiology. *Pharmacol. Ther.* **171**, 30-42 (2017).

16. M. C. Ferrero *et al.*, Proinflammatory response of human endothelial cells to *Brucella* infection. *Microbes Infect.* **13**, 852-861 (2011).

17. E. Freer, E. Moreno, I. Moriyon, J. Pizarro-Cerdá, A. Weintraub, J. P. Gorvel, *Brucella-Salmonella* lipopolysaccharide chimeras are less permeable to hydrophobic probes and more sensitive to cationic peptides and EDTA than are their native *Brucella* sp. counterparts. *J. Bacteriol.* **178**, 5867-5876 (1996).

18. H. Gerhardt, C. Betsholtz, Endothelial-pericyte interactions in angiogenesis. *Cell Tissue Res.* **314**, 15-23 (2003).

19. K. Gibby *et al.*, Early vascular deficits are correlated with delayed mammary tumorigenesis in the MMTV-PyMT transgenic mouse following genetic ablation of the NG2 proteoglycan. *Breast Cancer Res.* **14**, R67 (2012).

20. T. Girbl *et al.*, Distinct compartmentalization of the chemokines CXCL1 and CXCL2 and the atypical receptor ACKR1 determine discrete stages of neutrophil diapedesis. *Immunity.***46**, 1062-1076e (2018).

21. M. J. Grilló, J. M. Blasco, J. P. Gorvel, I. Moriyón, E. Moreno, What have we learned from brucellosis in the mouse model? *Vet. Res.***43**, 29-43 (2012).

22. C. N. Hall *et al.*, Capillary pericytes regulate cerebral blood flow in health and disease. *Nature.***508**, 55-60 (2014).

23. E. Ivanova, T. Kovacs-Oller, B. T. Sagdullaev, Vascular pericyte impairment and connexin 43 GAP junction deficit contribute to vasomotor decline in diabetic retinopathy. *J. Neurosci.* **37**, 7580-7594 (2019).

24. M. P. Jiménez de Bagüés *et al.*, The new species *Brucella microti* replicates in macrophages and causes death in murine models of infection. *J. Infect. Dis.*202, 3-10 (2010).

25. H. Kumar, T. Kawai, A. Shizuo, Pathogen recognition by the innate imune system. *Int. Rev. Immunol.* **30**, 16-34 (2011).

26. N. Lapaque *et al*., Differentila inductions of TNF-alfa and IGTP, IIGP by structurally diverse classic and non-classic lipopolysaccharides. *Cell. Microbiol.* **8**, 401-413 (2006).

27. N. Lapaque, I. Moriyon, E. Moreno, J. P. Gorvel, *Brucella* lipopolysaccharide acts as a virulence fator. *Curr. Opin. Microbiol.* **8**, 60-66 (2005).

28. F. Li *et al.*, Endothelial Smad4 maintains cerebrovascular integrity by activating N-cadherin through cooperation with Notch. *Dev. Cell.* **20**, 291-302 (2011).

29. K.J. Livak, T.D. Schmittgen. Analysis of relative gene expression data using real-time quantitative PCR and the 2(-Delta Delta C (T)) method. *Methods.* **25**, 402-408 (2001).

30. J. P. Luyendyk, J. G. Schoenecker, M. J. Flick, The multifaceted role of fibrinogen in tissue injury and inflammation. *Blood*. **133**, 511-520 (2019).

31. A. A. Macedo *et al.*, The abcEDCBA-encoded ABC transporter and the *virB* operon-encoded type IV secretion system of *Brucella ovis* are critical for intracellular trafficking and survival in ovine monocyte-derived macrophages. *PLoS One*. **10**, e0138131 (2015).

32. S. Maeda, T. Tsukihara. Structure of the gap junction channel and its implications for its biological functions. *Cell. Mol. Life Sci.* **68**, 1115-1129 (2011).

33. J. Manasson, T. Tien, C. Moore, N. M. Kumar, S. Roy, High glucose-induced downregulation of connexin 30.2 promotes retinal vascular lesions: implications for diabetic retinopathy. *Invest. Ophthalmol. Vis. Sci.* **54**, 2361-2366 (2013).

34. A. Martín-Martín, N. Vizcaíno, L. Fernández-Lago, Cholesterol, ganglioside GM_1 and class A scavenger receptor contribute to infection by *Brucella ovis* and *Brucella canis* in murine macrophages. *Microbes Infect.* **12**, 246-251 (2010).

35. A. Montagne, Z. Zhao, B. V. Zlokovic, Alzheimer's disease: A matter of blood-brain barrier dysfunction? *J. Exp. Med.***214**, 3151-3169 (2017).

36. E. Moreno, D. T. Berman, L. A. Boettcher. Biological activities of *Brucella abortus* lipopolysaccharides. *Infect. Immun.* **31**, 362-370 (1981).

37. W. A. Muller, Transendothelial migration: unifying principles from the endothelial perspective. Immunol. Rev. **273**, 61-75 (2016).

38. R. Navarro, M. Compte, L. Álvarez-Vallina, L. Sanz, Immune regulation by pericytes: modulating innate and adaptive immunity. *Front. Immunol.* **7**, 480 (2016).

39. A. M. Nikolakopoulou *et al.*, Pericyte loss leads to circulatory failure and pleiotrophin depletion causing neuron loss. *Nat. Neurosci.* **22**, 1089-1098 (2019).

40. S. Nourshargh, S. A. Renshaw, B. A. Imhof. Reverse migration of neutrophils: where, when, how, and why? *Trends Immunol.* **37**, 273-286 (2016).

41. K. Ochs *et al.*, Immature mesenchymal stem cell-like pericytes as mediators of immunosuppression in human malignant glioma. *J. Neuroimmunol.* **265**, 106-116 (2013).

42. S. Ogura *et al.*, Sustained inflammation after pericyte depletion induces irreversible blood-retina barrier breakdown. *JCI Insight.* **2**, e90905 (2017).

43. U. Ozerdem, K. A. Grako, K. Dahlin-Huppe, E. Monosov, W. B. Stallcup, NG2 proteoglican is expressed exclusively by mural cells during vascular morphogenesis. *Dev. Dyn.* **222**, 218-227 (2001).

44. U. Ozerdem, E. Monosov, W. B. Stallcup, NG2 proteoglycan expression by pericyte in pathological microvasculature. *Microvasc. Res.* **63**, 129-134 (2002).

45. U. Ozerdem, W. B. Stallcup, Early contribution of pericytes to angiogenic sprountin and tube formation. *Angiogenesis*. **6**, 241-249 (2003).

46. L. B. Payne *et al.*, Pericyte progenitor coupling to the emerging endothelium during vasculogenesis via connexin 43. *Arterioscler. Thromb. Vasc. Biol.* **42**, e96-e114 (2022).

47. C. Pieper, P. Pieloch, H. J. Galla, Pericytes support neutrophil transmigration via interleukin-8 across a porcine co-culture model of the blood-brain barrier. *Brain Res.* **1524**, 1-11 (2013).

48. R. Ponsaerts *et al.*, Intramolecular loop/tail interactions are essential for connexin 43-hemichannel activity. *FASEB J.* **24**, 4378-4395 (2010).

49. D. Proebstl *et al.*, Pericytes support neutrophil subendothelial cell crawling and breaching of venular walls in vivo. *J. Exp. Med.* **209**, 1219-1234 (2012).

50. O. Rasool, E. Freer, E. Moreno, C. Jarstrand, Effect of *Brucella abortus* lipopolysaccharides on the oxidative metabolismo and enzyme release of neutrophils. *Infect. Immun.* **60**, 4-7 (1992).

51. B. Schmeck *et al.*, *Listeria monocytogenes* induced Rac1-dependent signal transduction in endothelial cells. *Biochem. Pharmacol.***72**, 1367-1374 (2006).

52. M. Schnoor, P. Alcaide, M. B. Voisin, J. D. van Buul, Crossing the vascular wall: common nd unique mechanisms exploited by different leukocyte subsets during extravasation. *Mediators Inflamm.* **2015**, e946509 (2015).

53. T. M. A. Silva *et al.*, Putative ATP-binding cassette transporter is essential for *Brucella ovis* pathogenesis in mice. *Infect. Immun.* **79**, 1706-1717 (2011).

54. S. T. Smiley, J. A. King, W. W. Hancock, Fibrinogen stimulates macrophage chemokine secretion through toll-like receptor 4. *J. Immunol.* **167**, 2887-2894 (2001).

55. K. Stark *et al.*, Capillary and arteriolar pericytes attract innate leukocytes exiting through venules and 'instruct' them with pattern-recognition and motility programs. *Nat. Immunol.* **14**, 41-51 (2013).

56. I. Timmerman, A. E. Daniel, J. Kroon, J. D. van Buul, Leukocytes crossing the endothelium: a matter of communication. *Int. Rev. Cell. Mol. Biol.* **322**, 281-329 (2016).

57. O. Torok *et al.*, Pericytes regulate vascular immune homeostasis in the CNS. *Proc. Natl. Acad. Sci. USA.* **118**, E2016587118 (2021).

58. Z. Tu *et al.*, Retinal pericytes inhibit activated T cell proliferation. *Invest. Ophthalmol. Vis Sci.* **52**, 9005-9010 (2011).

59. B. Vallet, Bench-to-bedside review: endothelial cell dysfunction in severe sepsis: a role in organ dysfunction? *Crit. Care.* **7**, 130-138 (2003).

60. M. Varanat, R. G. Maggi, K. E. Linder, E. B. Breitschwerdt, Infection of human brain vascular pericytes (HBVPs) by *Bartonella henselae*. *Med. Microbiol. Immunol.* **202**, 143-151 (2013).

61. I. Wilkerson, J. Laban, J. M. Mitchell, N. Sheibani, D. J. Alcendor, Retinal pericytes and cytomegalovirus infectivity: implications for HCMV-induced retinopathy and congenital ocular disease. *J. Neuroinflammation.* **12**, 2 (2015).

62. E. A. Winkler, R. D. Bell, B. V. Zlokovic, Central nervous system pericytes in health and disease. *Nat. Neurosci.* **14**, 1398-1405 (2011).

63. K. K. Wu, K. Frasier-Scott, H. Hatzakis, Endothelial cell function in hemostasis and thrombosis. *Adv. Exp. Med. Biol.* **242**, 127-133 (1988).

64. H. Yamagami, S. Yamagami, T. Inoki, S. Amano, K. Miyata, The effects of proinflammatory cytokines on cytokine-chemokine gene expression profiles in the human corneal endothelium. *Invest. Ophthalmol. Vis. Sci.* **44**, 514-520 (2003).

65. T. Yamazaki, Y. S. Mukouyama, Tissue specific origin, development, and pathological perspectives of pericytes. *Front. Cardiovasc. Med.***5**, 78 (2018).

66. Y. Yin *et al.*, A hybrid sub-lineage of *Listeria monocytogenes* comprising hypervirulent isolates. *Nat. Commun.* **10**, 4283 (2019).

67. L. A. Zenewicz, H. Shen, Innate and adaptive immune responses to *Listeria monocytogenes*: a short overview. *Microbes Infect.* **9**, 1208-1215 (2007).

68. D. A. Portnoy, P. S. Jacks, D. J. Hinrichs. Role of hemolysin for the intracellular growth of *Listeria monocytogene*. *J. Exp. Med.* 167,1459-1471 (2019).

69. S. W. Barthold, G. L. Coleman, R.O. Jacoby, E. M. Livestone, A. M. Jonas. Transmissible murine colonic hyperplasia. *Vet. Pathol.* 15, 223-226 (1978.

70. D. B. Schauer, S. Falkow. Attaching and effacing locus of a *Citrobacter freundii* biotype that biochemical characterization of *Citrobacter rodentium* sp. nov. *J. Clin Microbiol.* 33, 2064-2068, 1995.

Chapter III

Pericyte depletion and bacterial dissemination to the central nervous system – preliminary results

Introduction

The blood brain barrier (BBB) is composed of the microvasculature of the central nervous system (CNS). CNS vessels are continuous non-fenestrated vessels that selectively regulate molecules that pass from the bloodstream to the nervous tissue as well as in the opposite direction (Zlokovis 2008; Daneman 2012). The blood vessels maintain CNS homeostasis, which is important for neuronal function as well as for protecting the brain from the action of toxins and pathogens. Pericytes are a critical component of the BBB. Pericytes localize in capillaries as umbrella-like structures (Daneman et al., 2010; Sengillo et al., 2013; Keller et al., 2013), and they are also found at the luminal aspect of astrocyte end-feet, with the basement membrane separating and allowing pericytes to play a crucial role in endothelial function. Pericyte malfunction or reduction increases BBB permeability and dysregulated brain immune homeostasis (Daneman et al., 2010; Sengillo et al., 2013; Keller et al., 2013).

A bacterial meningo-encephalitis infection results in inflammation in the meninges and nervous system parenchyma. The condition requires fast diagnosis and treatment (Ramgopal et al., 2019; Fuentes-Antrás et al., 2019); Lien et al., 2019). Bacteremia can promote dissemination of bacteria to different various regions, including the BBB. The BBB can distinguish between systemically circulating and nervous system resident immune cells (Ransohoff et al., 2003). Pathogens can breach vascular blood vessels via transcytosis through endothelial cells, paracytosis between endothelial cells or inside recruited and infected leukocytes, process known as “Trojan horse” (Guitiérrez-Jiménez et al., 2019; Anil and Banerjee, 2020). One new model for *in vitro* BBB studies is organoids. Studies of brain penetrating compounds can be conducted using these models (Cho et al., 2017). One advantage of this system is that all the cell types are in

direct interaction with one another. These interactions play a role in the maintenance of the BBB (Cecchelli et al., 2014). *In vitro* models for mimicking the BBB in cell culture have been developed and used since the 1980s (Bowman et al., 2023). These are an essential tool for understanding cell interactions and selective permeability. Reproducing BBB properties *in vivo* remains a challenge. In a transwell system, brain endothelial cells are cultured at the apical level and astrocytes or pericytes on the bottom side are co-cultured. The transwells are useful to evaluate transmigration and permeability models, but some holes can be formed in the monolayer of endothelial cells (Hatherell et al., 2011). Currently, researchers use organoids (spheroids) models. Under low-adherence conditions, endothelial cells, pericytes, and astrocytes spontaneously form a multicellular sphere. Organoids showed similar selective permeability *in vivo* as well. Besides, these co-culture systems are easier and cheaper than transwell cultures for the study of BBB (Cho et al., 2017). These BBB organoids models can be comparable to what is seen in the BBB. They showed high levels of tight/adherent junctions, selective permeability (Cho et al. 2017). For specific study the function of pericyte in the BBB, we will used transgenic model with the depletion of pericyte in systemic bacterial diseases.

Material and methods

NG2 cell depletion and mouse infection

NG2 cell depletion was performed as described (Kunisaki et al., 2013). Briefly, 4 to 6-week-old mice received 1 mg of tamoxifen (Sigma - Aldrich) IP twice a day (12-hour intervals) for five consecutive days. Two days later (7th day of the protocol), diphtheria toxin (DT), which triggers NG2cre cell depletion, was intraperitoneally injected at a single dose of 100 µg/Kg of body weight. Seven days later (14th day of the protocol), mice were 6 to 8-weeks-old and used for experimental infections. NG2+ pericyte-depleted C57BL/6 mice (n = 10) and iDTR C57BL/6 mice (n = 14) were IP injected with 100 µL of a suspension containing 1 x 107 CFU/mL of *B. ovis,* or *L. monocytogenes* 1x106 CFU/ml. Mice were euthanized at 1, 3, and 15 dpi. Liver and spleen were collected for bacteriology and histopathology.

For experiments with higher infectious doses, C57BL/6 were inoculated with 100 µL of a suspension containing 1 x 10^8, 1 x 10^9, or 1 x 10^{10} CFU/mL of wild type *B. ovis*, and subjected to euthanasia and sampling at 1, 3, and 7 dpi.

GAP19 treatment

C57BL/6 mice (5 to 7 weeks old) will be intraperitoneally treated with a Cx43-specific inhibitor (Gap19; 25 mg/Kg every 24 hours). These chemical inhibitors have been previously used *in vivo* in mice with no relevant deleterious effects (Burkovetskaya et al, 2014; Sasaki et al, 2018; Wang et al, 2013). Treated and untreated control mice will then be intraperitoneally inoculated with 10^7 CFU of *B. ovis*. Mice will be euthanized 3 obtained for CFU counting, histopathology and transcription analyses.

Bacteriologic cultures

Tissue samples were placed in sterile PBS (pH 7.4), and maintained on until they were macerated and serially diluted (10-fold dilutions) in PBS. One hundred µL of each dilution were plated on hTSA or LB, in duplicates. Plates were incubated at 37ºC in a humidified incubator supplemented with 5% CO_2 for 1 to 5 days, when colonies were counted.

Results

Pericyte depletion and bacteremia are associated with brain colonization by *Brucella ovis* and *Listeria monocytogenes*

In previous studies, intraperitoneal infection of pericyte-depleted mice with wild type *B. ovis* and *L. monocytogenes* resulted in clinical signs, fibrous peritonitis, and mortality, showing the role of pericyte in regulating inflammation and increased bacterial colonization in the liver and spleen (Chapter 2). For bacterial spread systemically, the organism is initially present in the blood. We investigated bacteremia in each group. *B. ovis* and *L. monocytogenes* infections resulted in higher bacteremia in the depleted and infected mice in *B. ovis* (Figure 3.1A). However, no difference between the two groups infected with *L. monocytogenes* (Figure 3.1B).

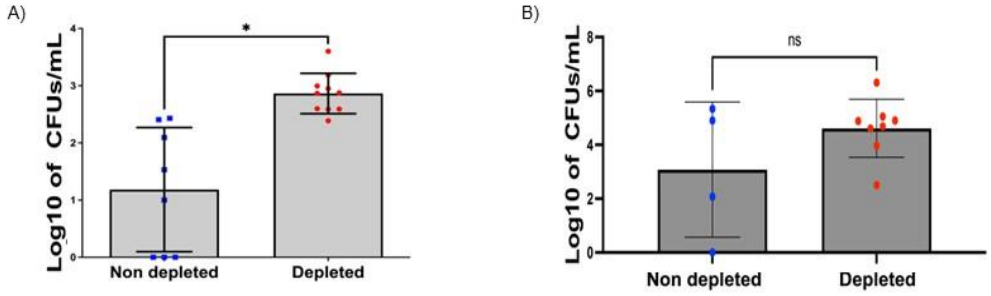

Figure 3.1 Bacteremia in depleted of pericytes. Blood bacterial count of non-depleted and depleted infected with $1x10^6$ CFU of *Brucella ovis* per animal at 24 hours pos infection (A) or $1x10^5$ CFU of *Listeria monocytogenes* after 48 hours post infection (B). The bar column in each group indicates the mean. Each point represents one animal. All data were logarithmically transformed prior to ANOVA, and the means were compared by the Student T test. Statistically significant differences are indicated by asterisks (* $p<0.05$).

Increased bacteremia and a lack of pericytes may favor bacterial colonization of CNS. No gross lesions were found in the CNS. Bacteriological analysis of the brain revealed that NG2-deficient mice were highly colonized by *B. ovis* and *L. monocytogenes* compared to non-depleted mice (Figure 3.2 A and 3.2 B). It is noteworthy that absence of pericytes did not reverse the requirement of the T4SS for full virulence since even pericyte-depleted mice were still able to

largely control *B. ovis* Δ*virB2* colonization, in the brain had not colonized in the brain at 6 dpi (Figure 3.3 A).

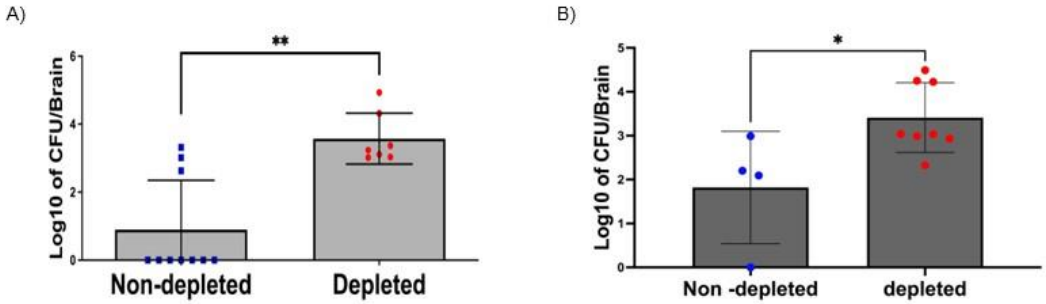

Figure 3.2 Brain colonization in the model of pericyte depletion. Experimental infection of non-depleted mice and pericyte-depleted mice with $1x10^6$ CFU of *Brucella ovis* per animal at 6 days after infection (A) or $1x10^5$ CFU of *Listeria monocytogenes* after 48 hours pos infection (B). The bar column in each group indicates the mean. Each point represents one. All data were logarithmically transformed prior to ANOVA, and the means were compared by the Student t test. Statistically significant differences are indicated by asterisks (* $p<0.05$; ** $p<0.01$).

For the purpose of determining if it is just an increase in bacteria in the bacteremia of the blood stream. We performed the infection with high doses of *B. ovis* infections (10^7, 10^8, 10^9) (Figure 3 B). In these experiments, we not found any difference between the doses of infection and bacteriology in the presence pericyte. The pericyte is responsible for controlling the level of bacteria in the blood. We analyzed the bacteriology of the high dose infection to determine whether the bacteria in the blood could influence brain colonization. Bacteria were isolated in the brain at 6 dpi (Figure 3 C).

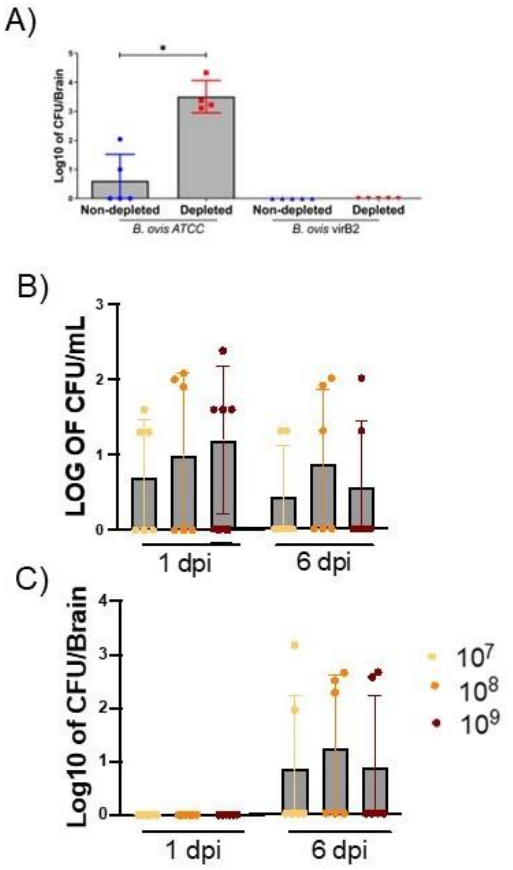

Figure 3.3 Bacteria colonization of the brain different host or challenge condition. Non depleted and pericyte depleted mice infected with *Brucella ovis* ATCC or *B. ovis* Δ*virB2* with 10^6 CFU/ animal after 6 days pos infection (A). Experimental high dose infection in C57BL-6 mice with *B. ovis* ATCC in different time of infection 1, 3, and 6 dpi in the blood (B) and in the Brain (C). The bar column in each group indicates the mean. Each point represents one animal. All data were logarithmically transformed prior to ANOVA, and the means were compared by the Student t test. Statistically significant differences are indicated by asterisks (* $p<0.05$; ** $p<0.01$).

Connexin 43 is essential to bacteremia and central nervous system colonization

Pericytes and endothelial cells interact through via peg-and-socket junctions. These junctions are rich in gap junctions, which are composed of connexin , mostly connexin 43 (Payne

et al., 2022). In previous studies, the blockage of connexin channels resulted in an upregulation of inflammatory genes (IL-6 and CCL-2), as well as adhesion molecules (PECAM-1 and ICAM-1) (Chapter 2). We treated the mice with GAP-19, favored *B. ovis* dissemination resulting in significant increased CFU numbers in blood and (Figure 4 A and 4 B) when compared to other group.

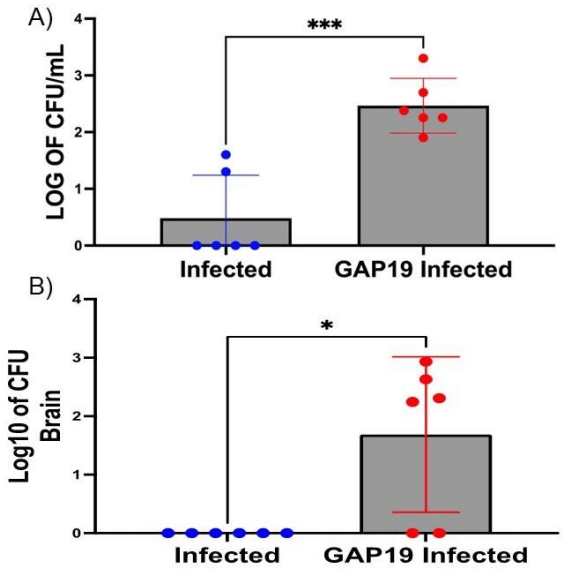

Figure 3.4 Effects of connexin 43 block (Gap junction channels) systemically in *Brucella ovis* infection colonization of blood and brain. C57bl-6 mice were infected with $1x10^{6}$ CFU of *B. ovis* per animal. After 6 days post-infection, blood (A) and brain (B) were collected for bacteriology analysis. A LOG transformation normalized the CFU numbers. Each point represents the mouse value, while the bars represent the mean of each group and the standard difference. The statistical analysis was performed by ANOVA (p*p<0.05; ***p<0.001)

Discussion

In this study, we demonstrated the importance of pericytes in the BBB in bacteria-related diseases. Bacteremia is critical for bacteria spread throughout many tissues (Aronson et

al., 2019). Between these systemic tissues, the CNS and meninges are significant places for bacterial multiplication and can result in a variety of clinical symptoms or mortality (John et al., 2015; Robertson et al., 2018). A second key point is that BBB effectively controls the access of the immune cell to CNS (Engelhard et al., 2017). These permeability controls avoid damaging immune mediated inflammation (Louveau et al., 2015). In addition, pathogens such as bacteria, viruses, and fungi, pass through the BBB. In the CNS, bacterial infections are associated with immunocompromised individuals, such as those with HIV infection or malnutrition. Bacteria involved in CNS infections include *L. monocytogenes, Neisseria meningitidis, Streptococcus pneumoniae, Staphylococcus aureus, Haemophilus influenza,* and *Brucella* spp. (Engelhardt et al., 2017).

In our study, we demonstrated that Cx-43 contributes to maintenance of the BBB by perycites. Our previous research indicates that pericytes and endothelial cells maintain tissues' homeostasis, and pericytes regulate inflammatory responses to Cx-43. Gap junction channels are essential to endothelial-pericytes communication during angiogenesis (Payne et al., 2022). Specifically, CX-43 defects lead to heart outflow tract defects in mice, for example (Rhee et al., 2009; Francis et al., 2011). The block or absence of Cx-43 also increases inflammatory (CCL-2 and Il-6) and adhesion molecules (PECAM-1 and ICAM-1) (Chapter 2).

With the depletion of number of pericytes, we found an increased bacterial colonization in the CNS during *B. ovis* and *L. monocytogenes* infection. In terms of keeping pathogens out of the central nervous system, the BBB plays an extremely important role. Pericytes are essential components of these systems. These cells increase the selective permeability, protecting brain tissue from damaging molecules. Pericyte depletion increased liquid permeability and plasma protein in the brain (Armulik et al., 2010). Several intracellular microorganisms survive in the intracellular environment, including *Brucella* spp., *Chlamydia pneumonia, Leishmania major,* and others. In the case of these pathogens, Trojan horse leukocytes serve as a crucial mechanism of dispersion for tissues, including the brain (Laskay et al., 2008; Gutierrez-Jimenez et al., 2019). Future experiments will investigate the role of pericyte in the leukocyte’s migration to brain. Besides investigate whether leukocytes infected (Trojan horse) with *B. ovis* and *L. monocytogenes*are more likely to pass through the BBB when pericytes are absent or decrease in

the BBB and in cell culture models. In addition, we will adapt the organoids model to understand the role of pericytes in bacterial neurological invasion in the BBB.

REFERENCES

ANIL, A.; BANERJEE, A. Pneumococcal Encounter With the Blood-Brain Barrier Endothelium. **Front. Cell Infect. Microbiol.**, v.10, p.590682, 2020.

ARMULIK, A.; GENOVÉ, G.; BETSHOLTZ, C. Pericytes: developmental, physiological, and pathological perspectives, problems, and promises. **Dev. Cell,** v. 21, n. 2, p. 193-215, 2011.

ARMULIK, A.; GENOVÉ, G.; MÄE, M.; et al. Pericytes regulate the blood-brain barrier. **Nature**, v. 468, v. 7323, p. 557-561, 2010.

BOWMAN, C.; MA, F.; MAO, J.; et al. Evaluation of bottom-up modeling of the blood-brain barrier to improve brain penetration prediction via physiologically based pharmacokinetic modeling. **Biopharm. Drug Dispos.**, v. 44, n.1, p. 60-70, 2023.

CECCHELLI, R.; ADAY, S.; SEVIN, E.; et al. A stable and reproducible human blood-brain barrier model derived from hematopoietic stem cells. **PLoS One**, v.9, n. 6,p. e99733,2014.

CHO, C. F.; WOLFE, J. M.; FADZE, C. M., et al., Blood brain barrier spheroids as an *in vitro* screening platform for brain penetrating agents. **Nature Communications**, v.8, p.15623, 2017.

DANEMAN, R.; ZHOU, L.; KEBEDE, A. A.; et al. Pericytes are required for blood-brain barrier integrity during embryogenesis. **Nature,** v. 468, n. 7323, p.562-566, 2010.

ENGELHARDT, B.; VAIKOCZY, P.; WELLER, R. O. The movers and shapers in immune privilege of the CNS. **Nat. Immunol.,** v.18, p. 123-131.

FRANCIS, R.; XU, X.; PARK, H.; et al. Connexin 43 modulates cell polarity and directional cell migration by regulating microtubule dynamics. **PLoS One**, v.6, p. e26379, 2011.

FUENTES-ANTRÁS, J.; RAMÍREZ-TORRES, M.; OSORIO-MARTÍNEZ, E.; et al. Acute Community-Acquired Bacterial Meningitis: Update on Clinical Presentation and Prognostic factors. **New Microbiol.**, v. 41, n.2, p. 81-87, 2019.

GAIESKI, D. F.; O'BRIEN, N. F.; HERNANDEZ, R. Emergency Neurologic Life Support: Meningitis and Encephalitis. **Neurocrit. Care**, v.27, n.1, p.124-133, 2017.

GUTIÉRREZ-JIMÉNEZ, C.; MORA-CARTÍN, R.; ALTAMIRANO-SILVA, P.; et al. Neutrophils as trojan horse vehicles for *Brucella abortus* macrophage infection. **Front. Immunol.,** v.10, p. 1012, 2019.

HATHERELL, K.; COURAUD, P. O.; ROMERO, I. A.; et al. Development of a three-dimensional, all-human in vitro model of the blood-brain barrier using mono-, co-, and tri-cultivation Transwell models. **J. Neurosci. Methods.**, v.199, n.2, p. 223-229, 2011.

KELLER, A.; WESTENBERGER, A.; SOBRIDO, M. J.; et al. Mutations in the gene encoding PDGF-B cause brain calcifications in humans and mice. **Nat. Genet.**, v.45, p. 1077-1082, 2013.

KUNISAKI, Y.; BRUNS, I.; SCHEIERMANN, C. et al. Arteriolar niches maintain haematopoietic stem cell quiescence. **Nature**, v.502, n. 7473, p. 637-643, 2013.

LASKAY T, VAN ZANDBERGEN G, SOLBACH W. Neutrophil granulocytes as host cells and transport vehicles for intracellular pathogens: apoptosis as infection-promoting factor. **Immunobiology**, v.213, p. 183-191, 2008.

LOUVEAU, A.; SMIRNOV, I.; KEYES, T.J.; et al. Structural and functional features of central nervous system lymphatic vessels. **Nature**, v.523, p. 337-341, 2015.

PAYENE, L. B.; TEWARI, B. P.; DUNKENBERGER, L.; et al. Pericyte progenitor coupling to the emerging endonthelium during vasculogenesis via connexin 43. **ATVB**, V. 42, n.4, p. e96-114, 2022.

RAMGOPAL, S.; WALKER, L. W.; VITALE, M. A; NOWALK, A. J. Factors associated with serious bacterial infections in infants ≤60 days with hypothermia in the emergency department. **Am. J. Emerg. Med.**, v. 37, n. 6, p. 1139-1143, 2019.

RANSOHOFF, R.M.; KIVISÄKK, P.; KIDD, G. Three or more routes for leukocyte migration into the central nervous system. **Nat. Rev. Immunol.**, v.3, n.7, p. 569-581, 2003.

RHEE, D. Y.; ZHAO, X. Q.; FRANCIS, R. J.; et al. Connexin 43 regulates epicardial cell polarity and migration in coronary vascular development. **Development**, v. 136, p.3185-3195, 2009.

SENGILLO, J. D.; WINKLER, E. A.; WALKER, C. T.; et al. Deficiency in mural vascular cells coincides with blood-brain barrier disruption in Alzheimer's disease. **Brain Pathol.**, v. 23, p. 303-310, 2013.

ZLOKOVIC, B. V. The blood-brain barrier in health and chronic neurodegenerative disorders. **Neuron**, v. 57, n.2, p.178-201, 2008.

Supplementary data

Table 1. Cells used for study with *Brucella* sp.

Cell type	Origin	*Brucella* species	MOI	Outcome of infection	References
Macrophages derivated of BMDMs	Primary of murine BMDMs	*B.abortus* *B.melitensis*	1-200	Cell infection and proliferation without inducing cytotoxicity	Celli et al, 2003 Barqueiro-Calvo et al, 2007 Surendran et al, 2011 Lacey et al, 2021
Dendritic cells (DC) or macrophages	Primary of human, canine, ovine, bovine PBMC and murine peritonel and alveolar	*B. abortus* *B.suis* *B.canis* *B. ovis*	1-300	Cell infection and proliferation. *Brucella* induced DC maturation	Billard et al, 2007. Zwerdling et al, 2008. Heller et al, 2012 Scian et al, 2013 Gorvel et al, 2014. Ferreiro et al,

					2014. Pujol et al, 2017. Pujol et al, 2019 Eckstein et al, 2020.
Macrophage DH82 THP-1 RAW 264.7 J774.A1	Commercial line of canine, human or murine macrophage-like of a tumor	*B.abortus* *B.suis* *B.melitensis* *B.canis* *B. ovis* *B.neotomae* *B.pinnipedialis* *B.* sp. frog isolated	1-1000	Cell infection and proliferation.	Delpino et al, 2009. Silva et al, 2011 Larsen et al 2013 Scian et al, 2013 Chacon-Diaz et al, 2015. Soler-Llorens et al, 2016 Verdiguel-Fernandez et al, 2017 Kang and

					Kirby, 2017 Kang and Kirby, 2019 Milillo et al, 2019 Arriola Benitez et al, 2020. Varesio et al, 2021 Park et al, 2021.
Neutrophil	Primary of human, goat, bovine blood stream or bone marrow of mice	*B.abortus* *B.melitensis* *B.canis* *B.suis*	50-1000	Cells infection, and without pro-inflammatory stimulus *Brucella* can survive in intracellular environment. Neutrophil could be a Trojan horse for macrophage infection with *Brucella*	Zwerdling et al, 2009 Delpino et al, 2010. Ferrero et al 2011 Scian et al, 2013 Keleher and Skyberg, 2016 Gutierrez-Jimenez et al,

					2019 Trotta et al, 2020
Trophoblast	Prymary isolated of placents of dogs, mice and immortalized of goats	*B.canis* *B.suis* *B. melitensis*	100-250	Cell infection and proliferation without inducing cytotoxicity. Decrease of cell multiplication.	Wang et al, 2016. Fernandez et al, 2017. Liu et al, 2019
Trophoblast Bewo, JeG-3 And SW.71	Commercial line of human choriocarcinoma	*B. melitensis* *B.papionis* *B.abortus* *B.suis* *B. ovis*	100-250	Cell infection and proliferation. *B.melitensis* caused changes in hormonal production.. *Brucella* spp can be localized in "*Brucella*-inclusions" *B.papionis* induced a decrease of cells fusion	Salcedo et al, 2013. Sidhu-Munoz et al, 2018. Garcia-Mendez et al, 2019. Bialer et al, 2021 Mena-Bueno et al, 2022

HELA	Commercial line of human epithelial cells	*B.canis* *B.melitensis* *B.abortus* *B. ovis* *B.pinnipedialis* *B.* sp. frog isolate *B.neotomae*	200-500	Cell infection and proliferation without inducing cytotoxicity.	Barqueiro-Calvo et al, 2007 Larsen et al 2013 Chacon-Diaz et al, 2015. Soler-Llorens et al, 2016 Verdiguel-Fernandez et al, 2017 Sidhu-Munoz et al, 2018 Waldrop and Sriranganathan, 2019
Colorectal Epithelial cells HT-29 CACO2	Commercial lines human cells of colorectal epithelia	*B.suis* *B.abortus* *B.melitensis* *B.canis*	100-200	Cell infection and proliferation with cytotoxic and low inflammatory response	Ferrero et al, 2012 Bialer et al, 2021

Alveolar epithelial	Commercial line of human type II alveolar epithelial	*B. abortus* *B.suis* *B.canis*	200-500	Cell infection and proliferation With a low cytotoxic	Ferrero et al, 2009 Ferrero et al, 2010
Esophagus epithelial cells	Primary cells of hooded seal (*Cystophora cristata*)	*B.pinnipedialis*	500	Cell infection without multiplication intracellular, with a significativly reduction of CFU at 24 hpi	Larsen et al, 2016
Testis epithelial cells OA3.Ts	Commercial line of sheep testis epithelial cells	*B. ovis*	200	Cell infection and proliferation.	Sidhu-Munoz et al, 2018.
Endometrial epithelial cells	Immortalized caprine endometrial epithelial cells or commercial human line	*B.suis* *B.abortus*	100-250	Cell infection and proliferation with a low cytotoxic	Wang et al, 2015 Zavattieri et al, 2020
Osteoblast	Primary of murine newborn-mouse calvaria	*B.suis*	100	*Brucella* adherence	Bialer et al, 2021
Osteoblat	Comercial lines of human osteosarcomas	*B.abortus*	10-1000	Cell infection and	Delpino et al, 2009.

SaOS-2 MG-63 MC3T3-E1	or (MC3T3-E1) murine preosteoblasts cells	*B.suis* *B.melitensis* *B.canis*		proliferation. *Brucella* invasion inhibits bone formation. Cortisol levels increased *Brucella* intracellular multiplication. However 50h after infection no recovery of *B.canis.*	Gentilini et al, 2018.
Osteoclast	Differenciation of primary cells of BMDMs	*B.abortus*	50-500	Cell infection and proliferation.	Khalaf et al, 2020
Osteocyte MLO-Y4	Commercial line of murine osteocyte cells with high expression of osteocalcin	*B.abortus*	100-1000	Cell infection and proliferation. *Brucella* infection decreased the expression of cx-43.	Pesce Viglietti et al, 2015 Pesce Viglietti et al, 2019

Synoviocytes	Commercial immortalized cell of human synovial sarcoma or primary human line	*B.abortus*	100-1000	Cell infection and proliferation.	Scian et al, 2011 Scian et al, 2013 Gentilini et al, 2019
Fibroblast	Immortalized human fibroblast like cells SW982 or primary synovial fibroblast	*B. abortus* *B.suis*	100-1000	Cell infection and proliferation.	Scian et al, 2011 Bialer et al, 2021
Endothelial cells HBMECs HUVEC	Immortalized line of human brain or primary umbilical veins	*B.abortus*	25-1000	Cell infection and proliferation.	Ferrero et al 2011 Miraglia et al 2018 Rodriguez et al, 2020
Hepatocytes	Commercial line of human hepatoma HepG2	*B.abortus*	10-1000	Cell infection and proliferation with cytotoxic effect	Delpino et al, 2010.
Hepatic stellate cells	Immortalized human hepatic	*B.abortus*	100-1000	Cell infection. *Brucella*	Arriola Benitez

	stellate cells line LX-2			induced increased of MHC-II in co-culture with macrophages	et al, 2013. Arriola Benitez et al, 2017 Arriola Benitez et al, 2020.
Lymphocyte B	Primary line of murine spleen cells	*B.abortus*	100-1000	Cell infection and proliferation	Pessce Viglietti et al, 2016
Lymphocytes T	Primary cells of human PBMC	*B.abortus*	25-1000	Low cell infection, with low CFU countings. Infection induced apoptosis	Vélasquez et al, 2012
Microglia BV-2 C13NJ HMC3	Commercial line or primary cells of murine and human cells	*B.suis* *B.melitensis* *B.abortus*	10-1000	Cell infection and replication with low cytotoxity	Yan et al, 2019 Erdogan et al, 2013 Wang et al, 2021 Garcia Samartino et al, 2010

Astrocytes	Primary isolation of mice	*B.abortus* *B.melitensis* *B.canis*	50-1000	Cell infection and replication	Samartino et al, 2010 Miraglia et al, 2013
Adipocyte	Fibroblast 3T3-L1 exposed a differentiation media	*B.abortus*	100-1000	Cell infection and replication	Pesce Vigletti et al, 2020
Chorioallatoic membrane explants	Explants of bovine placenta	*B.abortus*	1000	Internalization of bacteria	Samartino and Enright 1996. Carvalho Neta et al, 2008. Mol et al, 2014
Plaquets	Isolated of human blood	*B.abortus*	1-30	*Brucella* internalization	Trotta et al, 2018

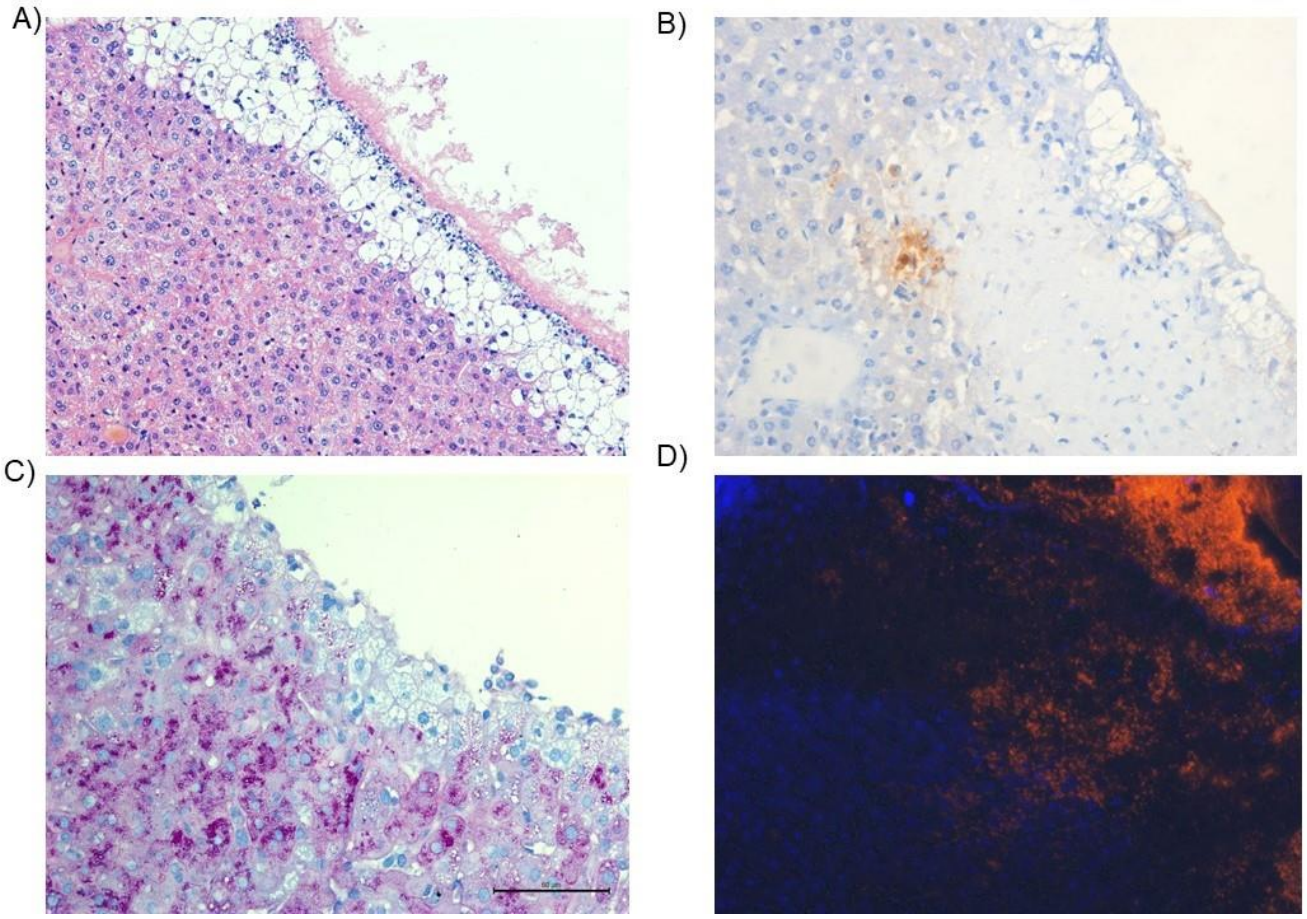

Supplementary Figure 1. Microscopic changes in the liver of pericyte depleted animals infected with *Brucella ovis*. Liver of infected mice depleted in hematoxilyn and Eosin staining (A) and Immunohistochemistry for NG2 (B). PAS staining of the liver of depleted mice (C). In situ Hibrydization for *Pecam1* of depleted mice infected with *B.ovis* (D).